

# Adaptive Morphology for Multi-Modal Locomotion

THÈSE N° 6608 (2015)

PRÉSENTÉE LE 9 JUIN 2015

À LA FACULTÉ DES SCIENCES ET TECHNIQUES DE L'INGÉNIEUR  
LABORATOIRE DE SYSTÈMES INTELLIGENTS  
PROGRAMME DOCTORAL EN SYSTÈMES DE PRODUCTION ET ROBOTIQUE

ÉCOLE POLYTECHNIQUE FÉDÉRALE DE LAUSANNE

POUR L'OBTENTION DU GRADE DE DOCTEUR ÈS SCIENCES

PAR

Ludovic DALER

acceptée sur proposition du jury:

Prof. M.-O. Hongler, président du jury  
Prof. D. Floreano, Prof. A. Ijspeert, directeurs de thèse  
Prof. C. Stefanini, rapporteur  
Dr M. Kovac, rapporteur  
Prof. J. Paik, rapporteur



ÉCOLE POLYTECHNIQUE  
FÉDÉRALE DE LAUSANNE

Suisse  
2015



Wings are a constraint that makes it possible to fly.  
— Robert Bringhurst

To my five sisters...





# Acknowledgements

The achievement of this thesis would not have been possible without the help and contributions of many people. To start with, I want to thank my supervisor Dario Floreano for his guidance throughout these four years of research. Dario introduced me his idea of using adaptive morphology for multi-modal locomotion while giving me a lot of freedom in the project. Dario taught me the importance of communicating my work outside of the lab and always forced me to think about the big picture, in order to understand where my work stands in the scientific world. Dario provided me with excellent work conditions and I enjoyed very much the four years spent in his lab.

Then, I would like to thank the members of my jury; Max-Olivier Hongler, Cesare Stefanini, Mirko Kovac, Jamie Paik and Auke Ijspeert who took the time to read my thesis and travel to Lausanne for my thesis defense.

Thanks is also due to the Swiss National Science Foundation through the National Centre of Competence in Research Robotics, whose funding made this research possible.

I would like to thank my colleague and friend, Adam Klaptocz, who supervised me during my semester and master projects within the lab. Adam convinced me to start a PhD thesis and transmitted me his passion for flying robots; without him I probably would not have started this project. Adam, together with Adrien Briod, taught me a lot during my first year of PhD and it has been a great opportunity for me to collaborate with them on the AirBurr project.

One of my colleague, Stefano Mintchev, who joined the lab in the middle of my PhD, was instrumental in the development of the platforms presented in this thesis. I would like to thank him for the time we spent together on brainstorming about new concepts and designing, manufacturing and testing prototypes. His passion for biology helped to understand better the concepts that are discussed in this thesis. Finally, I would like to thank him for his motivation and support, it has been a great pleasure to work with him on various projects.

I would like to express my gratitude to all my colleagues and friends at the LIS. I thank those who took the time to read this thesis; Adrien Briod, Stefano Mintchev, Giovanni Iacca, Julien Lecoeur and Ramon Pericet. I also would like to thank those with whom I spent time outside of the lab, doing all sorts of activities; Nicolas, Grégoire, Julien, Adrien, Adam, Przemek, Géraud, Stefano and many others.

## Acknowledgements

---

During my four years in the lab, I have supervised 22 students doing semester and master projects, some of their work contributed directly or indirectly to this thesis, most notably the work of Eric Nguyen and David Wuthier who continued to work with me even after their semester projects had ended.

Finally, I would like to express my gratitude to my friends and family who supported me through good and bad times. I would like to thank my parents, Frédéric and Ilona and their new spouses, and all my lovely younger sisters Charlotte, Saskya, Léa, Shanna and Kayla for all the happiness, love and support that they gave me. I also thank my closest friends who were always here to cheer me up; Gilles, Kevin, Pedro, Fabien, Cédric, Daniel and many others.

*Lausanne, 11 May 2015*

L. D.



# Abstract

There is a growing interest in using robots in dangerous environments, such as for exploration, search-and-rescue or monitoring applications, in order to reduce the risks for workers or rescuers and to improve their efficiency. Typically, flying robots offer the possibility to quickly explore large areas while ground robots can thoroughly search specific regions of interest.

While existing robotic solutions are very promising, they are often limited to specific use cases or environments. This makes them impractical for most missions involving complex or unpredictable scenarios, such as search-and-rescue applications. This limitation comes from the fact that existing robots usually exploit only a single locomotion strategy, which limits their flexibility and adaptability to different environments. In this thesis, multi-modal locomotion is investigated as a way to increase the versatility of mobile robots. We explore integrated design approaches, where the same actuators and structure are used for different modes of locomotion, which allows a minimization of the weight and complexity of the robot. This strategy is challenging because a single locomotor system must accommodate the potentially conflicting dynamics of multiple modes of locomotion. Herein, we suggest taking inspiration from nature, in particular the common vampire bat *Desmodus rotundus*. The goal being to make multiple modes of locomotion dynamically compatible (i.e. have compatible speeds and torques requirements), by optimizing the morphology of the locomotor system and even by adapting the morphology of the robot to a specific mode of locomotion.

It is demonstrated in this thesis that the integrated design approach can be effectively implemented on a multi-modal aerial and terrestrial robot, and that two modes of locomotion can be made dynamically compatible by optimizing the morphology. Furthermore, an adaptive morphology is used to increase the efficiency of the different modes of locomotion. A locomotor system used both for walking on the ground and controlling flight, has been successfully implemented on a multi-modal robot, which further has deployable wings to increase its performances on the ground and in the air. By successfully exploiting the concepts of integrated design and adaptive morphology, this robot is capable of hovering, forward flight and ground locomotion. This robot demonstrates a very high versatility compared to state of the art of mobile robots, while having a low complexity.

**Keywords:** Flying robots, multi-modal robots, integrated design, adaptive morphology.







## Résumé

L'utilisation de robots dans des environnements dangereux présente un intérêt grandissant pour des applications telles que l'exploration, la recherche de personnes en danger ou la surveillance. Les robots volants offrent la possibilité d'explorer rapidement de grandes surfaces alors que les robots terrestres permettent d'examiner minutieusement une région d'intérêt.

Les solutions robotiques existantes, bien que prometteuses, sont souvent limitées à des situations ou des environnements spécifiques, ce qui les rend inutilisables dans des missions aux scénarios complexes ou imprévisibles, telles que pour des missions de secours. Cette limitation vient du fait que les robots existants exploitent généralement une stratégie de locomotion unimodale, ce qui limite leur adaptabilité à des environnements différents de ceux pour lesquels ils ont été conçus. Dans cette thèse, une stratégie de locomotion plurimodale est investiguée dans le but d'augmenter la versatilité des robots mobiles. Nous explorons une approche de conception intégrée, selon laquelle les mêmes actionneurs et structures sont utilisés pour plusieurs modes de locomotion, permettant ainsi de minimiser le poids et la complexité du robot. Cette stratégie est ambitieuse car un unique système locomoteur doit satisfaire les dynamiques conflictuelles de plusieurs modes de locomotion. Ici, nous proposons de prendre inspiration de la nature, en particulier la chauve-souris vampire commun *Desmodus rotundus*. Le but étant de rendre plusieurs modes de locomotion dynamiquement compatible, c'est-à-dire ayant des exigences en vitesses et couples compatibles. Pour se faire, nous proposons d'optimiser la morphologie du système locomoteur et aussi d'adapter dynamiquement la morphologie du robot au mode de locomotion.

Il est démontré dans cette thèse qu'une conception intégrée peut-être efficacement implémentée sur un robot aérien et terrestre plurimodal, deux modes de locomotions sont rendus dynamiquement compatible en optimisant la morphologie. De plus, une morphologie adaptative permet d'augmenter l'efficacité des différents modes de locomotion. Un système locomoteur utilisé pour marcher au sol et pour contrôler le vol a été implémenté avec succès sur un robot plurimodal. Ce robot utilise également des ailes à géométrie variable pour augmenter ses performances au sol et dans les airs. En exploitant avec succès les concepts de conception intégrée et de morphologie adaptative ce robot, capable de vol stationnaire, de vol à plat et de déplacement au sol, démontre avoir une haute versatilité comparé à l'état de l'art des robots mobiles, tout en ayant une faible complexité.

**Mots clés :** Robots volants, robots plurimodaux, conception intégrée, morphologie adaptative.



# Contents

<b>Acknowledgements</b>	<b>i</b>
<b>Abstract (English/Français)</b>	<b>iii</b>
<b>List of figures</b>	<b>ix</b>
<b>List of tables</b>	<b>xi</b>
<b>1 Introduction</b>	<b>1</b>
1.1 Motivation . . . . .	2
1.1.1 Autonomous Robots Limitations . . . . .	2
1.1.2 Multi-Modal Locomotion . . . . .	3
1.1.3 Integrated Design Approach . . . . .	7
1.1.4 Adaptive Morphology . . . . .	8
1.2 Main Contributions and Thesis Organization . . . . .	9
<b>2 Platform Configuration Selection</b>	<b>11</b>
2.1 Functional Analysis . . . . .	12
2.2 Possible Solutions . . . . .	12
2.3 Evaluation of Solutions . . . . .	15
2.4 Solutions Selection . . . . .	17
2.5 Implementation of the Selected Solution . . . . .	19
<b>3 Integrated Design Approach</b>	<b>23</b>
3.1 Introduction . . . . .	24
3.2 Integrated Structure . . . . .	24
3.2.1 Ground Locomotion Analysis . . . . .	24
3.2.2 Morphology Optimization . . . . .	27
3.2.3 DALER v6 Mechanical Design . . . . .	28
3.2.4 DALER v6 Locomotion Capabilities . . . . .	29
3.3 Integrated Structure and Actuation . . . . .	31
3.3.1 Dual Use Walkerons . . . . .	31
3.3.2 DALER v9 Locomotion Capabilities . . . . .	41
3.4 Integrated Design Approach Analysis . . . . .	42
3.5 Conclusion . . . . .	44

## Contents

---

<b>4 Adaptive Morphology for Multi-Modal Locomotion</b>	<b>47</b>
4.1 Introduction . . . . .	48
4.2 DALER v9 Adaptive Mechanical Design . . . . .	49
4.3 Ground Locomotion Measurements . . . . .	50
4.4 Adaptive Morphology Model . . . . .	52
4.5 DALER v9 Adaptive Locomotion Capabilities . . . . .	57
4.6 Adaptive Morphology Analysis . . . . .	57
4.7 Conclusion . . . . .	58
<b>5 Integrated &amp; Adaptive Robot with Three Modes of Locomotion</b>	<b>59</b>
5.1 Introduction . . . . .	60
5.2 Platform Configuration . . . . .	60
5.3 DALER v11 Mechanical Design . . . . .	62
5.4 DALER v11 Prototype . . . . .	66
5.5 Electronics Design . . . . .	68
5.6 DALER v11 Locomotion Capabilities . . . . .	69
5.7 Multi-Modal Locomotion Analysis . . . . .	72
5.7.1 Mass Distribution & Integration Analyses . . . . .	72
5.7.2 Versatility and Complexity Analyses . . . . .	75
5.8 Conclusion . . . . .	78
<b>6 Concluding Remarks</b>	<b>79</b>
6.1 Main Accomplishments . . . . .	80
6.2 Future Work . . . . .	82
6.3 Outlook . . . . .	85
<b>A History of the DALER Project</b>	<b>87</b>
<b>B Weight of Criteria for Platform Configuration Selection</b>	<b>99</b>
<b>Bibliography</b>	<b>107</b>
<b>Curriculum Vitae</b>	<b>109</b>
<b>Publications</b>	<b>111</b>

# List of Figures

1.1	Multi-modal robots based on a fully additive strategy . . . . .	4
1.2	Multi-modal robots based on a semi-additive strategy . . . . .	5
1.3	Common vampire bat <i>Desmodus rotundus</i> running on the ground . . . . .	7
1.4	Multi-modal robot based on an integrated strategy . . . . .	8
1.5	Multi-modal robots with adaptive morphology . . . . .	9
1.6	Thesis outline . . . . .	10
2.1	Different modes of locomotion of the DALER . . . . .	19
2.2	Definition of the roll, pitch and yaw axes of the DALER . . . . .	19
2.3	Ground locomotion mode of the DALER . . . . .	20
2.4	Final demonstration scenario of the DALER project . . . . .	21
3.1	DALER v6 prototype . . . . .	24
3.2	Model of the DALER v6 . . . . .	25
3.3	Ground locomotion analysis of the DALER v6 . . . . .	25
3.4	Morphology optimization of the DALER v6 . . . . .	28
3.5	Mechanical design of the DALER v6 . . . . .	29
3.6	Ground locomotion capabilities of the DALER v6 . . . . .	30
3.7	DALER v9 prototype . . . . .	31
3.8	Model of the DALER v9 . . . . .	32
3.9	Operating range of a DC motor . . . . .	34
3.10	Working points of the walkerons . . . . .	37
3.11	Resulting working points of the walkerons . . . . .	42
4.1	Model of the DALER v9 Adaptive . . . . .	48
4.2	DALER v9 Adaptive prototype . . . . .	49
4.3	Mechanical design of the DALER v9 Adaptive . . . . .	49
4.4	Cost of transport vs speed of the robot on the ground . . . . .	51
4.5	Cost of transport vs speed of the robot on the ground with a wheel . . . . .	52
4.6	Efficiency of the DC motors as a function of their rotational speed . . . . .	54
4.7	Travelled distance for one revolution of the walkerons . . . . .	55
4.8	Comparison between measured data and model for the cost of transport . . . . .	55
4.9	Cost of transport of the robot as a function of the wing opening . . . . .	56

## List of Figures

---

5.1	Solutions for adding hovering capabilities . . . . .	61
5.2	Mechanical design of the DALER v11 . . . . .	62
5.3	Morphology configurations of the DALER v11 . . . . .	63
5.4	Wings' actuation mechanism . . . . .	64
5.5	Mechanical design of the left rib B and its walkeron . . . . .	65
5.6	DALER v11 prototype . . . . .	66
5.7	Morphology configurations of the DALER v11 prototype . . . . .	67
5.8	Modes of locomotion of the DALER v11 prototype . . . . .	67
5.9	Schematic of the electronics of the DALER v11 . . . . .	68
5.10	Ground locomotion capabilities of the DALER v11 . . . . .	69
5.11	Hover capabilities of the DALER v11 . . . . .	70
5.12	Attitude log during a hover flight . . . . .	71
5.13	Mass distribution by modes of locomotion of the components . . . . .	72
5.14	Mass distribution analyses . . . . .	74
5.15	Versatility versus complexity of multi-modal robots . . . . .	77
5.16	Versatility versus autonomy of DALER prototypes . . . . .	78
6.1	Model of the deployable wings. . . . .	82
6.2	Prototypes used to compare flight performance . . . . .	83
6.3	Experimental prototype used to test the hover controller and transitions . . . . .	84
6.4	Mass-and-power model diagram . . . . .	85
A.1	DALER v1. . . . .	88
A.2	DALER v2. . . . .	89
A.3	DALER v3. . . . .	90
A.4	DALER v4. . . . .	91
A.5	DALER v5. . . . .	92
A.6	DALER v6. . . . .	93
A.7	DALER v7. . . . .	94
A.8	DALER v8. . . . .	95
A.9	DALER v9. . . . .	96
A.10	DALER v10. . . . .	97
A.11	DALER v11. . . . .	98

# List of Tables

2.1	Functional decomposition . . . . .	12
2.2	Morphological matrix . . . . .	13
2.3	List of criteria for all the sub-functions . . . . .	14
2.4	Solution selection for providing lift . . . . .	15
2.5	Solution selection for providing thrust . . . . .	16
2.6	Solution selection for controlling the orientation . . . . .	16
2.7	Solution selection for moving on the ground . . . . .	17
2.8	Best solutions . . . . .	17
3.1	Friction coefficients for different types of ground . . . . .	28
3.2	Summary of performance of the DALER v6 . . . . .	30
3.3	Working points and power requirements for walkerons . . . . .	38
3.4	Working points and power requirements for optimized walkerons . . . . .	40
3.5	Summary of performance of the DALER v9 . . . . .	41
3.6	Mass distribution and integration analyses of the DALER v6 and v9 . . . . .	43
4.1	Summary of performance of the DALER v9 Adaptive . . . . .	57
4.2	Mass distribution and integration analyses of the DALER v9 and v9 Adaptive . . . . .	58
5.1	Summary of performance of the DALER v11 . . . . .	70
5.2	Mass distribution and integration analyses of the DALER v9 Adaptive and v11 . . . . .	73
5.3	Versatility analysis . . . . .	76
5.4	Complexity analysis . . . . .	77
6.1	Transition capabilities of a DALER prototype . . . . .	83
B.1	Weights calculation based on pairwise comparison for providing lift . . . . .	99
B.2	Weights calculation based on pairwise comparison for providing thrust . . . . .	100
B.3	Weights calculation based on pairwise comparison for controlling orientation . . . . .	100
B.4	Weights calculation based on pairwise comparison for moving on the ground . . . . .	101





# 1 Introduction

Autonomous robots have a great potential for replacing humans in high risk missions, however current robots are limited by their locomotion capabilities in complex unstructured environments. In this introductory chapter, the main locomotion limitations of mobile robots are discussed, multi-modal locomotion is described as a possible solution to increase versatility. The state of the art of multi-modal robots is presented and solutions to improve their design are proposed, such as using an integrated design approach and adaptive morphology. Finally, the main contributions of this thesis are described and followed by an outline of the work accomplished.



### 1.1 Motivation

In this section, the motivations for using mobile robots in dangerous environments are introduced. The main limitation of the state of the art of mobile robots is discussed; using a single mode of locomotion limits their flexibility and adaptability to different terrains. Multi-modal locomotion is described as being a solution to increase the versatility of mobile robots. The state of the art of multi-modal robots is presented; most existing solutions are based on an additive strategy (i.e. additional actuators and structures are added for each new mode of locomotion), or on a semi-additive strategy (i.e. only passive structures are added for the new mode of locomotion, no additional actuators are added). The concept of integrated design (i. e. a single locomotor system is used for multiple modes of locomotion) is proposed as a solution to achieve efficiently multi-modal locomotion. Finally, adaptive morphology is presented as a solution to improve integrated designs where two modes of locomotion would require different placement of the center of mass relatively to the locomotor system. The state of the art of mobile robots using adaptive morphology is described at the end of this section.

#### 1.1.1 Autonomous Robots Limitations

There is a growing interest in the use of autonomous robots for applications such as exploration, search-and-rescue or monitoring of the environment. These robots have to deal with very complex terrains, such as semi-collapsed buildings, deep caverns, or forests with a lot of vegetation. Autonomous robots are appealing for these tasks due to their ability to explore areas that are risky and inaccessible to humans [1, 2, 3, 4, 5]. For example robots could be used to fly over a village, enter inside houses and search for victims trapped in partially collapsed buildings after an earthquake. In such a scenario, the robots must be able to move indoor and outdoor, to pass over large obstacles, and to move in narrow spaces.

However, existing platforms have limited locomotion abilities. Most existing mobile robots exploit only a single locomotion strategy, such as rolling, walking, flying, hovering, climbing, swimming, crawling, or jumping. Operating in unstructured environments is very challenging for mobile robots since the topology of the terrain could be subject to significant variations. State of the art search-and-rescue robots are designed to perform specific tasks in particular terrains; as soon as the terrain is slightly different from what they were designed for, these robots can hardly move and become inadequate. Using only a single locomotion strategy limits their flexibility and adaptability to different environments. Obstacles of the same size or larger than a robot represent a significant challenge for ground locomotion based robots [3]. In confined indoor environments, flying is very challenging, thus a common characteristic of indoor flying robots is their capability to hover or to fly very slowly [6, 7, 8, 9, 10], as opposed to outdoor flying robots, which have to fly fast in order to cover long distances and resist to wind. Flying requires to gain speed and hovering with a prop-hanging system is very power consuming [11, 12]. For these reasons, a robot capable of forward flight, hover and ground locomotion represents an interesting research direction to navigate in complex environments.

### 1.1.2 Multi-Modal Locomotion

Our approach to improve the versatility of current mobile robots is to use a *Multi-Modal Locomotion Strategy*; if a given mode of locomotion is no longer profitable due to a change of environmental conditions, then another mode of locomotion that is more adequate in this new environment should be used. The combination of forward flight and ground locomotion brings dual advantages of travelling quickly over long distances and thoroughly exploring a specific region of interest on the ground. In a search-and-rescue scenario, forward flight can be used for covering long distances, ground locomotion can be used for local exploration and finding potential victims and finally, hover locomotion can be used to switch between forward flight and ground locomotion, and also to transition from outdoor to indoor and to fly in cluttered environments.

Multi-modal locomotion is a feature that increases the environmental adaptability, the locomotion versatility, and the operational flexibility of mobile robots [13]. Although multi-modal locomotion has a potentially high impact in robotics and has recently attracted much attention [5, 14], robots that successfully demonstrate competences in diverse environments are still at an early stage. Current prototypes show that the implementation of any additional locomotion mode can potentially lead to performance losses (i.e. manoeuvrability, speed, energetic efficiency) [15, 16, 17, 18, 19]. This effect is mainly caused by the weight added to the platform and the increased complexity of the robot, which in turn reduces the operating capabilities of each mode of locomotion and thus the overall mobility of the robot. For flying robots this disadvantage is even more significant, since increasing the weight could lead to the inability to take-off. Indeed, similarly to animals [14, 20, 21, 22], multi-modal robots are subject to various trade-off due to conflicting requirements imposed by locomotion on different surfaces or fluids. Therefore, the main challenge to successfully implement multi-modal locomotion is to identify design strategies that maximize performance in diverse environments.

For the design of a multi-modal robot, two different design approaches exist, the first one being the additive design described above. For each new mode of locomotion, a new locomotor apparatus is added (i.e. more actuators and an additional structure are added), this approach increases the weight and the complexity of the robot, leading to a potential loss of performance of the two modes of locomotion. The second design approach is the integrated design approach, the same actuators and structure are used for different modes of locomotion. This strategy allows a minimization of the weight and complexity of the robot. An integrated strategy is potentially advantageous because it limits the number of mechanisms, actuators and sensors. However, the integrated strategy is more challenging than the additive strategy because a single locomotor system must accommodate potentially conflicting dynamics of multiple modes of locomotion.

### Robots based on an Additive Design Approach

To the best of the author's knowledge, there is no robot capable of effective forward flight, hover, and ground locomotion. Current implementations of aerial and terrestrial robots are mainly based on an additive strategy, where secondary locomotion modes are obtained by using additional actuators and mechanisms [15, 19] (see Fig. 1.1) or dedicated appendices, such as legs [17], spherical cage [23], wheels [24], cylindrical cage [25], or large ring [26] (see Fig. 1.2) that are not used during flight. These additions have an impact on the weight and drag during flight, decreasing aerial efficiency and manoeuvrability. Furthermore, most of these robots have a morphology highly optimised for a primary locomotion mode, and are therefore less effective in the secondary one.

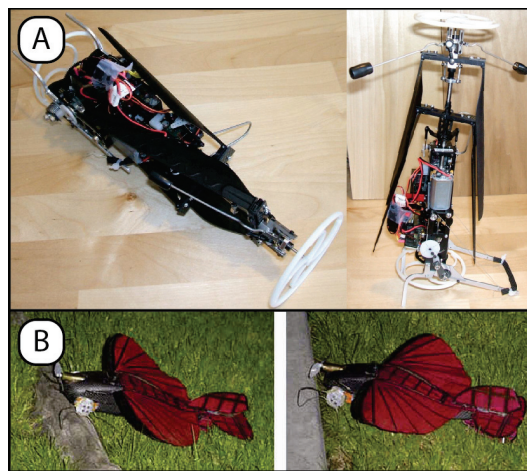


Figure 1.1: Multi-modal robots based on a fully additive strategy. A) Land/Air Miniature Robot in ground and flight configurations [15]. B) Micro Air-Land Vehicle, with wings for flight and wheel-legs (i.e. wheel-legs) for terrestrial locomotion [19].

A small ground robot [15] (see Fig. 1.1.A), which has the ability to fly, utilizes a minimalistic wheeled ground mode to minimize weight, and a rotary-wing flight mode, enabling transformations at will. This design is ideal for hovering in an indoor environment and rolling on a flat ground, but it is not yet capable of rolling in rough terrains or flying outdoors. A biologically inspired Micro Air-Land Vehicle called *MALV* [19] (see Fig. 1.1.B) flies using a chord-wise, under-cambered, bat-like compliant wing and walks over rough terrains using passively compliant wheel-leg running gears. *MALV* performs transitions from flight to walking but most of the time cannot get back to the air, since it can only take-off from the roof of a building of at least 6 meters high.

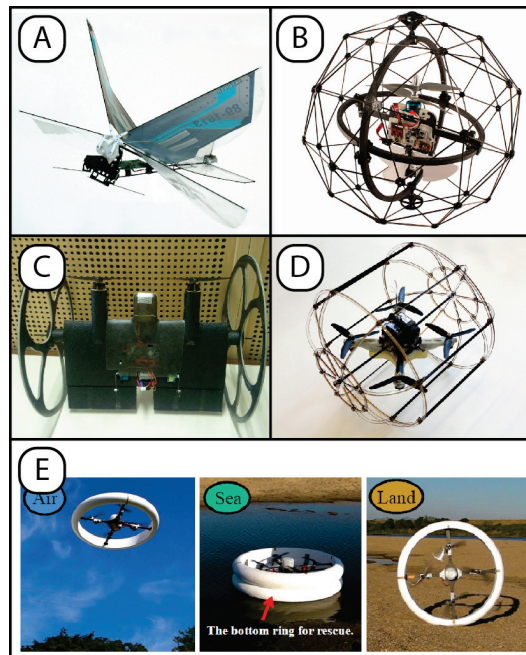


Figure 1.2: Multi-modal robots based on a semi-additive strategy. A) Bipedal Ornithopter for Locomotion Transitioning, with flapping wings for flight and rotary legs for walking [17]. B) GimBall flying robot, with freely rotating protective cage for ground locomotion and coaxial propellers for flight [23]. C) MAVion Roll & Fly, a bi-rotor hovering platform with passive wheels for rolling on the ground [24]. D) Hybrid Terrestrial and Aerial Quadrotor with a passively rotating cage for ground locomotion [25]. E) Multi-field Universal Wheel for Air-land (MUWA) vehicle, with quadrotor with variable-pitch propellers for flight and a large ring for ground and water locomotion [26]

### Robots based on a Semi-additive Design Approach

*BOLT* [17] (see Fig. 1.2.A) is a lightweight bipedal ornithopter capable of high-speed dynamic running and effecting transitions between aerial and terrestrial locomotion modes. This robot, due to its small size, can only run on an obstacle free ground and is not capable to fly outdoors. *GimBall* (see Fig. 1.2.B) is a flying robot that is resistant to collisions with its environment, it has a freely rotating protective cage which has three degrees of freedom allowing to decouple the torques applied on the cage from the inner frame. GimBall can use its protective cage to move on the ground, however while moving on the ground it happens that two rings of the gimbal system get in the same plane provoking a gimbal lock and thus the loss of control of the platform. Furthermore, this gimbal system and protective cage add weight and drag to the platform and thus reduce the flight time. *MAVion Roll and Fly* [24] (see Fig. 1.2.C) is a Vertical Take-Off and Landing (VTOL) aircraft, it has carbon fibre wheels to roll along grounds, walls and ceilings. The ground capabilities of this robot are limited since the wheels are only passive and its hovering skills are disrupted by its wings creating a lot of drag when moving

## Chapter 1. Introduction

---

through the air. *HyTAQ* [25] (see Fig. 1.2.D) is a Hybrid Terrestrial and Aerial Quadrotor which can hover and has a cylindrical protective cage that can freely rotate around its axial axis. This protective cage acts as a wheel on the ground and provides support to the quadrotor, thus reducing the energy needed to travel a given distance. Adding a freely rotating cage around a hovering platform such as *HyTAQ* or *GimBall* is a simple solution to add ground locomotion and to reduce the cost of transport, however the weight that is added for the cage could be replaced by a bigger battery. *MUWA* [26] (see Fig. 1.2.E) is a Multi-field Universal Wheel for Air-land (MUWA) vehicle. It is a quadrotor with variable-pitch propellers with a large ring for ground and water locomotion. It can stand on the ground at a given tilt angle, roll on the ground like a wheel, and float/move on the water. The combination of four propellers with variable pitch and a large ring enables three modes of locomotion with a relatively simple design, however, as for the other robots, this ring adds weight and drag and thus reduces flight performances.

### Robots Capable of Flying & Hovering

In 2008, Thipyopas *et al.* [27] presented a comparative aero-dynamical study of tilt-rotor, tilt-wing and tilt-body for multi tasks Micro Air Vehicle (MAV). In a tilt-rotor configuration, also known as thrust vectoring, only the rotors rotate to adjust the direction of the thrust vector, the thrust can be either aligned with the wing for forward flight or perpendicular to the wing for vertical take-off and landing. The tilt-wing configuration is similar except that this time it is the wing that rotates with respect to the fuselage. The rotors are mounted on the wing and thus move with it. In the tilt-body configuration, the fuselage, the wing and the rotors rotate together to transition from hover to forward flight. Very often, landing gears are used to upright the platform on the ground in order to put the fuselage in a vertical take-off ready position. Analytical study and wind tunnel tests presented in [27] have been done to compare different configurations by using the same power system. The results of this study showed that the tilt-wing and the tilt-rotor configurations have no advantage over the tilt-body configuration. Tilt-rotor configuration has poor aero-dynamical performances and consumes more power than the two other configurations. Tilt-wing configuration leads to many drawbacks, both in the design and in the practical aspect. The results concluded that tilt-body concept seems to be most efficient for VTOL MAV applications.

The MAVion was used to perform wind tunnel testing in order to characterize longitudinal flight behaviour during a transition between vertical and horizontal flight modes. The *Quadshot*, a commercial product sold by *Transition-robotics*, is another tilt-body aircraft, it can both fly horizontally like a flying wing and hover like a quadrotor. The MAVion and the *Quadshot* cannot fly in cluttered indoor environments because of their large size and the *Quadshot* cannot move on the ground. Even if these robots are capable of transitioning between hover and forward flight, their designs are not ideal for both. However, both these designs are good sources of inspiration for the control of the transition phase between hover and forward flight.

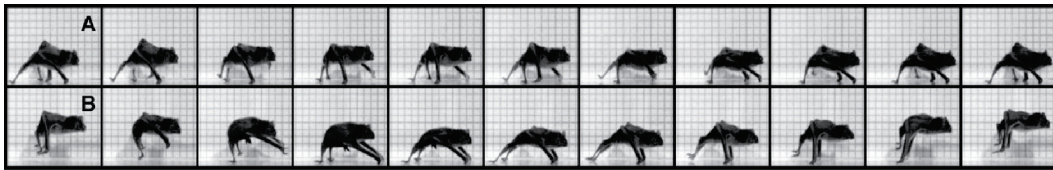


Figure 1.3: Common vampire bat, *Desmodus rotundus*, running on the ground. A) Walking at 0.12 m/s and B) bounding at 0.6 m/s.

### 1.1.3 Integrated Design Approach

Many animals perform multi-modal locomotion by using an integrated strategy; this means that a single locomotor apparatus, composed of actuators (i.e. set of muscles for animals or motors for robots) and appendices (i.e. limbs for animals or mechanical structures for robots), is used for multiple modes of locomotion. For example, seabirds of the *Alcidae* family exploit wing propulsion for both flight and swimming [28]. Among all the animals with mixed aerial and terrestrial locomotion capabilities, the common vampire bat *Desmodus rotundus* is a relevant case study. In general, bat's muscles and morphology are highly adapted for flapping flight [29] and, compared to other mammals, bats move awkwardly on the ground. *D. rotundus* is a notable exception because, most probably due to its blood-based diet [21], it evolved remarkable terrestrial capabilities such as running [30] and jumping [31]. According to the literature, these terrestrial competences do not appear to negatively affect its flight ability, although further biological data would be necessary to validate this hypothesis [32]. *D. rotundus* has evolved an integrated strategy to multi-modal locomotion; a single locomotor apparatus, the pectoral muscles and the wings, are used to locomote in the air and on the ground (see Fig. 1.3). In order to implement efficiently the integrated design approach, it will be demonstrated in Chapter 3 that the two different modes of locomotion must be dynamically compatible, which means that they must require compatible speeds and torques. Morphology optimization will be introduced as a way to make two modes of locomotion dynamically compatible.

#### Robots based on an Integrated Design Approach

A biologically inspired miniature integrated jumping and gliding robot, MultiMo-Bat [33], is capable of jumping heights of more than 6 meters with a total weight of less than 100 grams (see Fig. 1.4). The robot is composed of two four-bar mechanisms that provide the structure for both jumping and gliding. This robot uses an integrated design approach for multi-modal locomotion, since the legs used for the jump can deploy to become the structure of the wings. Robots presented in Fig. 1.2 are examples of semi-integrated (or semi-additive) designs since no additional actuators are added for the second mode of locomotion, however they all have additional structures which are used only for one mode of locomotion. These structures add weight to the platform and thus reduces the performance of the primary mode of locomotion.

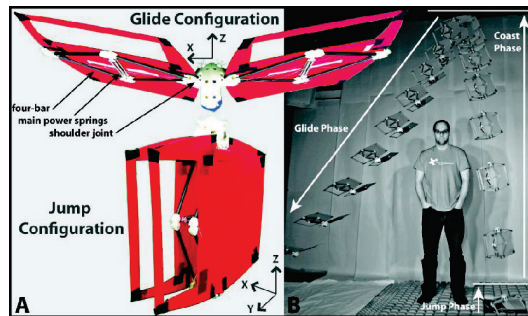


Figure 1.4: Multi-modal robot based on an integrated strategy. The MultiMo-Bat robot uses legs for jumping which then can deploy to become the structure of the wings [33].

### 1.1.4 Adaptive Morphology

Animals such as flying snakes, seabirds and some salamanders adapt their morphology to the desired locomotion mode in order to enhance performance. Flying snakes, for example, flatten their body in order to increase lift and to travel longer distances during gliding [34, 35]. Before diving into the sea, alcids partially fold their wings into a shape better suited to swimming. Johansson et al. [36] suggested that the partly folded wings of the alcids may act as efficient aft-swept wingtips, reducing the induced drag and increasing the lift-to-drag ratio. The salamander is another example of animal that uses adaptive morphology. Salamanders retract their legs along their body when they transition from walking to swimming [37]. Some other species of salamanders are also capable of rolling. Their body, originally shaped for walking, can take the shape of a large wheel to rapidly roll downhill [38]. The *D. rotundus* remarkably combines the integrated strategy discussed above with adaptive morphology, by adapting the morphology of its wings during the transition from flight to terrestrial locomotion. This explains the small trade-offs in the multi-modal capabilities of this animal and is our principal source of inspiration for the design of robots capable of flying and walking. It will be demonstrated in Chapter 4 that, by using an adaptive morphology strategy to transition between the different modes of locomotion, the efficiency of locomotion can be improved.

#### Robots with an Adaptive Morphology

Robots capable of adaptive morphology can self-adjust the shape of their structure in order to switch between one mode of locomotion to another, Fig. 1.5 shows two examples of multi-modal robots that use adaptive morphology. A palm sized jumping robot [39] (see Fig. 1.5.A), designed by Kovac *et al.*, is able to open its wings, recover in mid-air and glide. A string is attached to the wing tip and is rolled on a spool to fold the wings. An unlocking mechanism disconnects the spool from its gear box, and the springs in the joints of the wings provide the unfolding energy. The robot can jump higher when the wings are folded than when they are open. MALV closes its wings during ground locomotion in order to reduce its wingspan and then can go through narrower openings (see Fig 1.5.B).



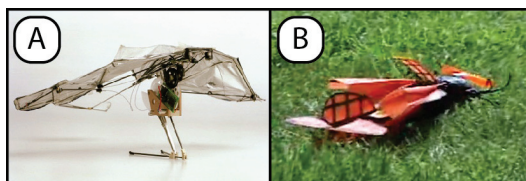


Figure 1.5: Multi-modal robots with adaptive morphology. A) Jumping, gliding robot with deployable wings [39]. B) A version of MALV with foldable wings [19].

Other examples of adaptive morphology can be found in the state of the art of morphing wings [40, 41]. These examples do not use adaptive morphology for multi-modal locomotion but to adapt the shape of the wings for different flight conditions. For example swifts can transition from efficient steady flight to aggressive manoeuvres or precision descents by adjusting the swept angle of their wings [42]. Grant *et al.* [43], inspired by seagulls, designed a vehicle that adopts a series of joints and structures to alter the dihedral and swept angles of the wings in order to expand MAV's mission capabilities. Ifju *et al.* [44] successfully developed a series of MAVs with flexible wings that can passively change the angle of attack along the wing to reduce inherently sensitivity to disturbances.

## 1.2 Main Contributions and Thesis Organization

The main novelty of this thesis is to combine the integrated design approach with the concepts of adaptive morphology and morphology optimization in a multi-modal robot<sup>1</sup>. In a robot designed according to the integrated approach, morphology optimization can be used to make two modes of locomotion dynamically compatible while adaptive morphology can improve the efficiency of the robot. In addition, the design of a multi-modal flying, hovering and walking robot brings together many different topics, such as mechanical design, electronics, control theory and aerodynamics.

This thesis is organized around the main topics that it addresses; platform configuration, integrated design approach, adaptive morphology and multi-modal locomotion. Figure 1.6 gives an overview of the locomotion capabilities of the prototypes presented in the next chapters and provides the design approaches studied with each of these robots.

---

<sup>1</sup>This robot is called *DALER*, which is an acronym for *Deployable Air Land Exploration Robot*.

## Chapter 1. Introduction

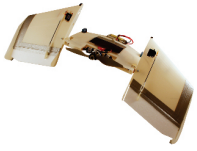

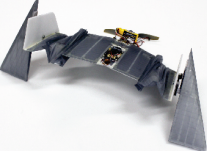

				
<b>Version</b>	DALER v6	DALER v9	DALER v9 adaptive	DALER v11
<b>Chapter</b>	Chapter 3		Chapter 4	Chapter 5
<b>Locomotion modes</b>	Ground locomotion	X	X	X
	Forward flight	X	X	X
	Hover			X
<b>Design approach</b>	Integrated structure	X	X	X
	Integrated actuation		X	X
	Adaptive morphology			X

Figure 1.6: Thesis outline. Four main prototypes presented in this thesis, used to study the concepts of integrated design approach and adaptive morphology for multi-modal locomotion.

- Chapter 2 presents the selection of the configuration of the platform. A functional analysis is done, many solutions are evaluated and a possible design of the robot is selected and introduced.
- Chapter 3 presents two designs of multi-modal robots based the integrated design approach (see DALER v6<sup>2</sup> and v9 in Fig. 1.6). The first prototype, the v6, uses the same structure for flying and walking on the ground but with different actuators. The second prototype, the v9, adopts a fully integrated design approach, by using the same structure and actuators to control the flight and to walk on the ground. The results obtained with both prototypes are analysed and compared in order to study the benefits of the integrated design approach.
- Chapter 4 presents the concept of adaptive morphology. The design of a flying and walking robot which has deployable wings is introduced and its performance in the different modes of locomotion are characterized (see DALER v9 adaptive in Fig. 1.6).
- Chapter 5 presents a robot which is capable to walk on the ground, up-righting itself, hover and fly forward (see DALER v11 in Fig. 1.6). This prototype adopts an integrated design approach, has an adaptive morphology and its number of actuators is limited in order to minimize its complexity and weight.

<sup>2</sup>All the versions of the DALER prototypes are presented in Appendix A, numbered v1 to v11

## 2 Platform Configuration Selection

This chapter presents the selection of the type of platform configuration for a robot capable of three modes of locomotion; forward flight, hover and ground locomotion. First a functional analysis of the robot is done; this consists in listing all the functions that the robot must fulfil. Then, multiple solutions for each function will be defined and analysed according to specific criteria, different combinations of solutions will be evaluated and one final set of solutions will be selected for implementation.



### 2.1 Functional Analysis

This section presents the functional analysis of the robot. In order to travel quickly over long distances the robot should be capable to fly forward and for a thorough exploration of a small area the robot should be capable to move on the ground. Finally, for transitioning between ground locomotion and forward flight the robot should be capable to take-off and land vertically and to hover. Furthermore, hover locomotion can also be used to enter inside houses and to fly in cluttered environments. From these requirements, two main functions can be identified; *move in the air* and *move on the ground*. The first function can be further decomposed in three sub-functions; *provide lift*, *provide thrust* and *control orientation*. These three functions combined allow the robot to fly forward and to hover, Table 2.1 summarizes this functional decomposition. The possible solutions for each of these functions are described in the next section.

Functions	Sub-functions
Move in the air	Provide lift Provide thrust Control orientation
Move on the ground	

Table 2.1: Functional decomposition.

### 2.2 Possible Solutions

In this section possible solutions for each function are presented and are listed in Table 2.2. For providing thrust, solutions based on propellers actuated by electrical brushless motors are considered; it is the most used solution for RC airplanes and is the cheapest and most available solution. Therefore, this analysis is based on the number of propellers needed and on their placement on the platform. For controlling the orientation, only solutions compatible with the use of propellers are considered. For moving on the ground, in order to minimize the final weight of the platform, no additional structure should be added. The possible types of displacement on the ground are divided in three main categories; frontal rolling, tumbling and side rolling.

## 2.2. Possible Solutions

<b>Provide lift</b>	
Rigid wing	Rigid wings are used on standard airplanes, here only a basic flying wing without a fuselage and a tail is considered.
Inflatable wing	Inflatable wings are usually used for paragliders or kites.
Balloon	Balloons lighter than air provide lift.
<b>Provide thrust</b>	
Single rotor	A single rotor could be, for example, placed at the front or at the back of the platform.
Bi-rotor	A bi-rotor configuration is a common solution for airplanes. For example, one propeller can be placed on each side of the platform.
Coaxial rotors	Coaxial rotors, similarly to a single rotor, can be placed at the front or at the back of the platform.
Multi-rotor	Multiple rotors can be used to provide thrust, for example, they can be placed in a quadrotor-like configuration.
<b>Control orientation</b>	
Flaps	Flaps provide a force that applies a torque on the platform which is then used to control the orientation. The main requirement for these flaps is to be under a flow of air. Thus, when the platform is hovering the flaps must be under the airflow produced by the propeller(s).
Rotating wings	Instead of moving the trailing edge of the wing (i.e. flaps configuration) a portion of the wing can rotate along the wing length axis to change the lift force and thus control the platform orientation.
Differential speed	If the bi-rotor or the multi-rotor solution are selected for the previous function then this solution could be used. By changing the speed of the propellers, their thrust force is modified and therefore this variation of force can be used to control the platform.
Thrust vectoring	Thrust vectoring can also be used to control the orientation of the robot. It consists in changing the orientation of a propeller in order to control the orientation of its thrust force.
<b>Move on the ground</b>	
Frontal rolling	The main body stays horizontal and actuators on the sides are used to move forward.
Tumbling	Actuators on the sides are used to help the main body to perform flips.
Side rolling	Actuators are used to make the main body roll sideways.

Table 2.2: Morphological matrix, listing multiple solutions for each sub-function.

## Chapter 2. Platform Configuration Selection

---

<b>Provide lift</b>	
Robustness	Robustness is important especially to tolerate harsh landings and to not get damaged during ground locomotion.
Weight	The total weight of the robot should be kept low in order to minimize the kinetic energy and avoid injuring people in case of crashes.
Wind resistance	The robot should fly faster than the wind to avoid drifting. An indicative range for the wind speed is 15 km/h (i.e. a gentle breeze).
Complexity	The robot should be as simple as possible to manufacture, in order to minimize production time and cost.
Safety	The robot should be as safe as possible for humans.
Reuseability	
<b>Provide thrust</b>	
Force/weight	The thrust force should be high compared to the weight of the solution.
Robustness	The solution should be robust to landings.
Efficiency	The solution should not consume too much power. An indicative range for the minimum travelled distance is 10 km.
Complexity	The solution should be as simple as possible in order to minimize cost and risks of failure.
Safety	An operator should be able to launch the robot without risk of injury.
Reuseability	
<b>Control orientation</b>	
Power/weight	The torque produced to control the orientation should be high compared to the inertia of the robot and the platform should be able to perform fast manoeuvres such as transitioning between hover and forward flight thus the solution should be fast. High torque at high speed is therefore a high power requirement for a minimal weight of the solution.
Robustness	The solution should be robust to landings.
Complexity	The solution should be as simple as possible.
Reuseability	
<b>Move on the ground</b>	
Weight	The weight added for ground locomotion should be minimized.
Robustness	The solution should no break during ground locomotion and landings.
Complexity	The complexity of the solution should be minimized.
Speed	The speed of the robot on the ground should be sufficient in order to do local exploration of a small area. An indicative range for the speed is 0.5 km/h.
Efficiency	The ground locomotion should be efficient. An indicative range for the power consumption is 20% of the hovering power.
Manoeuvrability	The robot must be capable to move in any directions on the ground and also be capable to move in rough terrains; it should overcome obstacles of its height.
Reuseability	

Table 2.3: List of criteria for all the sub-functions.

## 2.3 Evaluation of Solutions

The first step of the evaluation process is to grade the solutions given in Table 2.2 based on different criteria. The main criterion for all the functions, according to the integrated design approach, is the reuseability of actuators and structure for multiple modes of locomotion. Therefore, this criterion is present for each function, otherwise Table 2.3 gives the criteria for all the sub-functions. A weight for each criterion can be assigned in order to represent its importance. The method of pairwise comparison is used to assign these weights. The weights are normalized in such a way that the mean of the weights for each function is 1. Thus, the differences between the grade and the weighted grade for each solution can be analysed. The details of the pairwise comparisons are presented in Appendix B. A grade between 1 (very bad) and 3 (very good) is given to each solution for each criterion. Then, each grade is multiplied by the weight of its criterion and the sum of the weighted grades is calculated for each solution.

For providing lift, Table 2.4 gives the evaluation of the solutions. The best solution according to this evaluation is the use of a rigid wing (16.60), which is the most used solution for similar applications. This solution is very robust to landings, gives a high lift force for its weight, is resistant to wind, has a very low complexity, is very simple to manufacture, and is also safe for humans. The two other possible solutions; inflatable wings (11.20) and balloons (11.20), are less effective and therefore will not be considered in the final selection. Moreover, the structure of the rigid wing could be used not only for providing lift but also as a support for the other modes of locomotion (i.e. hover and ground locomotion). Wings that inflate with airflow (e.g. kites or paragliders) would collapse during hovering and a balloon would not be ideal for ground locomotion in unstructured terrains.

Provide lift							
Criteria	Weight	Rigid wing		Inflatable wing		Balloon	
Robustness	1.20	3	3.60	2	2.40	2	2.40
Weight	1.20	2	2.40	3	3.60	3	3.60
Wind resistance	0.20	3	0.60	2	0.40	1	0.20
Complexity	1.20	3	3.60	2	2.40	2	2.40
Safety	0.20	2	0.40	2	0.40	3	0.60
Reuseability	2.00	3	6.00	1	2.00	1	2.00
Total		16	16.60	12	11.20	12	11.20

Table 2.4: Solution selection for providing lift.

## Chapter 2. Platform Configuration Selection

For providing thrust, Table 2.5 gives the evaluation of the solutions. The solution with the bi-rotor configuration obtains the best grade (13.80), it performs a little bit better in almost all the criteria than the other solutions. The three other solutions; coaxial-rotors (11.60), single rotor (11.40) and multi-rotor (11.20), are very close behind and thus will also be considered in the final selection process.

Provide thrust									
Criteria	Weight	Single rotor		Bi-rotor		Coaxial rotors		Multi-rotor	
Force/weight	1.20	2	2.40	2	2.40	3	3.60	2	2.40
Robustness	0.40	2	0.80	3	1.20	2	0.80	1	0.40
Efficiency	1.00	2	2.00	2	2.00	3	3.00	2	2.00
Complexity	1.00	3	3.00	3	3.00	1	1.00	2	2.00
Safety	0.40	3	1.20	3	1.20	3	1.20	1	0.40
Reuseability	2.00	1	2.00	2	4.00	1	2.00	2	4.00
Total		13	11.40	15	13.80	13	11.60	10	11.20

Table 2.5: Solution selection for providing thrust.

For controlling the orientation, Table 2.6 gives the evaluation of the solutions. The solution with the best grade is the rotating wings solution (11.33), this is mainly due to its high score for the reuseability criterion; rotating wings can be easily used as wheels to enable the ground locomotion. Flaps could also be used to move on the ground but would be much less efficient since they do not rotate continuously. The solution with differential speed can also be used to move on the ground if propellers are used as wheels. The solutions of differential speed (8.33) and flaps (6.67) are below the solution of rotating wings but still perform well and will thus be kept for the final analysis. Finally, the solution of thrust vectoring obtains a very bad grade (4.33) and is thus abandoned.

Control orientation									
Criteria	Weight	Flaps		Rotating wings		Dif. speed		Thrust vectoring	
Power/weight	1.33	2	2.67	3	4.00	2	2.67	1	1.33
Robustness	0.33	3	1.00	2	0.67	2	0.67	2	0.67
Complexity	0.33	3	1.00	2	0.67	3	1.00	1	0.33
Reuseability	2.00	1	2.00	3	6.00	2	4.00	1	2.00
Total		9	6.67	10	11.33	9	8.33	5	4.33

Table 2.6: Solution selection for controlling the orientation.



Finally, for moving on the ground, Table 2.7 gives the evaluation of the solutions. The solution with the best grade is the frontal rolling solution (18.17) which performs a little bit better in almost all the criteria than the tumbling solution (14.00) and the solution of side rolling obtains the lowest grade (11.00). Frontal rolling is simple to control, can potentially go at high speeds, and is probably more manoeuvrable than the other configurations.

Move on the ground							
Criteria	Weight	Frontal rolling		Tumbling		Side rolling	
Weight	1.50	3	4.50	2	3.00	2	3.00
Robustness	0.33	3	1.00	2	0.67	2	0.67
Complexity	1.33	3	4.00	2	2.67	2	2.67
Speed	0.50	2	1.00	2	1.00	2	1.00
Efficiency	0.33	2	0.67	2	0.67	2	0.67
Manoeuvrability	1.00	3	3.00	2	2.00	1	1.00
Reuseability	2.00	2	4.00	2	4.00	1	2.00
Total		18	18.17	14	14.00	12	11.00

Table 2.7: Solution selection for moving on the ground.

## 2.4 Solutions Selection

From the previous section the solutions that are kept for the final selection process are summarized in Table 2.8. The best solution for each sub-function is highlighted in bold characters. In this section, possible designs which combine these solutions are proposed.

Two functions have only one solution left and are thus directly selected; rigid wings will be used during forward flight for providing lift, thus this wing will be the main structure of the robot, and the frontal rolling strategy will be used for ground locomotion. The goal now is to see which solutions for the two other functions are the most compatible with the two selected solutions and between themselves.

Functions	Sub-functions	Solutions	
Move in the air	Provide lift	<b>Rigid wing</b>	
	Provide thrust	<b>Bi-rotor</b>	Coaxial rotors
		Single rotor	Multi-rotor
	Control orientation	<b>Rotating wings</b>	Differential speed
Move on the ground		Flaps	
		<b>Frontal rolling</b>	

Table 2.8: Best solutions given by the evaluation process, ranked by their score.

## Chapter 2. Platform Configuration Selection

---

The use of coaxial-rotors or of a single rotor would require having the propellers in the centre of the platform with flaps in their airflow. Therefore, these solutions are not compatible with the frontal rolling solution where actuators should be placed on each side of the platform to enable the ground locomotion. Two possible designs are left, either propellers can be used for the ground locomotion or control surfaces:

- A possible solution to move on the ground would be to use the propellers as wheels. The differential speed method could be combined with a multi-rotor configuration. This combination could lead to a quadrotor configuration for hovering with a rigid wing for forward flight and the use of the propellers for ground locomotion.
- Another possible solution is to use rotating wings both to move on the ground and to control the orientation of the platform. This solution requires to have one rotating wing on each side of the platform under an airflow. Thus, the most compatible solution for providing thrust is to use the bi-rotor configuration. This combination would lead to a rigid wing for forward flight with one rotating wing on each side of the platform and one propeller above each of these rotating wings.

The first solution would require a mechanism that would change the orientation of the propellers in order to switch between a hovering configuration (i.e. propellers axis at the vertical) and a ground locomotion configuration (i.e. propellers axis at the horizontal). Furthermore, the two modes of locomotion would require very different dynamics, hovering would require very high rotational speed of the propellers with low torque while ground locomotion would require very high torque at low speed. Therefore, the use of a gearbox would be necessary on each motor.

The second solution do not have these drawbacks and combines all the best solutions given in Table 2.8. This solution will be retained and detailed in the next section.

## 2.5 Implementation of the Selected Solution

The implementation of the set of solutions selected by the above analysis is presented in this section. Figure 2.1 shows the robot in the three modes of locomotion. The robot is a flying wing which has a delta shape and a self-stabilizing airfoil which provide stability during forward flight (see Fig. 2.1.A). During ground locomotion the wingspan of the robot could be reduced in order to go through small openings and the robot uses rotating wings for walking (see Fig. 2.1.B). Finally, during hover locomotion (see Fig. 2.1.C) the propellers placed on each side of the wing provide airflow on the rotating wings and the wingspan is also reduced compared to the forward flight configuration (e.g. for going through a window). The rotating wings which are used both for “walking” and as “elevons” to control the flight will be called “walkerons”.

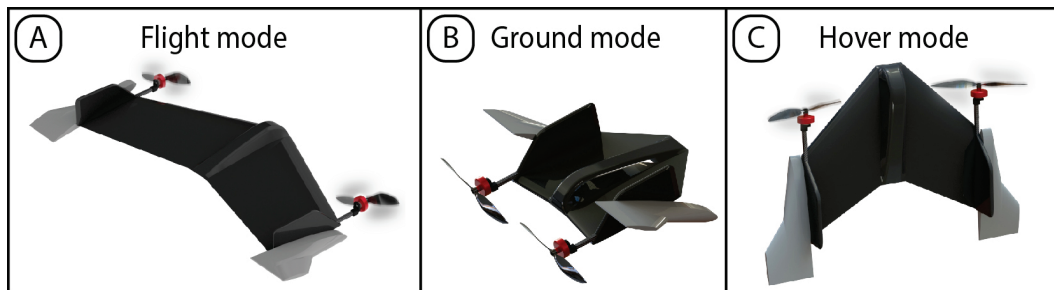


Figure 2.1: Different modes of locomotion of the DALER: A) forward flight, B) ground locomotion and C) hover.

Figure 2.2 shows the definitions of the roll, pitch and yaw axis of the robot. The two propellers placed on each side of the platform provide thrust in order to gain speed during forward flight and to counteract gravity during hover. By changing the differential speed of these propellers the yaw axis can be controlled. These propellers also provide airflow to the walkerons, this allows to create a force by tilting these walkerons and thus to create torques used to control the platform. By moving the walkerons in the same direction the pitch angle can be controlled and by moving them in opposite direction the roll angle can be controlled. Roll, pitch, and yaw can be controlled at all time during hover, forward flight and transitions between the two.

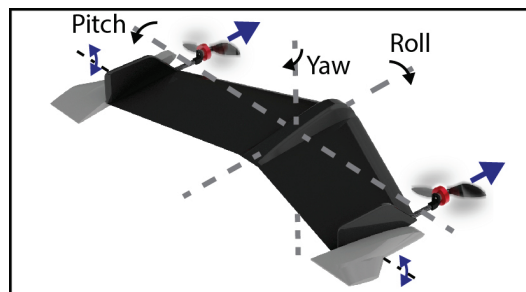


Figure 2.2: Definition of the roll, pitch and yaw axes of the DALER.

## Chapter 2. Platform Configuration Selection

The walkerons can be used as wheels to move on the ground as shown in Fig. 2.3. The forward direction of motion is opposite from the flight direction, the body of the robot is dragged on the ground. In order to move straight the robot has to turn both walkerons at the same speed as shown by Fig. 2.3.A. By changing the differential speed of the walkerons when they are moving in the same direction the robot can perform curves (see Fig. 2.3.B) and by rotating the walkerons in opposite directions the robot can turn on spot (see Fig. 2.3.C). Finally, by turning the two walkerons opposite to the walking direction, the body will upright itself in a take-off ready position (see Fig. 2.3.D). If a small mechanism is added, the body could stay in this take-off ready orientation while the walkerons are brought back to the hovering position (i.e. aligned with the wing).

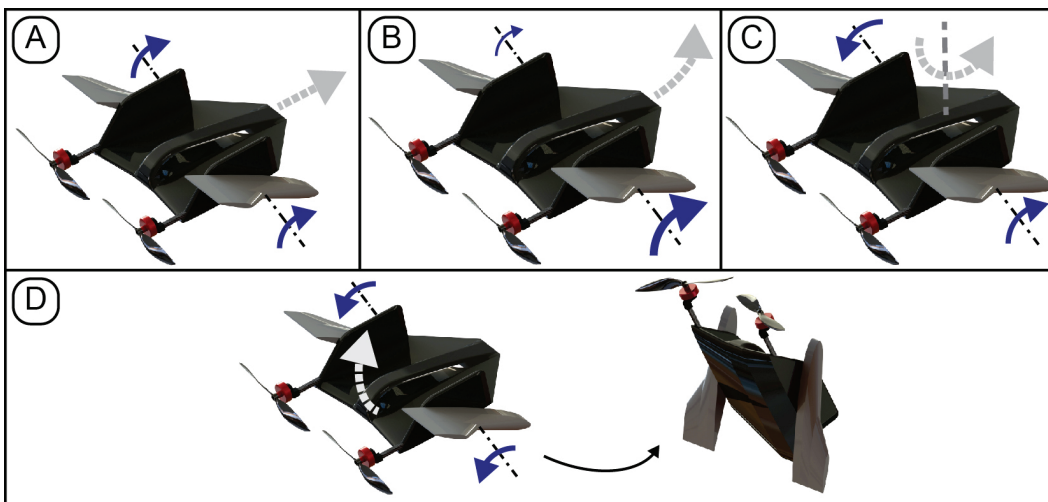


Figure 2.3: Ground locomotion mode of the DALER. A) Moving straight by turning the two walkerons at the same speed in the same direction. B) Performing curves by turning one walkeron faster than the other one. C) Turning on spot by turning the two walkerons in opposite directions. D) Uprighting by turning the two walkerons backwards at the same time.

Figure 2.4 shows the type of mission scenario that could be achieved by this robot capable of three modes of locomotion and of transitioning between these modes. The robot would start its mission by flying quickly to a region of interest, then it could transition to hover and enter inside houses or buildings, land on the ground, explore the area, upright itself, take-off, exit the building and transition back to forward flight in order to come back to its departure point.

This robot is based on an integrated design approach and has an adaptive morphology that increases the performance of the different modes of locomotion. This design is the case study used in this thesis, the next chapter focuses on the integration of a sub-set of locomotion modes of this platform (i.e. forward flight and ground locomotion) and the research questions involved in the integrated design approach.

## 2.5. Implementation of the Selected Solution

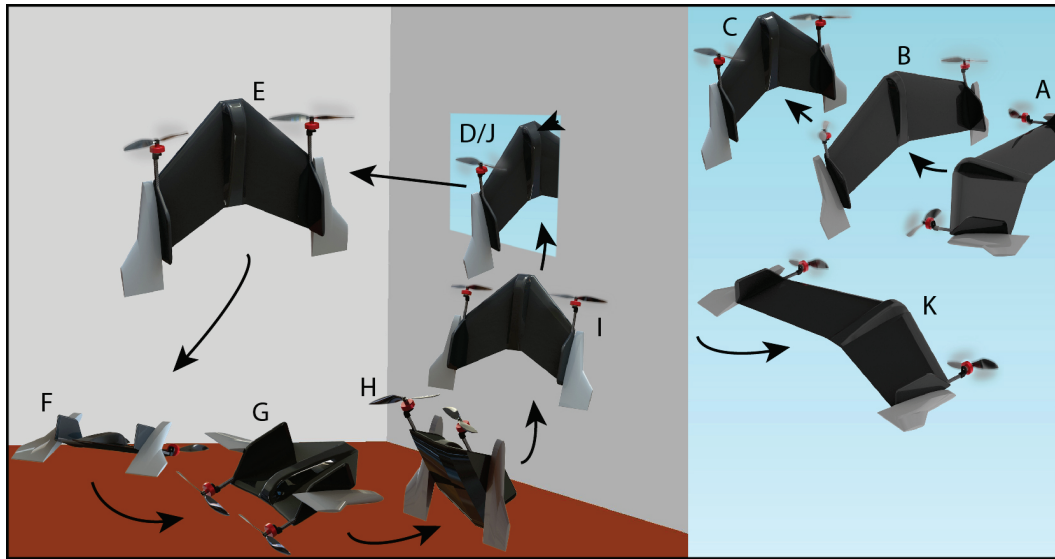


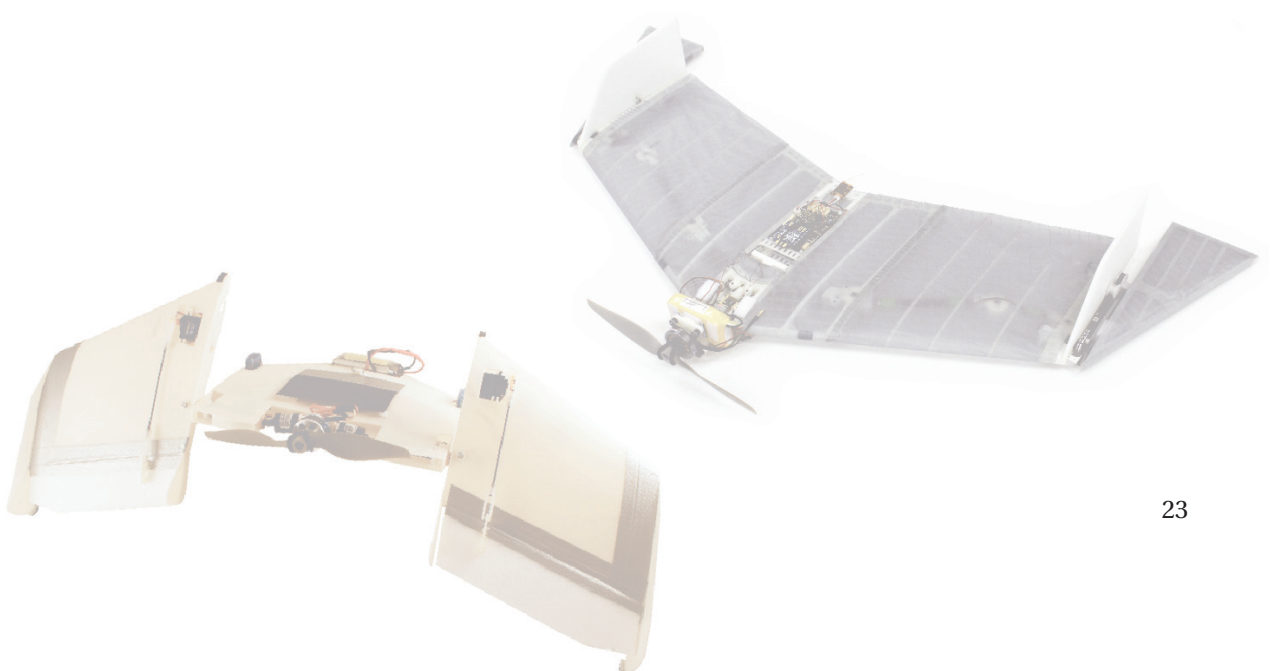
Figure 2.4: Final demonstration scenario of the DALER project. Each image shows the robot performing a different action: A) flying forward, B) transitioning to hover, C) folding the wings downwards (in this configuration the wingspan is smaller, thus reducing the impact of the wind on the platform and allowing to go through small openings), D) entering a building in hover, E) hovering indoors, F) landing on the ground and closing the wings frontwards (in this configuration the wingspan is at its minimum and the robot can walk between obstacles), G) walking on the ground in order to explore the area, H) uprighting in a take-off ready position, I) taking-off vertically and transitioning to hover, J) exiting the building and finally K) transitioning to forward flight in order to go back to the departure point.



### 3 Integrated Design Approach

Multi-modal robots can be designed according to two different design approaches; additive or integrated. An additive design approach implies that for each new mode of locomotion a new set of structure and actuator(s) is added to an existing design. This solution allows having an optimized locomotor system for each mode of locomotion, however it adds weight and complexity to the robot. In opposition, an integrated design approach uses the same structure and actuators for different modes of locomotion, this approach allows minimizing the total weight and complexity of the robot. However, it rises new challenges in the design of the robot; if the same actuator is used for two modes of locomotion then these modes should have compatible dynamics (i.e. compatible torque and speed requirements), this limitation will be discussed in this chapter.

This chapter is based on the publication *A Flying Robot with Adaptive Morphology for Multi-Modal Locomotion* [45] and partly on the publication *A bioinspired multi-modal flying and walking robot* [46].



### 3.1 Introduction

This chapter first presents a prototype based on the integrated design approach. In this prototype only the structure is shared for the terrestrial and aerial modes of locomotion, different actuators are used for the flight control and for the ground locomotion. Then, a second prototype is presented which further exploits the integrated design approach. In this second prototype, the same structure and the same actuators are used for the two modes of locomotion. Finally, these two prototypes are compared and conclusions about the integrated design approach are drawn based on their locomotion capabilities.

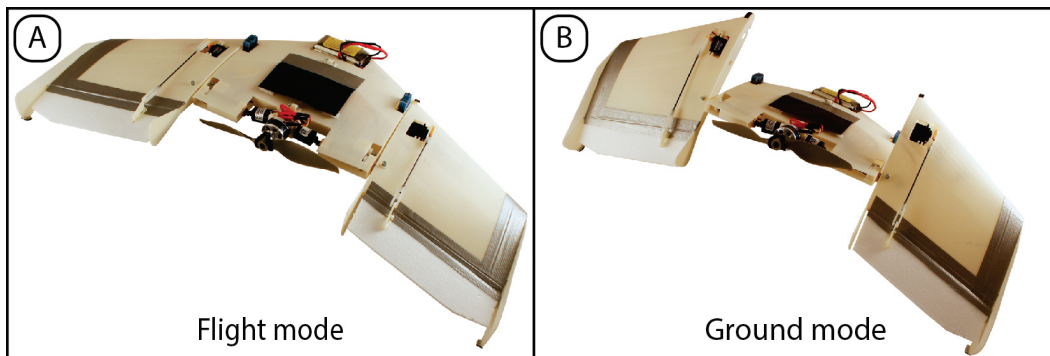


Figure 3.1: DALER v6 prototype, which can fly forward and walk. This robot can use its wings as wheels to move on the ground. A) Forward flight configuration and B) ground locomotion configuration.

### 3.2 Integrated Structure

In this section, the integration of the forward flight and ground modes of locomotion will be studied, by the means of the prototype shown in Fig. 3.1. In this platform, the wings' structure is used both for forward flight and for ground locomotion. The ground locomotion properties of this prototype will be analysed and the morphology of the robot, modelled in a physics based simulator, will be optimized for ground locomotion speed. Finally, the mechanical design of this DALER v6 prototype will be presented and its locomotion capabilities will be assessed.

#### 3.2.1 Ground Locomotion Analysis

This sub-section aims at analysing the ground locomotion of the DALER v6 shown in Fig. 3.1. The geometry of a flying wing airframe can be described with 3 parameters (see Fig. 3.2); the *taper ratio*  $T = C_t/C_r$ , which is the ratio between the tip chord  $C_t$  and the root chord  $C_r$ , the *swept angle*  $\theta$ , and the *half-wingspan*  $b/2$ . For the ground locomotion, a new parameter is defined which is called the *inner ratio*  $I = 2d/b$ . The inner ratio is the ratio between the distance  $d$ , distance between the center of the robot and the rotating wing, and the half-



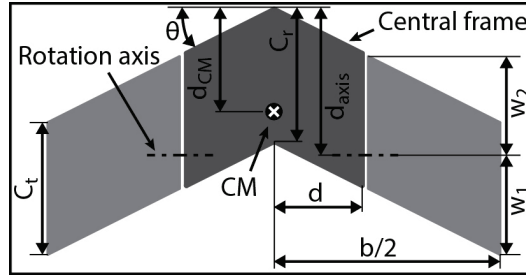


Figure 3.2: Model of the DALER v6 with dimension parameters.

wingspan. The position of the rotation axis of the wings  $d_{axis}$  is defined from the front tip of the platform. In order to minimize the maximum torque in the motors that actuate the wings this length is constrained in order to have  $w_1 = w_2 = w$ . Finally, the position of the center of mass (CM) is constrained, for flight stability reason, by the aerodynamic pressure center, which depends on the lift distribution of the platform [47].

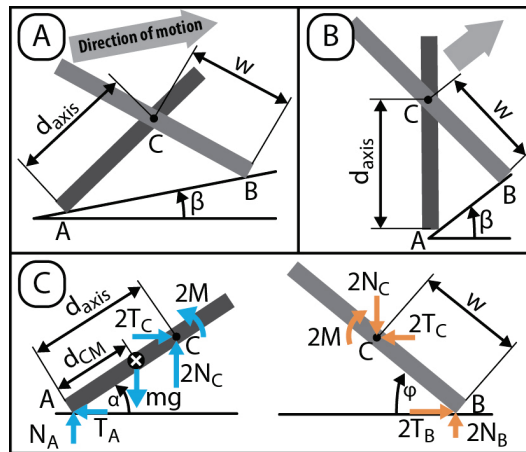


Figure 3.3: Ground locomotion analysis of the DALER v6. A) Schema of the robot seen from the side on a slope with dimension parameters; the central frame in dark grey and the wing in light grey. B) Limit of stability; for bigger values of  $\beta$  or  $w$ , the robot would fall backwards. C) Free body diagram; central frame on the left, and wings on the right.

The first important constraint to consider is that the center of the robot, the central frame, does not flip over when it is climbing on a slope. Figure 3.3.A shows a schema of the robot seen from the side on a slope of angle  $\beta$ . To prevent flipping, the following condition has to be maintained:

$$w < d_{axis} \cos(\beta) \tag{3.1}$$

### Chapter 3. Integrated Design Approach

---

Otherwise the center part of the robot would rotate instead of the wings, because the gravitational force would pull it backwards. Figure 3.3.B shows the corresponding limit situation.

The second important constraint to consider is that the wings do not slip on the ground, the static friction force  $T = \mu N$  at point A should be smaller than at point B, so that the contact point A slips on the ground but not the contact point B (see Fig. 3.3):

$$\mu_A N_A < \mu_B N_B \quad (3.2)$$

To evaluate this condition the model is separated into two bodies (see Fig. 3.3.C). The hypothesis that the mass of the wings can be neglected compared to the total mass of the robot is done; all the heavy components such as the battery and the electronics are in the central frame of the robot, the wings represent less than 10% of the mass of the robot. As there are two wings and two motors, the contact forces at point B and C are doubled. The following equations can be derived from Newton's and Euler's equations applied on this system (at angle  $\varphi = 0^\circ$ ):

$$N_A = mg \left( 1 - \frac{d_{CM}}{d_{axis} + w} \right) \quad (3.3)$$

$$N_B = mg \frac{d_{CM}}{2(d_{axis} + w)} \quad (3.4)$$

Which lead to the following inequality:

$$\frac{d_{axis} + w}{d_{CM}} < 1 + \frac{\mu_B}{2\mu_A} \quad (3.5)$$

The friction between the ground and the robot has an influence on the admitted limit values of the parameters. The friction coefficient at the contact point on the center part A should be reduced to a minimum to permit a slipping-less rotation of the wings.

When the constraint given by eq. 3.5 is satisfied, the transversal contact force is determined by the friction at point A and can be used to evaluate the torque required by the motors:

$$T_A = 2T_B = 2T_C = \mu_A N_A \quad (3.6)$$

Hence, the torque for one motor (at  $\varphi = 0^\circ$ ):

$$M = \frac{1}{2} mg \frac{d_{CM}}{1 + \frac{d_{axis}}{w}} \quad (3.7)$$

For higher values of  $\varphi$ , the required torque depends also on the friction coefficient between the contact point of the robot A and the ground. For a good locomotion efficiency, the required torque should be as small as possible and the covered distance per revolution should be as long as possible. The length of the covered distance  $l$  per rotation of the wings is proportional to  $w$ , assuming that the wings do not slip,  $l = 4w$ . Supposing that the robot moves forwards with a certain mean speed  $v$ , the required average rotational speed of the wings  $\Omega$  is:

$$\Omega = v \frac{2\pi}{l} = v \frac{\pi}{2w} \quad (3.8)$$

Equations 3.7 and 3.8 are used to dimension an optimal actuator for ground locomotion (a safety factor of 1.5 is used for the torque).

#### 3.2.2 Morphology Optimization

The morphology of the robot has been optimized for maximizing its speed in the ground locomotion mode. The robot has been modelled in a physics based simulator, using the Open Dynamic Engine (ODE) library. All the combinations of taper ratio, swept angle, and inner ratio were generated while keeping a constant wing area. Only the morphologies satisfying eq. 3.1 and eq. 3.5 were evaluated in the simulator. The optimized parameters do not have an impact on the lift generated by the wing since the area is kept constant, however the manoeuvrability, the stability and the drag will be influenced by the taper ratio and the swept angle. The airfoil profile and the placement of the centre of mass must be carefully adapted to the wing geometry. Figure 3.4 shows the distance travelled for the different configurations. Each point represents a different geometry of the robot and the color represents the travelled distance for one complete revolution of the wings. The x axis represents the inner ratio (from 20 to 80%), the y axis the taper ratio (from 30 to 100%), and the z axis the swept angle (from  $5^\circ$  to  $45^\circ$ ). Points that are missing on the graph are geometries where the axis of rotation of the wings would have been outside of the central frame of the robot, and thus are not evaluated. This figure also shows the extreme configurations of the robots. From the graph it can be seen that the best results are obtained for a medium swept angle (between  $20^\circ$  and  $30^\circ$ ), a large taper ratio ( $\geq 65\%$ ), and a small inner ratio ( $\leq 50\%$ ). The point with the highest value has the following parameters: inner ratio 35%, taper ratio 95%, and swept angle  $26^\circ$ . The prototype that was built to validate this concept was thus designed using these same parameters, and its mechanical design is presented in the next sub-section.

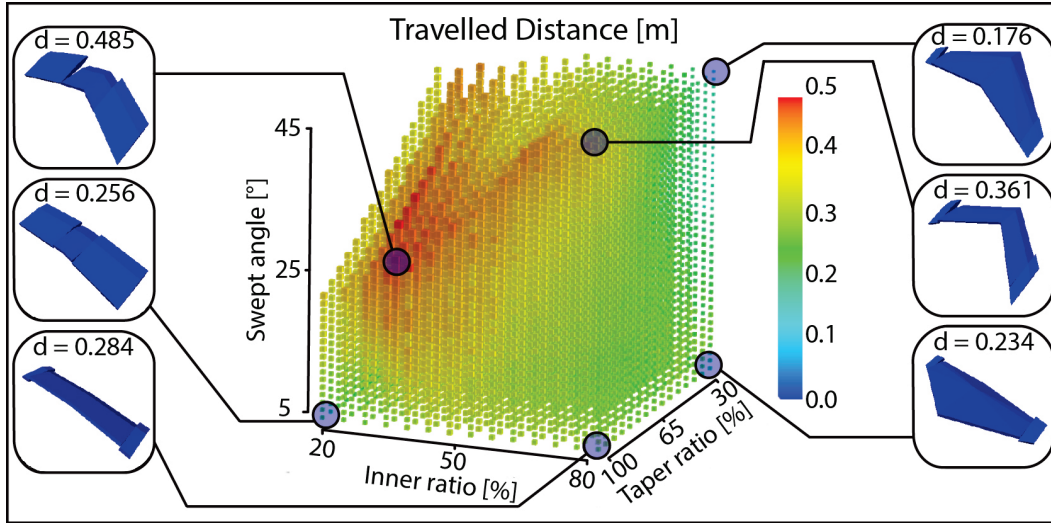


Figure 3.4: Morphology optimization of the DALER v6. Distance travelled for one revolution of the wings. The *swept angle* is the angle  $\theta$  shown in Fig. 3.2, the *taper ratio* is ratio between the tip chord and the root chord  $T = C_t/C_r$ , and the *inner ratio* is the ratio between the distance  $d$  and the half-wingspan  $I = 2d/b$ .

### 3.2.3 DALER v6 Mechanical Design

For the flight mode of locomotion the wings have to be sufficiently rigid in order to sustain the lift force and for the ground mode they must sustain high torsion forces during walking. The prototype is 3D printed in ABS, its total mass is 450 g for a wingspan of 60 cm.

Figure 3.5.A and D show small hooks that were added on the wings to increase the friction with the ground, they are covered with rough tape. Table 3.1 gives the friction coefficients on different surfaces for the wings and for the center of the robot. The relation between the parameters  $\frac{d_{axis+w}}{d_{CG}}$  for this robot is equal to 2.5. Equation 3.5, the none-slipping condition, is satisfied for all surfaces except for the parquet that is very slippery. However, the robot can still walk on parquet since it is slipping only on a small portion of each step, it is just less efficient than on the other surfaces (the robot has been optimized for locomotion on grass in the simulator).

	Parquet	Carpet	Asphalt	Grass
Robot center $\mu_A$	0.3	0.4	0.5	0.5
Wings $\mu_B$	0.45	1.8	1.7	1.6
$1 + \frac{\mu_B}{2\mu_A}$	1.75	3.25	2.7	2.6

Table 3.1: Friction coefficients for different surfaces.

The rotation of the wings must be locked during flight because the gears of the DC motors which actuates the wings have backlash (4-5 degrees), thus a locking mechanism is used to prevent unwanted fluttering of the wings during flight. Figure 3.5.C and D show this locking mechanism, and B shows the axis of rotation of the wing, the DC motor that is mounted inside the robot, the gears, and the slip ring (slip rings prevent the servo-motors' cables, used for the flaps on the wings, from being twisted).

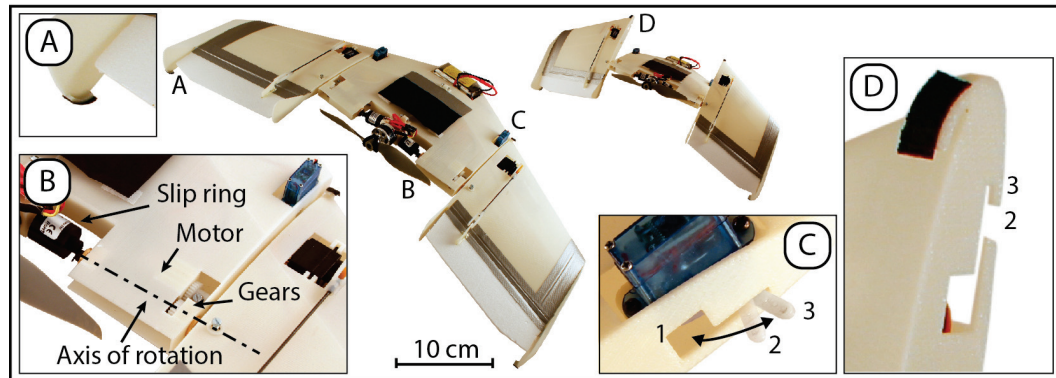


Figure 3.5: Mechanical design of the DALER v6. A) & D) Small hooks added on the wings, covered with rough tape to increase the friction with the ground. C) Locking mechanism; the servo-motor arm is in position 1 (arm retracted) when the robot walks on the ground, then it can be opened to position 2 and the wings rotate until the arm of the servo-motor slices into the corresponding slot 2 (shown in D), and finally the wings are locked when the arms are in position 3. B) Slip ring, DC motor, gears and axis of rotation of the wings.

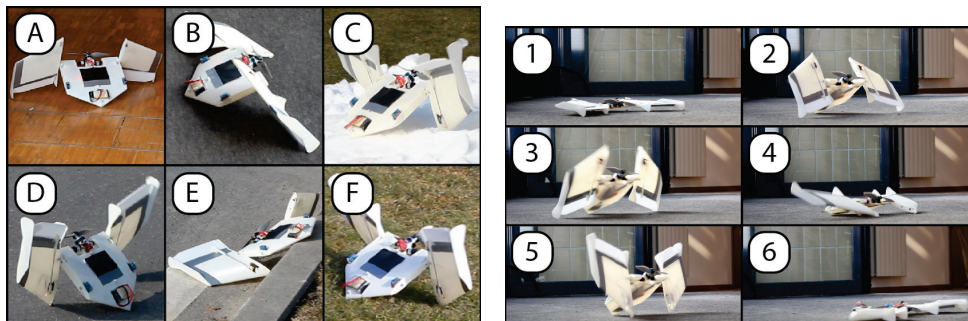
#### 3.2.4 DALER v6 Locomotion Capabilities

The DALER v6 prototype is capable to walk on different terrains, such as on parquet, on carpet, in snow, on asphalt, and on grass (see Fig. 3.6.a). Different experiments have been performed in order to evaluate the capabilities of the robot on the ground. The maximum gap that the robot can overcome repeatedly (100% success over 5 trials) is 12 cm, which corresponds to 0.4 body-length (BL); above this distance the robot gets stuck or falls in the gap. The maximum step that the robot can climb is 8 cm, which corresponds to 1.2 body-height (BH). The maximum upward slope, on a wooden floor, that the robot can walk on is  $15^\circ$ . When the wings rotate synchronously (see Fig. 3.6.b) the robot can go at 12 cm/s (or 0.4 BL/s) and can rotate on spot at  $25^\circ$ /s. The autonomy of the robot is very much dependent on the type of terrain. On a flat wooden surface the maximum autonomy has been measured at close to 30 minutes and in rough terrains the robot can walk for about 15 minutes with a full battery (3 cells LiPo, 0.7 Ah). It can fly at about 14 m/s, is robust to landings at that speed, and the autonomy of such a flying wing is about 10-15 minutes in forward flight. Table 3.2 summarizes the performances of the prototype in the air and on the ground.

			DALER v6
Terrestrial	Obst.	Gap max.	12 cm (0.4 BL)
		Step max.	8 cm (1.2 BH)
		Slope max.	15°
	Speed	Forward max.	12 cm/s (0.4 BL/s)
		Rotational max.	25 °/s
		Autonomy	15-30 min.
Aerial	Speed min.	8 m/s	
	Speed max.	14 m/s	
	Autonomy	10-15 min.	
Battery capacity			0.7 Ah

Table 3.2: Summary of performance of the DALER v6.

The DALER v6 shows good ground locomotion performances, but its flying capabilities are impaired by its weight. The use of the structure of the wing for ground locomotion allows to minimize the structural mass of the robot, yet the robot has 7 actuators in total; 3 for forward flight (i.e. one brushless motor for the propeller and two servo motors for the flaps) and four are added for the ground locomotion (i.e. 2 DC motors for the rotation of the wings and two servo motors for the locking mechanisms). To further investigate the benefits of the integrated design approach, another prototype which uses the same actuators for flight control and for ground locomotion is presented in the next section.



(a) DALER v6 on different terrains, A) on parquet, B) on carpet, C) in snow, D) on asphalt, E) going down a step, and F) on grass. (b) Ground locomotion sequence of the DALER v6.

Figure 3.6: Ground locomotion capabilities of the DALER v6.

## 3.3 Integrated Structure and Actuation

The present section describes the implementation of another flying wing with walking capabilities, the DALER v9, which this time fully exploits the integrated design approach. The robot adopts the same actuators and appendices, called walkerons, for both flight control and walking on the ground. With the proposed design, terrestrial competences are successfully endowed on a flying wing while losses of aerial performance are minimized in terms of flight manoeuvrability and cost of transport during flight, because the drag in the air is not increased compared to a regular flying wing since no additional structures are added. In the proposed design (see Fig. 3.7), the two walkerons are used to control the pitch and the roll axes of the robot during flight and are also used as wheels to power the ground locomotion in unstructured environments. These walkerons are designed in such a way that the two modes of locomotion have compatible dynamics as described below. The mechanical design of this robot will be presented in the next chapter (see section 4.2)

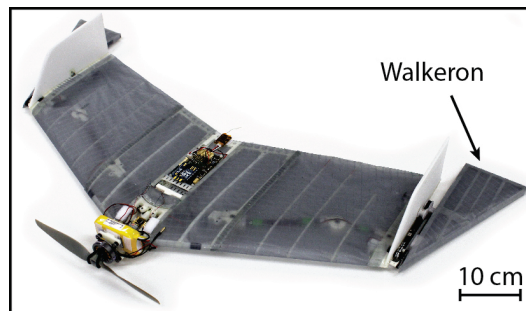


Figure 3.7: DALER v9, multi-modal flying and walking robot. The robot is equipped with walkerons that seamlessly integrate flight control and terrestrial walking.

### 3.3.1 Dual Use Walkerons

The effective use of the walkerons for multiple modes of locomotion in a flying wing (see Fig. 3.8.A) is achieved using a two-step design process:

- Identifying the best shape of walkerons in order to accommodate the different constraints imposed by flight control and ground locomotion.
- Selecting suitable actuators and sizing walkerons for their double use with the smallest possible flight efficiency loss.

Regarding the first step, three important aspects constrain the shape of the walkerons (see Fig. 3.8.B):

1. The axis of rotation of the walkeron should be close to its aerodynamic centre. The aerodynamic centre of any airfoil is the point where the pitching moment coefficient

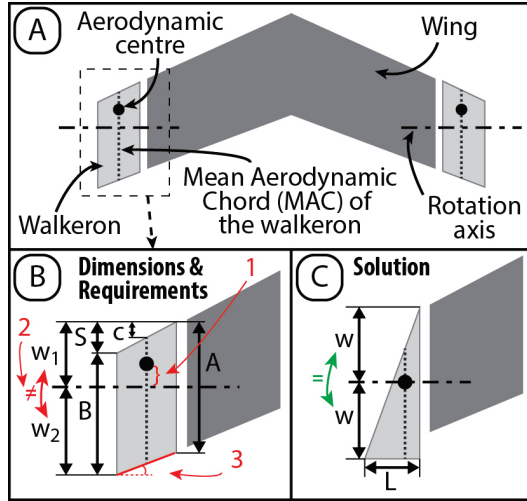


Figure 3.8: Model of the DALER v9. A) The walkeron is the portion of the wing used to control the flight. B) Zoom on one of the walkerons, which shows the different parameters which have to be dimensioned and the constraints; 1) the centre of aerodynamic pressure (black dot) should be on the rotation axis, 2) the axis of rotation should be in the centre of the walkeron ( $w_1 = w_2$ ) and 3) the trailing edge should be horizontal. C) The solution that fulfils all these requirements.

does not change with the angle of attack; this is also the point where the lift is applied [48]. Thus, if the axis of rotation of the walkeron goes through the aerodynamic centre, the torque that must be applied by the motor to turn the walkeron is minimized and it also makes the calculations easier since this torque will not change with the angle of attack. The aerodynamic centre is located at approximately 25% of the Mean Aerodynamic Chord (MAC) [48].

2. For the ground locomotion, the axis of rotation of the walkeron has to be in its centre in order to minimize the peak torque required by the motor.
3. The trailing edge of the walkeron should be parallel with its axis of rotation, in order to maximize the grip on the ground.

In order to satisfy these three requirements, it is demonstrated below that the walkerons should have a triangular shape, as in Fig. 3.8.C. The MAC length is given by the following equation:

$$MAC = A - \left[ \frac{2(A-B)\left(\frac{A}{2} + B\right)}{3(A+B)} \right] \quad (3.9)$$



### 3.3. Integrated Structure and Actuation

Where  $A$  is the root chord of the walkeron and  $B$  is its tip chord (see Fig. 3.8.B). The swept distance at  $MAC$ ,  $c$ , is given by:

$$c = S \frac{A + 2B}{3(A + B)} \quad (3.10)$$

Where  $S$  is the swept distance at the tip of the walkeron (see Fig. 3.8.B). The following equations must be satisfied in order to, respectively, minimize the motor torque, have an horizontal trailing edge, and have the centre of rotation at 25% of the  $MAC$  distance:

$$w_1 = w_2 \quad (3.11)$$

$$A = S + B \quad (3.12)$$

$$w_1 = c + \frac{MAC}{4} \quad (3.13)$$

Thus, by replacing  $c$  and  $MAC$  by their expression and with  $w_1 + w_2 = S + B$ :

$$S^2 - 2AS + A^2 = 0 \quad (3.14)$$

This equation has only one solution:  $S = A$  and therefore  $B = 0$ . It follows that the walkerons should have a triangular shape as shown in Fig. 3.8.C. This triangular shape has a large swept angle which creates a vortex at the tip of the walkeron. This vortex prevents stalling of the walkerons at large angles of attack and thus increases the performance during aerobatics manoeuvres that require high deflection of the walkerons.

Regarding the second step, namely the selection of actuators and the sizing of the walkerons, it is important to consider that flight manoeuvrability requires rapid walkeron movements and low torque, while ground locomotion demands high torque and lower rotational speed. These differences in torque and rotational speed requirements make the selection of a single actuator difficult.

To appreciate this issue, let's consider the operating range of a conventional DC motor (see Fig. 3.9). It is constrained by two main factors: the torque that can be continuously delivered by the motor is limited by heat dissipation, and the maximum speed is primarily limited by the wear effect in the commutations systems and in the bearings. Moreover, the maximum continuous torque decreases with the speed, thus there is a trade-off between torque and speed that can be delivered by the motor. Usually, if two locomotion modes have very different dynamics (i.e. one needs very high speed and the other very high torque), an actuator

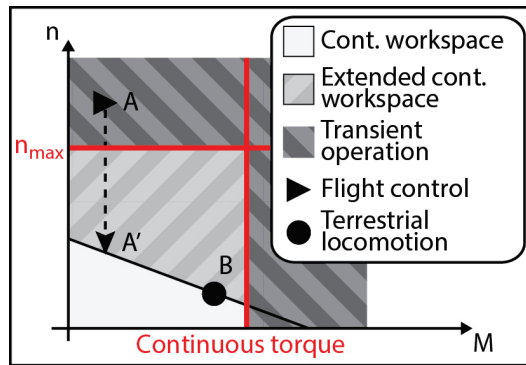


Figure 3.9: Operating range of a DC motor suited for terrestrial locomotion (rotational speed  $n$  vs. torque  $M$ ). The dynamics of flight control and terrestrial locomotion are shown at point  $A$  and  $B$ , respectively. The diagonal line illustrates the dynamics of a DC motor operating at  $V = V_{nominal}$ , where  $V$  is the voltage applied to the motor and  $V_{nominal}$  is the maximum voltage recommended by the manufacturer. The continuous torque is the maximum torque that can be applied continuously by the motor without overheating and  $n_{max}$  is the maximum speed of the motor. The optimisation of the walkerons' size moves the dynamics of flight control within the continuous workspace of the actuator dimensioned for terrestrial locomotion.

dimensioned for one locomotion mode will not be suited for the other and vice-versa. For example, an actuator dimensioned for terrestrial locomotion, which operating range is shown in Fig. 3.9 (slow with high torque, point  $B$ ), is not able to continuously provide the high speed required by flight control because its working point  $A$  is outside of the continuous workspace of this actuator. Alternatively, an actuator dimensioned for flight control, which would have a different operating range compared to the one shown in Fig. 3.9 (i.e. higher  $n_{max}$  and lower continuous torque), would overheat during ground locomotion because of the too high torque.

A similar problem is encountered in the skeletal muscles required for animal locomotion. Skeletal muscles generate their maximum power and efficiency in a small range of fibre strain, contraction speeds and load [49]. Birds need less power to fly due to favourable environmental conditions, instead of reducing the contraction speed of the muscles, they alternate between gliding and flapping phases in order to maintain an optimal contraction speed of the muscle during the flapping phase [50]. Using this strategy, avian muscles work in their optimal range, maximizing efficiency and output power. Similarly, when transitioning between substrates with different physical properties [51], animals, like robots have to address the limitations of their biological actuators. In our situation, three solutions exist to address the limited operating range of DC motors:

1. The use of a single oversized DC motor that is simultaneously compatible with both locomotion modes. A single DC motor that matches both dynamics has to be simultaneously fast and strong resulting in a heavier solution than the use of two different motors each independently optimized for a single working point. Hence, an integrated

approach with a single locomotor apparatus can be heavier than using two locomotion systems as suggested by the additive strategy. A numerical example below supports this conclusion.

2. The use of a transmission with controllable gear ratio which would allow a single actuator to match the dynamics imposed by flight control and terrestrial locomotion by changing this ratio. This approach involves additional components (i.e. clutch, gear shift actuator and multiple gear trains) that increase both the complexity and the weight of the robot. Therefore, the advantage with respect to an additive strategy is questionable.
3. The rotational speed of the walkerons during flight control could be reduced until it is compatible with the operating range of the actuator suited for ground locomotion (as shown by the dotted arrow in Fig. 3.9). This can be achieved without loss of flight manoeuvrability if the size of the walkerons is increased proportionally to the reduction of speed.

In the third solution, the two locomotion modes become dynamically compatible within the limited operating range of a single actuator; hence they can be seamlessly integrated in a single locomotor system optimized for one of the mode of locomotion. In this condition, the additional terrestrial competences have a minimal impact on the aerial performances of the robot. Furthermore, because the walkerons are already part of the flying wing, additional weight and drag are minimized, hence reducing the impact of walking on the aerial cost of transport.

#### Analysis of Solution 1

When two locomotion modes have different dynamics, the use of a single apparatus is not convenient. To this aim, the dynamic data reported in Table 3.3 are considered, and two actuation strategies have been compared:

- A single actuator dimensioned to match the dynamics of both working points (integrated design strategy).
- Two different actuators for flight control and for ground walking (additive design strategy).

Weight is a good metrics to compare the different strategies since it is a key parameter in the design of flying robots. Weight comparison is based on the fact that biological and artificial effectors (the system that converts an input energy into an output mechanical work) have constant power densities [52, 53]: their weight increases with rated power capabilities. Considering a complete actuator (i.e. electromagnetic effector + reduction stage), it is still possible to assume that its weight increases with its rated power. According to this assumption, the

### Chapter 3. Integrated Design Approach

---

weights of the two strategies can be compared by evaluating the maximum power associated with the actuators that are involved.

DC motors have been selected for actuating the walkerons since they can be easily implemented and because their control techniques are well established. Nevertheless, the overall methodology presented here can be generalized to other actuators (e.g. SMAs, EAPs). The dynamic behaviour of a DC motor is described by the following equation, which expresses the rotational speed,  $n$ , as a function of the motor output torque,  $M$ :

$$n(M) = n_0 - kM \quad (3.15)$$

Where  $n_0$  is the no-load speed and  $k$  is the speed/torque gradient. The output power of the motor,  $P$ , is given by:

$$P(M) = n(M)M = (n_0 - kM)M \quad (3.16)$$

The maximum power,  $P_{max}$ , that can be delivered by the actuator is then evaluated as follows:

$$\frac{dP(M)}{dM} = n_0 - 2kM \quad (3.17)$$

$$P_{max} = P\left(M = \frac{n_0}{2k}\right) = \frac{1}{4} \frac{n_0^2}{k} \quad (3.18)$$

The two strategies of actuation are illustrated in Fig. 3.10, which shows rotational speed,  $n$ , vs. torque,  $M$ . The points  $A$  and  $B$  represent the working points of the walkerons during flight control and walking, respectively. According to eq. 3.15, each DC motor is associated with a line connecting the no-load speed to the stall torque. An actuator is suited for a specific working point if it lies on the actuator line. The additive strategy requires a single actuator for each locomotion mode: actuator  $a$  for flight control and actuator  $b$  for terrestrial operations. In the integrated design approach a single actuator  $c$  can be used for both.

Evaluating at first the strategy of multiple actuators, the motor parameters ( $n_0$  and  $k$ ) can be optimized in order to minimize the peak power of each actuator, and therefore their weight. Considering a generic working point ( $n_x, M_x$ ), the actuator dynamics are described by:

$$n_x = n_{0,x} - k_x M_x \quad (3.19)$$

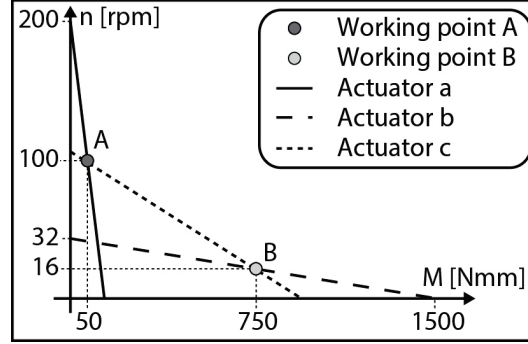


Figure 3.10: Working point *A* of walkerons during flight, working point *B* of walkerons during ground locomotion and dynamic capabilities of motors *a*, *b* and *c*.

Thus, according to eq. 3.18:

$$P_{max,x} = \frac{1}{4} \frac{(n_x + k_x M_x)^2}{k_x} \quad (3.20)$$

$P_{max,x}$  has a minimum value for  $k_x = \frac{n_x}{M_x}$  corresponding to:

$$P_{max,x} = \frac{1}{4} \frac{(n_x + n_x)^2}{n_x / M_x} = n_x M_x \quad (3.21)$$

In conclusion, power expressions associated with optimized actuators that work in the dynamic conditions *A* and *B*,  $P_{max,a}$ ,  $P_{max,b}$  and  $P_{max,a+b}$ , are:

$$P_{max,a} = n_a M_a \quad (3.22)$$

$$P_{max,b} = n_b M_b \quad (3.23)$$

$$P_{max,a+b} = n_a M_a + n_b M_b \quad (3.24)$$

where  $n_i$  and  $M_i$  are respectively the speed and the torque outputs of a motor *i*. This example shows that, within the additive design approach, in order to minimize weight, an optimal actuator delivers its maximum power in the working point of interest.

### Chapter 3. Integrated Design Approach

---

By adopting an integrated design approach, a single actuator  $c$  is used. With this strategy, the two motor parameters ( $n_{0,c}$  and  $k_c$ ) are constrained by the following equations:

$$\begin{cases} n_a = n_{0,c} - k_c M_a \\ n_b = n_{0,c} - k_c M_b \end{cases}, \quad (3.25)$$

which leads to:

$$k_c = \frac{n_a - n_b}{M_b - M_a} \quad (3.26)$$

$$n_{0,c} = \frac{n_a M_b - n_b M_a}{M_b - M_a} \quad (3.27)$$

Finally, the maximum power associated with the actuator  $c$ ,  $P_{max,c}$ , can be evaluated according to eq. 3.18 as:

$$P_{max,c} = \frac{1}{4} \frac{n_{0,c}^2}{k_c} = \frac{1}{4} \frac{(n_a M_b - n_b M_a)^2}{(M_b - M_a)(n_a - n_b)} \quad (3.28)$$

The values of torque and speed associated with the two working points  $A$  and  $B$  are measured on the DALER v6 prototype, the flight control working point is given by the dynamical capabilities of the servo motors used for the flaps and the ground locomotion working point by the DC motors used for rotating the wings (see Fig. 3.5). According to eq. 3.22-3.24 and eq. 3.28, the overall power consumption of the two actuation strategies are summarized in Table 3.3.

Working point	Additive	Integrated
Flight control	$M_a = 50 \text{ Nmm}$ $n_a = 100 \text{ rpm}$	$P_a = 520 \text{ mW}$
Ground locomotion	$M_b = 750 \text{ Nmm}$ $n_b = 16 \text{ rpm}$	$P_b = 1260 \text{ mW}$
Total power consumption	$P_{a+b} = 1780 \text{ mW}$	$P_c = 2450 \text{ mW}$

Table 3.3: Working points and power requirements for flight control and terrestrial locomotion. Data experimentally measured from the DALER v6 prototype. Comparison between additive and integrated design strategies.

It can be observed that the power required by the single actuator strategy is 37% higher than the overall power required by multiple actuators. Since power is assumed as an index of weight, the conclusion is that an integrated design approach with a single actuator is not optimal in terms of weight. This is due to the fact that the two operational points have very different dynamics, and therefore a single DC motor that matches both requirements has to be both fast and strong, thus resulting in a heavier solution than two single motors each optimized for a single working point. For example, considering motors from Maxon (Sachseln, Switzerland), good candidates are the following: RE8 with a 64:1 reduction, weighs 7.8 grams for flight control; DCX 10L with a 400:1 reduction, weighs 18.7 grams (considering the weight of the available 1024:1 reduction stage) for ground locomotion; RE-max 13 with a 100:1 reduction, weighs 31 grams with plastic gears and 41 grams with metal gears (considering the available 67:1 reduction stage) for both locomotion modes. In summary, the weight associated with a single actuator strategy is 19% to 57% heavier than the solution with two different motors, which is in good agreement with the calculation presented above.

#### Analysis of Solution 3

In the authors' opinions, the best solution for a successful integrated design consists of translating the working point  $A$  to point  $A'$  in order to match the properties of actuator  $b$ , as illustrated in Fig. 3.9. In fact, the working points  $A'$  and  $B$  are dynamically well matched to actuator  $b$ , which can be effectively selected to power both locomotion modes. By doing this the velocity of the walkerons decreases, thus the manoeuvrability of the flying wing may be compromised. The question is then if it is possible to optimize the size of the walkerons in order to make the two operational points dynamically compatible, with minimal impact on flight manoeuvrability. To answer this question, let us consider the lift generated by a walkeron,  $L$ :

$$L = \frac{1}{2} \rho v^2 A_{wn} C_L \quad (3.29)$$

Where  $\rho$  represents the air density,  $v$  is the air speed,  $A_{wn}$  is the area of the walkeron and  $C_L$  is the lift coefficient. The lift coefficient of an airfoil in a steady airflow can be expressed as a function of its angle of attack,  $\alpha$ , as:

$$C_L = K_c \alpha + C_{L0} \quad (3.30)$$

Where  $K_c$  is a parameter that allows to evaluate the lift variation depending on the angle of attack and  $C_{L0}$  is the lift coefficient for  $\alpha = 0$ . Since the aim is to preserve flight manoeuvrability, the walkerons must generate the same lift variation (that is ultimately responsible for pitch

### Chapter 3. Integrated Design Approach

---

and roll control) in the same time interval, and therefore:

$$\frac{dL}{dt} = \frac{1}{2}\rho v^2 A_{wn} K_c \dot{\alpha}_{wn} = \frac{1}{2}\rho v^2 A_{wn} K_c n_{wn} = \text{const} \quad (3.31)$$

Where  $n_{wn}$  is the rotational speed of the walkeron. This equation demonstrates that the flight manoeuvrability is not compromised when the walkeron is slowed down if its area is increased according to the following relationship:

$$A_{wn} n_{wn} = \text{const} \quad (3.32)$$

Concerning torque requirements, in first approximation, walkerons producing the same manoeuvrability need the same actuation torque. For example, when the area of a walkeron is doubled its lift doubles as well. Nevertheless, the stroke (angle  $\alpha$ ) is reduced and consequently the velocity is divided by two. These two effects compensate each other, resulting in a constant torque requirement for each walkeron that ensures the same level of manoeuvrability. Thus, as shown by the dashed arrow in Fig. 3.9, the working point A can be translated vertically until it crosses in  $A'$  by simply increasing the width  $L$  of the walkeron (see Fig. 3.8).

Working point	Additive	Integrated
Flight control	$M_{a'} = 50 \text{ Nmm}$ $n_{a'} = 31 \text{ rpm}$	$P_{a'} = 160 \text{ mW}$
Ground locomotion	$M_b = 750 \text{ Nmm}$ $n_b = 16 \text{ rpm}$	$P_b = 1260 \text{ mW}$
Total power consumption	$P_{a'+b} = 1420 \text{ mW}$	$P_c = 1260 \text{ mW}$

Table 3.4: Working points and power requirements for optimized walkerons.

Torque and velocity of the working points  $A'$  and  $B$  ( $M_{a'}$ ,  $n_{a'}$ ,  $M_b$  and  $n_b$ ) are reported in Table 3.4 as well as the associated power requirements. In this condition, the integrated design approach is 13% lighter than the additive design approach.



3.3.2 DALER v9 Locomotion Capabilities

This sub-section presents the analysis of the performance of the DALER v9 prototype on the ground as well as in the air. Table 3.5 summarizes the performances of the robot and compares them to the performances of the DALER v6. As for the v6, different experiments have been performed in order to evaluate the capabilities of the robot on the ground. The maximum gap that the robot can overcome is 9 cm (0.25 BL). The maximum step that the robot can climb is 4 cm (0.7 BH). The maximum upward slope, on a wooden floor, that the robot can walk on is 7°. The maximum forward speed measured on a flat wooden floor is 4 cm/s (0.15 BL/s) and the maximum rotational speed of the robot (on spot) is 20°/s (18 s for one complete revolution). The autonomy of the robot on a flat wooden surface has been measured at close to 60 minutes and in rough terrains the robot can walk for about 30 minutes with a full battery.

		DALER v6	DALER v9	
Terrestrial	Obst.	Gap max.	12 cm (0.4 BL)	9 cm (0.25 BL)
		Step max.	8 cm (1.2 BH)	4 cm (0.7 BH)
		Slope max.	15°	7°
	Speed	Forward max.	12 cm/s (0.4 BL/s)	4 cm/s (0.15 BL/s)
		Rotational max.	25°/s	20°/s
		Autonomy	15-30 min.	30-60 min.
Aerial	Speed min.	8 m/s	6 m/s	
	Speed max.	14 m/s	20 m/s	
	Cont. pitch rate	-	120°/s	
	Cont. roll rate	-	180°/s	
	Autonomy	10-15 min.	25-30 min.	
Battery capacity		0.7 Ah	1.5 Ah	

Table 3.5: Summary of performance of the DALER v9.

The drag force during flight is the same as on a wing capable of only flying since no additional appendices have been added for ground locomotion. The minimum flight speed of the robot, before stalling, has been measured at 6 m/s and therefore the robot can easily be launched by hand. The maximum flight speed of the robot has been measured above 20 m/s. The autonomy of the robot at cruise speed (approx. 12 m/s) is between 25 and 30 minutes. The maximum constant pitch and roll rates, measured by performing an inside loop manoeuvre and a full roll manoeuvre, are 120°/s and 180°/s respectively.

The working range of the walkerons' motors has been measured during flight. For a standard flight, the speed of the walkerons varies between 0 and 25 rpm and the torque varies between 100 and 150 Nmm. This torque is mainly caused by friction in the transmission of the mechanism that actuates the walkerons and does not change with the speed of the robot in the air. The speed during ground locomotion varies between 0 and 15 rpm and the torque varies between 650 and 850 Nmm depending on the speed of the robot and on the friction with the ground. Figure 3.11 shows the two designed working points, *A'* and *B*, for flight and

ground locomotion respectively and the two measured working areas of the motor during flight and ground locomotion. The two measured areas are below the line of the actuator and this demonstrates that the same motor can be used for the two modes of locomotion and that these modes of locomotion are dynamically compatible.

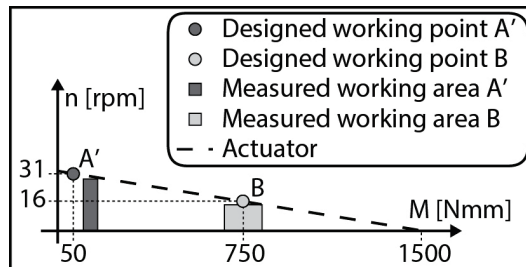


Figure 3.11: Designed working points  $A'$  of walkerons during flight and  $B$  during ground locomotion and measured working areas of the motors during the two modes of locomotion.

### 3.4 Integrated Design Approach Analysis

In this section, the levels of integration of the two prototypes are compared in order to evaluate the benefits of the integrated design approach. The level of integration of a robot can be evaluated with the mass integration metrics recently introduced by [33]; the mass integration metrics is “a measure of the percentage of the total integrated robot mass”. Thus, the mass integration value is given by the sum of the mass required by each mode of locomotion divided by the mass of the robot (i.e. for  $n$  modes of locomotion a fully integrated design will score  $n$  and a fully additive design 1). Table. 3.6 provides the mass distribution of the two DALER prototypes. The components are sorted into three categories; the components shared for both modes of locomotion, the components used only for terrestrial locomotion and those used only for aerial locomotion.

#### DALER v6 Mass Distribution

For the v6, the shared components are: the *mechanics* composed of the central frame and the two wings, the *electronics*, and the *battery*. These shared components weigh a total of 257 g. The components which are added only for terrestrial and aerial modes of locomotion are both separated into three categories; *mechanics*, *actuators* and *electronics*. The mechanical parts for the ground locomotion include all the components added to allow the rotation of the wings (i.e. gears, shaft, bearings and slip rings), the actuators are the two DC motors and the two servo motors for the locking mechanism and the electronics is composed of two speed controllers for the DC motors. The mechanical parts added for forward flight are the two flaps and a propeller, the actuators are two servo motors and a brushless motor and the electronics is a speed controller. The total masses for the terrestrial and aerial modes of locomotion are equivalent and are equal to 353 g. The total mass of the robot is 449 g.

### 3.4. Integrated Design Approach Analysis

Components		DALER v6 Mass [g]		DALER v9 Mass [g]	
Shared	Mechanics	184		162	
	Actuators	0		22	
	Electronics	8		27	
	Battery	65		130	
	$M_S$	257		341	
Ground	Mechanics	42		0	
	Actuators	34		0	
	Electronics	20		0	
	$M_G$	96		0	
	$M_G^{tot}$	$M_S + M_G$	353	$M_S + M_G$	341
Flight	Mechanics	19		10	
	Actuators	55		26	
	Electronics	22		14	
	$M_F$	96		50	
	$M_F^{tot}$	$M_S + M_F$	353	$M_S + M_F$	391
$M_{Robot}$		<b>449</b>		<b>391</b>	
Integration		$\frac{M_G^{tot} + M_F^{tot}}{M_{Robot}}$	<b>1.57</b>	$\frac{M_G^{tot} + M_F^{tot}}{M_{Robot}}$	<b>1.87</b>

Table 3.6: Mass distribution and integration analyses of the DALER v6 and v9.

#### DALER v9 Mass Distribution

For the v9, the shared components are all the mechanical parts which are needed to build a fixed wing (i.e. central frame, ribs, carbon rods, walkerons and fabric), the actuation and the transmission used to control the walkerons, the autopilot board, the DC motor board, and finally the battery. These shared components weigh a total of 341 g. There are no components added only for ground locomotion. The parts used only for the flight are one brushless motor, one propeller, one speed controller and a motor holder. These components weigh 50 g, which brings the total mass for the flight mode of locomotion to 391 g. The total mass of the robot is 391 g.

#### Mass Integration Comparison

The mass integration value of the v6 prototype is 1.57 and for the v9 1.87. These results show that 87% of the mass is used by both modes of locomotion for the v9 and 57% for the v6; the v9 is 46.6% lighter than it would be with a fully additive design approach and the v6, 36.4%. The only other multi-modal robot evaluated with this metric is the MultiMo-Bat [33], which scores 1.69. The result achieved by the v9 is even more remarkable considering that it combines active aerial and terrestrial locomotion, while in the MultiMo-Bat flight is passive (gliding), and therefore does not require actuators. In the v9, such high level of integration can be achieved since the same actuators are used for both flight control and walking on the ground.

### Locomotion Capabilities Comparison

From Table 3.5 it can be seen that the ground locomotion capabilities of the v9 prototype are lower than for the v6 prototype. The ground locomotion of the v6 could be optimized since it is decoupled from the flight mode of locomotion. The position of the axis of rotation of the wings is optimized for ground speed (i.e. close from the center of mass of the robot), whereas for the DALER v9 it is constrained by the flight requirements (i.e. away from the center of mass). On the other hand, the flight performances of the v9 are much higher, the high mass integration of the prototype allows to minimize the total weight of the robot and therefore it increase its agility in the air. The prototype can fly at a lower speed, facilitating take-off, and has a higher flight time, the battery has a double capacity compared to the v6.

### 3.5 Conclusion

Nature has evolved multiple strategies to implement multi-modal locomotion. These strategies can be successfully applied to the development of robots with locomotion capabilities in multiple environments with minimal compromises. A comparison can be made between animals that exploit an additive strategy with multiple single-use locomotor apparatus, or an integrated strategy with a single apparatus with competences in multiple substrates. For robots, it is shown that the latter strategy is convenient if the two locomotion modes impose dynamics that are compatible with the operating range of the actuator used in the single locomotor apparatus. In this condition, secondary locomotion modes can be added with minor impact on the primary locomotion mode. In the DALER v9 prototype, ground locomotion can be performed with walkerons, introducing minimal losses in flight manoeuvrability and minimal increase in robot weight. In addition, robotics could provide new perspectives for understanding multi-modal locomotion in animals. For example, the concept of dynamically compatible locomotion modes could explain why the *Desmodus rotundus* does not apparently show compromises caused by terrestrial competences in a body optimized for flight. It is possible to speculate that this bat evolved a unique running gait compatible with a locomotor apparatus already used for flight [32].

The following observations can be drawn from the results obtained with the two prototypes presented in this chapter:

- The integration of the structure for multiple modes of locomotion allows to reduce the total mass of a multi-modal robot, which increases its locomotion performances.
- If different actuators are used for the two modes of locomotion, each mode can be individually optimized; the dynamics and the placement of the actuators are optimized specifically for one mode of locomotion. In our situation it led to better ground locomotion capabilities of the DALER v6. However, the total weight of the robot is high, which reduces its flight capabilities and its autonomy (i.e. a small battery has to be used).

- If the same locomotor system is to be used for multiple modes of locomotion, then these modes should be dynamically compatible (i.e. they should require compatible speeds and torques). Morphology optimization can be used in order to make two modes of locomotion dynamically compatible.
- A fully integrated design approach, where the structure and actuators are shared, allows to minimize the total weight of the robot. In our situation, it led to good flight capabilities of the DALER v9 and a high autonomy, however the ground locomotion capabilities are sub-optimal since the placement of the axis of rotation of the walkerons is constrained by flight requirements.

A solution to solve this latest constraint is the use of adaptive morphology, by adapting the morphology of the robot to a shape better suited to ground locomotion, the performances of the robot can be improved. Adaptive morphology has been studied on the DALER v9 and is the core of the next chapter.



## 4 Adaptive Morphology for Multi-Modal Locomotion

The previous chapter showed the benefits of the integrated design approach compared to the additive design approach. However, using a single locomotor apparatus for multiple modes of locomotion introduces issues in the design of the robot. Eventually, the different modes of locomotion could require different placements of the locomotor structures, positions of the centre of mass or body sizes. A solution that is introduced in this chapter is to use adaptive morphology to modify the shape of the robot, in order to accommodate the opposing constraints of two modes of locomotion. For the DALER v9 Adaptive, ground locomotion and forward flight require different position of the walkerons relatively to the centre of mass of the robot. Deployable wings provide morphological adaptation for switching from a wing shaped for flight to a more compact morphology adapted to ground locomotion; deployed wings maximize lift during flight, while folded wings enhance the efficiency of the robot on the ground by increasing the grip of the walkerons. This chapter presents the design of a robot identical to the DALER v9 but with adaptive morphology; this robot will be called DALER v9 Adaptive.

This chapter is partly based on the publication *A bioinspired multi-modal flying and walking robot* [46].



## 4.1 Introduction

The challenge of adapting a morphology mainly optimized for flight to one more suited for terrestrial locomotion is discussed in this chapter. Forward flight and walking require different positions of the centre of mass of the robot. For ground locomotion the centre of mass (CM) of the robot must be close to the centre of rotation of the walkerons to avoid the walkerons slipping on the ground (see Fig. 4.1.B). In flight the centre of mass must be instead far from the centre of rotation of the walkeron in order to create torques required to control the flight (see Fig. 4.1.A). Furthermore, for flight stability reasons, the centre of mass must be in front of the aerodynamic pressure of the wing. In this prototype, the use of foldable wings to adapt the morphology of the robot to either flight or ground locomotion is proposed. With reference to Fig. 4.1, when the wings are deployed, the robot has a flight-adapted morphology:

- The lift is augmented due to the large wingspan.
- The distance between the axis of rotation of the walkerons and the centre of mass is increased, enhancing flight manoeuvrability.

When the wings are folded, the morphology of the robot becomes suitable for ground locomotion:

- A short wingspan improves the robot's agility in cluttered terrestrial environments due to its reduced size.
- The axis of rotation of the walkerons is closer to the centre of mass, thus enhancing the grip between the walkerons and the ground.

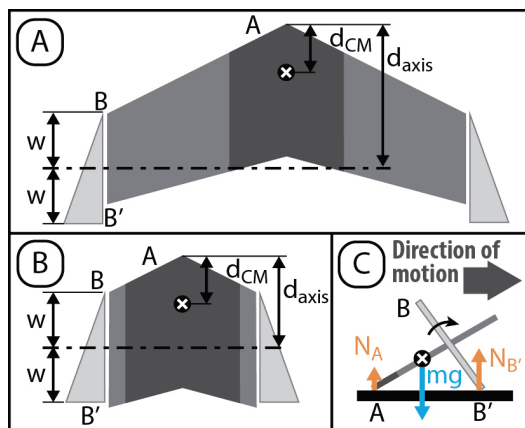


Figure 4.1: Model of the DALER v9 Adaptive. A) Robot seen from above with deployed wings. B) Robot seen from above with folded wings. C) Robot seen from the side walking on a flat terrain.



## 4.2. DALER v9 Adaptive Mechanical Design

The use of these deployable wings allows adaptation of the morphology of the robot and therefore, it satisfies the requirements on the relative positioning of the centre of mass and of the walkeron axis of rotation for the two modes of locomotion. Adaptive morphology is studied on the DALER v9 Adaptive prototype which has deployable wings as shown in Fig. 4.2.

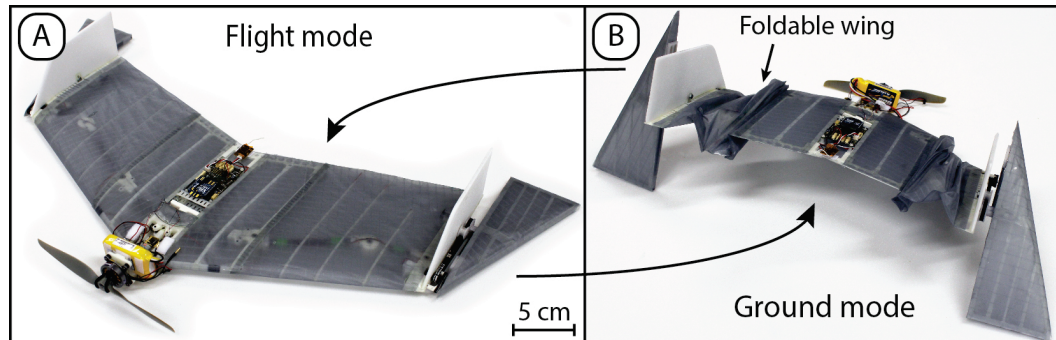


Figure 4.2: DALER v9 Adaptive, multi-modal flying and walking robot. The robot has deployable wings which adapt its morphology either to A) forward flight or to B) ground locomotion.

## 4.2 DALER v9 Adaptive Mechanical Design

This section presents the mechanical design of the DALER v9 Adaptive prototype. As illustrated in Fig. 4.3 the DALER v9 Adaptive comprises five main body sections: a central frame housing the propeller, electronics and battery, two foldable sections and two walkerons for flight control and ground locomotion. The robot has a wingspan of 72 cm and a weight of 391 g. The frame of the DALER v9 Adaptive is designed in order to minimize weight, while providing enough stiffness for efficient flight. To this aim, the structure has a central frame and multiple ribs connected together by carbon fiber spars. This frame is covered with Icarex, a lightweight polyester fabric, inextensible and resistant to wear.

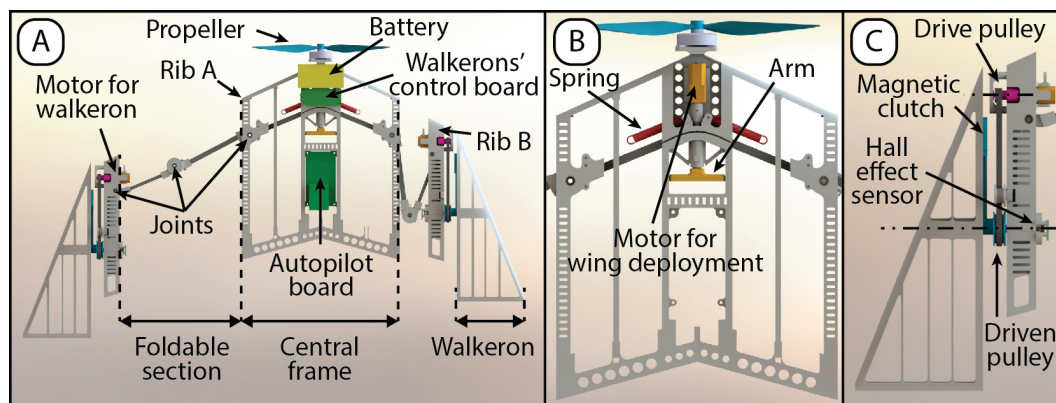


Figure 4.3: Mechanical design of the DALER v9 Adaptive. A) Left wing deployed and right wing folded. B) Central frame. C) Walkeron's drive mechanism.

## Chapter 4. Adaptive Morphology for Multi-Modal Locomotion

---

Flight control and ground locomotion rely on a single locomotor system composed of two independent walkerons and their actuators. DC motors are housed in the external ribs (rib B) and are coupled with the walkerons using a synchronous belt. For control purposes, the angular positions of the walkerons are measured by Hall effect sensors, which detect the orientation of small magnets mounted on the walkerons' axis of rotation. The two foldable sections of the robot are equipped with an articulated frame controlled by a single DC motor. The foldable structure is composed of two carbon spars that are serially connected together and also to ribs A and B through revolute joints. Each foldable section is controlled by two separate cables, one to open and the other to close the wings. The two cables are connected to a double arm that is directly controlled by the DC motor. The arm is used instead of a pulley because it acts as a self-locking mechanism that prevents unwanted rotation of the motor when the wings are fully deployed or collapsed. The cable responsible for wing folding is connected to a spring and when the wing is deployed, the spring is pulled and the covering fabric is tensioned. This is of paramount importance in order to pre-load the fabric to avoid fluttering, thus maximizing flight efficiency. Furthermore, the spring can absorb energy, limiting damage to the wings in case of a frontal collision. If a wing collapses due to a collision, the spring is stretched. Each spring can absorb a maximum energy of 12.5 J which corresponds to a collision at 8.4 m/s. Wing morphing can be performed in 1 to 2 seconds. The length of each foldable section can be reduced from 17 cm to 6 cm (65%); this corresponds to a 30% reduction in the overall wingspan.

### 4.3 Ground Locomotion Measurements

This section presents measurements of the cost of transport (COT) of the robot on the ground. In Fig. 4.4 the COT of the robot on a wooden floor as a function of its speed can be seen for different openings of the wings. For each measurement two complete revolutions of the walkerons were performed and the following parameters were measured:

- The time,  $t$ .
- The travelled distance,  $d$ .
- The current in the DC motors,  $I$ .
- The voltage applied to the DC motors,  $V$ .

A controller running at 100 Hz controls the rotational speed of the walkerons. At each update of the controller (every 10 ms) the current in both motors is measured along with their voltage. The electrical power is computed at each step and then low-pass filtered. At the end of the run, the mean power is computed and multiplied by the time of the run in order to find the total energy used for the run. Finally, the COT is computed by dividing the energy by the mass of the robot and by the travelled distance.

### 4.3. Ground Locomotion Measurements

Concerning the experiments presented in Fig. 4.4, the walkerons were set to seven different revolution speeds and each experiment was repeated five times. The smaller dots represent all the measurements and the larger dots represent the mean COT at the mean speed of the robot for the seven imposed rotational speeds of the walkerons. The three different makers' shapes (diamonds, triangles and squares) represent the configurations with the wings open, half-closed and fully closed respectively. With reference to Fig. 4.1 and Fig. 4.3 the width of the foldable section for the three different openings was set to 17 cm, 11 cm and 6 cm respectively, imposing a distance between the centre of mass and the axis of rotation of the walkerons ( $d_{axis} - d_{CM}$ ) of 13 cm, 11 cm and 9 cm.

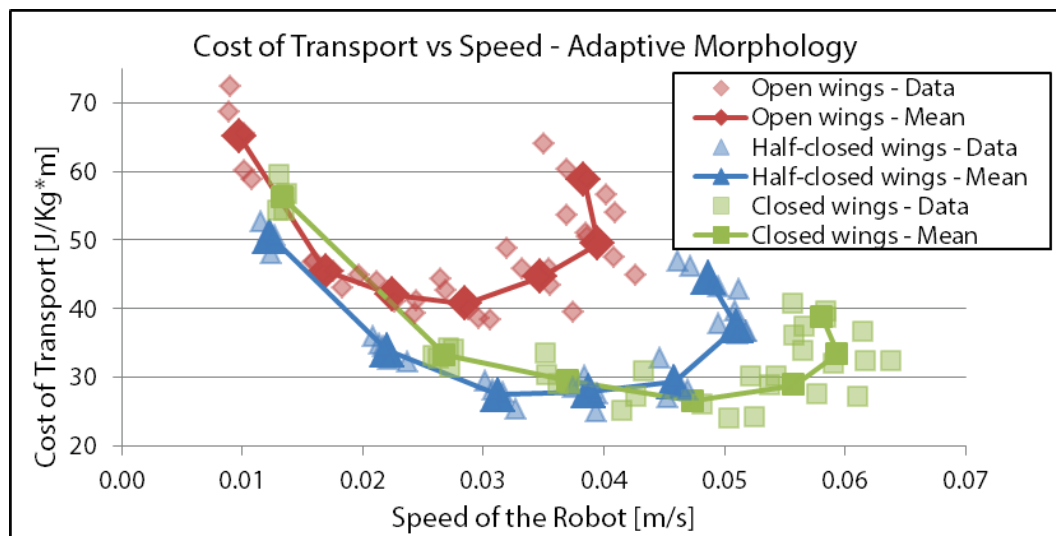


Figure 4.4: Cost of transport versus speed of the robot on the ground, with three different wing openings (open, half-closed and closed).

It can be seen that the three lines show the same trend; a high COT at low speeds, then a minimal COT at around 75% of the maximum rotational speed of the walkerons, and again a high COT at high rotational speeds of the walkerons. At high rotational speeds there is a sharp increase of COT due to the fact that the walkerons slip more on the floor. The COT of the robot when the wings are closed (i.e. folded) is much lower than the COT for open wings, especially at high speeds. Furthermore, the speed of the robot is much higher for the same rotational speed of the walkerons (35% increases). These two arguments clearly demonstrate the need and the advantage of having an adaptive morphology (i.e. foldable wings) for terrestrial locomotion.

Another interesting observation is that at speeds lower than 0.04 m/s the configuration with half-closed wings has a lower COT than the one with fully closed wings. This indicates that the morphology of the robot (i.e. wings opening) should be continuously adapted as a function of the speed to minimize the COT. This can be explained by the fact that, on one hand, when the wings are folded the centre of mass of the platform has to rise higher at each step than when

## Chapter 4. Adaptive Morphology for Multi-Modal Locomotion

the wings are open, while on the other hand, at low speeds there is static friction between the ground and the walkerons while at very high speeds the friction is mainly dynamic (i.e. lower), therefore the wings start to slip more. By adapting the morphology of the robot an optimal trade-off between centre of mass lifting and walkerons slippage can be found in order to minimize the cost of transport.

Figure 4.5 shows the same experiments but with a small wheel at the tip of the robot that is used to reduce the friction between the central frame of the robot and the ground. It can be seen that if this friction is reduced to almost zero the adaptive morphology has less benefits than previously and also that the robot travels much faster for the same rotational speed of the walkerons. In outdoor field applications, the friction of the central frame cannot be so drastically reduced, thus this situation will not happen, however it demonstrates the importance of maximizing the friction on the walkerons and minimizing the friction on the central frame. From these experiments it can be seen that COT values between 15 and 20 J/Kg·m at speeds of more than 0.1 m/s can be reached, similar to small running animals [54].

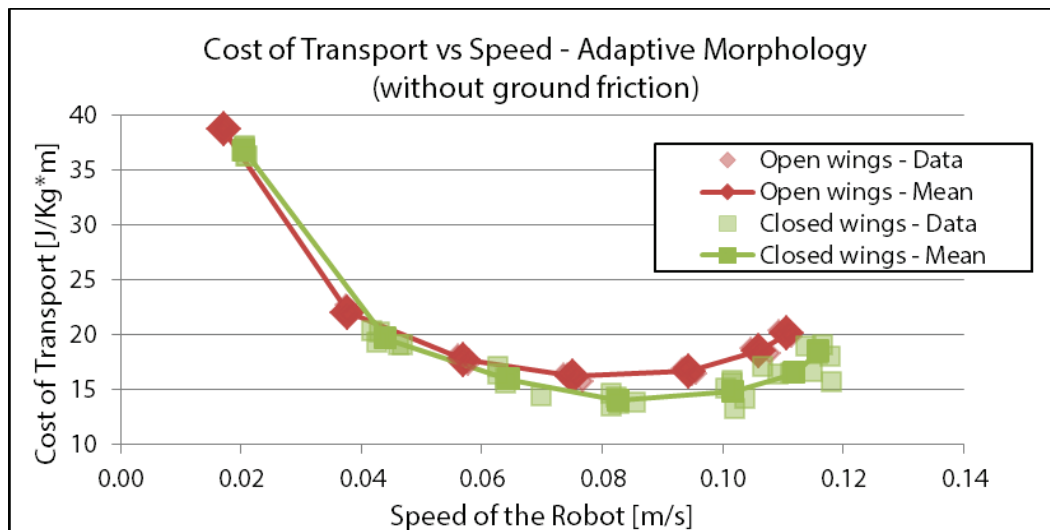


Figure 4.5: Cost of transport versus speed of the robot on the ground, with two different wing openings (open and closed) and a small wheel on the tip of the robot that is used to reduce friction with the ground.

### 4.4 Adaptive Morphology Model

This section has for objective to analyse the results presented in section 4.3 in order to establish a model of the cost of transport of the robot on the ground as a function of its morphology (i.e. the opening of the wings).

The experimental cost of transport is calculated from the following equations:

$$COT_{data} = \frac{E}{md} \quad (4.1)$$

$$E = Pt \quad (4.2)$$

$$P = UI \quad (4.3)$$

Where  $E$  is the energy,  $m$  is the mass of the robot,  $d$  is the travelled distance,  $P$  is the electrical power of the motor,  $t$  is the time and  $U$  and  $I$  are the voltage and the current in the motors. Therefore, the cost of transport can be directly calculated from the experimental data as:

$$COT_{data} = \frac{UI t}{md} \quad (4.4)$$

The theoretical cost of transport can be evaluated from the theoretical mechanical power:

$$P = \frac{M\omega}{\eta} \quad (4.5)$$

Thus,

$$COT_{model} = \frac{M\omega t}{\eta md} \quad (4.6)$$

Where  $M$  is the torque that must be applied by the DC motors which control the walkerons,  $\omega$  is the rotational speed of the motors and  $\eta$  is the efficiency of the motors. The torque required by the DC motor can be evaluated based on Fig. 3.3.C. By using Newton's and Euler's equations this torque can be evaluated as:

$$M = mg \frac{d_{CM} \cos \alpha [\cos \varphi - \mu \sin \varphi] + d_{axis} \mu \left[ \frac{w}{d_{axis}} \cos \varphi \sin \varphi + \sin \varphi \cos \alpha \right]}{\cos \varphi + \frac{d_{axis}}{w} \cos \alpha} \quad (4.7)$$

With,

$$\alpha = \sin^{-1} \left( \frac{w}{d_{axis}} \sin \varphi \right) \quad (4.8)$$

## Chapter 4. Adaptive Morphology for Multi-Modal Locomotion

Where  $d_{CM}$  is the distance between the tip of the robot and the center of mass, which changes with the morphology of the robot,  $\alpha$  is the angle between the central frame of the robot and the horizontal,  $\varphi$  is the angle between the walkerons and the horizontal,  $d_{axis}$  is the distance between the tip of the robot and the axis of rotation of the walkerons, which changes as well with the morphology and  $w$  is the radius of the walkerons. It can be observed in eq. 4.7 that the torque increases when  $d_{axis}$  is close to  $d_{CM}$  (i.e. wings folded) and decreases when  $d_{axis}$  is larger than  $d_{CM}$  (i.e. wings deployed).

The efficiency of the motor as a function of its rotational speed can be evaluated from:

$$\eta = \frac{M\omega t}{UI} \quad (4.9)$$

Where,  $M$  is the torque given by eq. 4.7,  $\omega$  the rotational speed and  $U$  and  $I$  are the voltage and current measured in the motors during the experiments. Figure 4.6 shows the efficiency of the motors as a function of their rotational speed. The diamond, triangular and squared marker' shapes represents respectively the experiments with the wings open, half-closed and closed. The solid grey line shows the average of these three experiments and the black dotted line shows the second order polynomial fit of this average. Figure 4.7 shows the distance that is travelled by the robot for one revolution of the walkerons as a function of their rotational speed. The three dotted lines show the linear fit of the experiments with the wings open, half-closed and closed. The distance travelled by the robot decreases almost linearly with the increase of the rotational speed of the walkerons (i.e. the friction between the walkerons and the ground is lower at high speed) and the morphology of the robot (i.e. the distance between the centre of mass and the axis of rotation of the walkerons) changes the offset of this function.

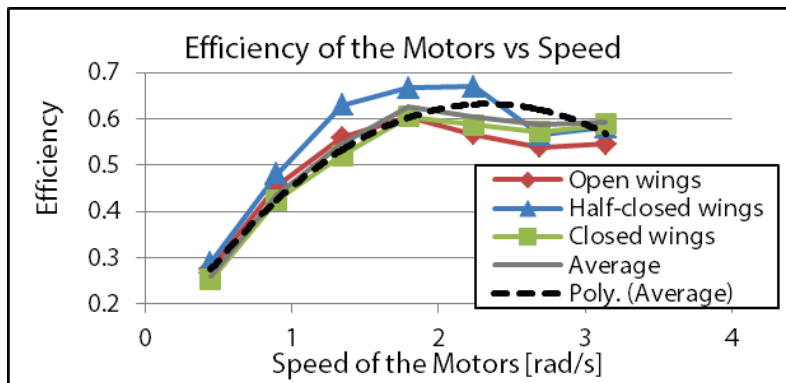


Figure 4.6: Efficiency of the DC motors as a function of their rotational speed.

Figures 4.6 and 4.7 allow to understand better the measurements of the cost of transport shown in Fig. 4.4. At low speeds, the motors are not efficient, which increases the COT. Then, there is an optimal rotational speed which minimizes the COT at around 75% of the maximal speed.

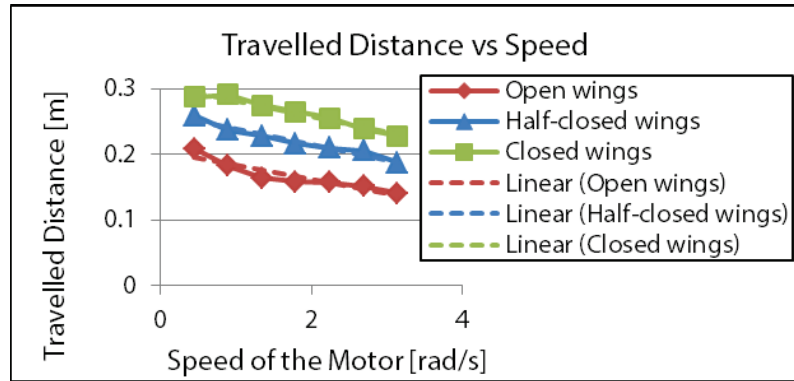


Figure 4.7: Travelled distance for one revolution of the walkerons as a function of their rotational speed.

At high speeds, the motors are again less efficient and the travelled distance is reduced due to the slippage of the walkerons on the ground. There is an optimal wing opening, depending on the speed of the robot, which optimizes the trade-off between centre of mass lifting (i.e. the centre of mass has to be lifted higher when the wings are folded) and walkerons' grip (i.e. the grip is higher when the wings are folded) and therefore minimizes the cost of transport.

The measurements from Fig. 4.4 can be fitted by three second order polynomial equations such as:  $f_i(x) = a_i x^2 + b_i x + c_i$  (see Fig. 4.8). The three equations for the three different openings of the wings have thus different  $a_i$ ,  $b_i$  and  $c_i$  coefficients. For each coefficient their three values can be used to find another second order polynomial fit. It can be observed from Fig. 4.8 that the model fits closely the data in the region around the minimum COT, which is the region of interest.

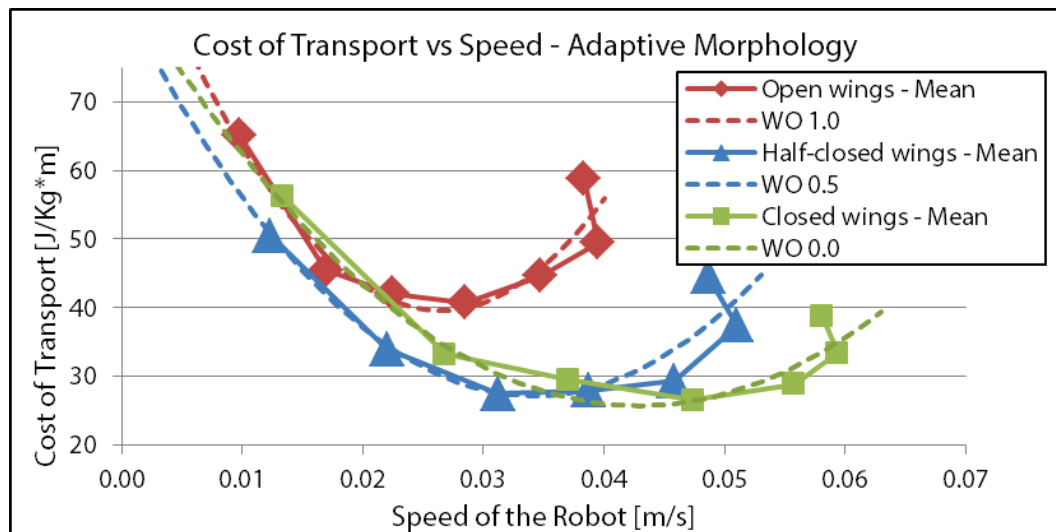


Figure 4.8: Comparison between measured data and model for the cost of transport.

## Chapter 4. Adaptive Morphology for Multi-Modal Locomotion

From these three polynomial fits, the cost of transport of the robot can be evaluated for any opening of the wings. Figure 4.9 shows the cost of transport for ten different wing openings (WO), from the wing completely opened, WO 1.0, to completely closed, WO 0.0. The thick solid lines show the minimum of the cost of transport as a function of the speed. The morphology of the robot that minimizes the cost of transport changes as a function of the speed of the robot, which is represented by the color of the thick solid line. This shows that the morphology of the robot should be continuously adapted as a function of the speed in order to minimize the cost of transport.

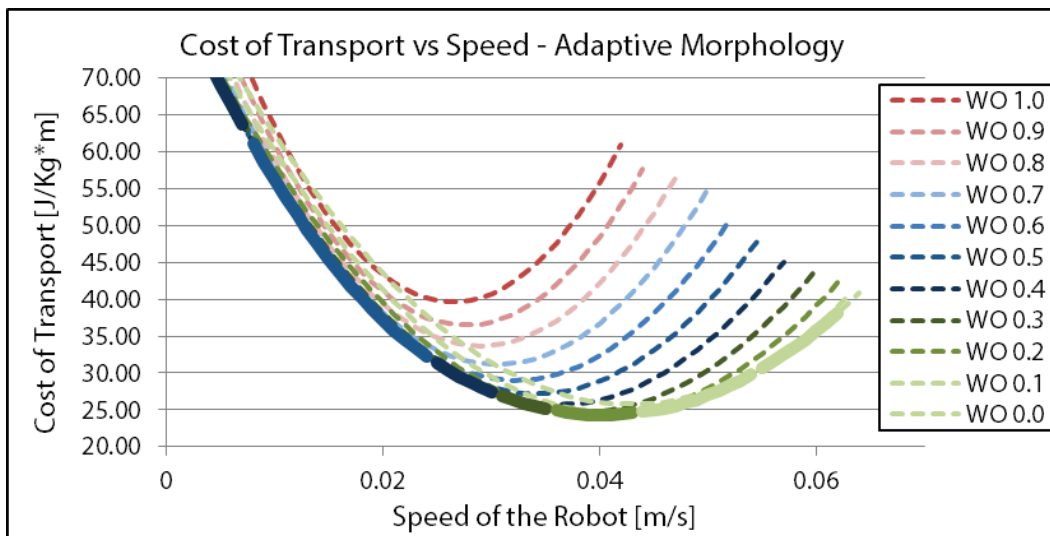


Figure 4.9: Cost of transport of the robot as a function of the wing opening.



## 4.5 DALER v9 Adaptive Locomotion Capabilities

Table 4.1 summarizes the performance of the robot, compared to the v9 without adaptive morphology and the v6. The same experiments have been performed in order to characterize the locomotion capabilities. Compared to the v9 without adaptive morphology, the maximum step that the robot can climb on is 6 cm instead of 4 cm, the maximum slope inclination is 9 ° instead of 7 °, the maximum speed is 6 cm/s instead of 4 cm/s and the maximum rotational speed is 24 °/s instead of 20 °/s. The ground locomotion capabilities are improved by adaptive morphology however, the deployable wings add weight to the robot. Thus, the battery has to be reduced in order to keep a constant wing loading. The 1.5 Ah battery (130 g) used on the v9 without adaptive morphology is replaced by a 1 Ah battery (90 g), representing a capacity loss of 33%. Nevertheless, the COT of the robot on the ground is reduced by approximately 35% thanks to adaptive morphology (see Fig. 4.4). Therefore, the autonomy of the robot on ground is the same for the prototypes with and without adaptive morphology (30 to 60 min depending on the terrain), while the speed is increased by 50% and with it the travelled distance. The flight performances are identical, only the autonomy is reduced by 33% for the version with adaptive morphology.

		DALER v6	DALER v9	DALER v9 Ad.	
Terrestrial	Obst.	Gap max.	12 cm (0.4 BL)	9 cm (0.25 BL)	9 cm (0.25 BL)
		Step max.	8 cm (1.2 BH)	4 cm (0.7 BH)	6 cm (1 BH)
		Slope max.	15 °	7 °	9 °
	Speed	Forward max.	12 cm/s (0.4 BL/s)	4 cm/s (0.15 BL/s)	6 cm/s (0.2 BL/s)
		Rotational max.	25 °/s	20 °/s	24 °/s
		Autonomy	15-30 min.	30-60 min.	30-60 min.
Aerial	Speed min.	8 m/s	6 m/s	6 m/s	
	Speed max.	14 m/s	20 m/s	20 m/s	
	Cont. pitch rate	-	120 °/s	120 °/s	
	Cont. roll rate	-	180 °/s	180 °/s	
	Autonomy	10-15 min.	25-30 min.	15-20 min.	
Battery capacity		0.7 Ah	1.5 Ah	1 Ah	

Table 4.1: Summary of performance of the DALER v9 Adaptive.

## 4.6 Adaptive Morphology Analysis

Table 4.2 shows the mass distribution and integration analyses of the v9 Adaptive. Since the mass of the battery is reduced by 40 g compared to the v9 without adaptive morphology, the total mass of the shared components is now 301 g. The mass added for the deployable wings is 42 g, which brings the total for the ground locomotion to 343 g. The total mass for the forward flight is 351 g and the total mass of the robot is 393 g. The mass integration value is 1.77, which is less than for the v9 without adaptive morphology (1.87) but still higher than the

## Chapter 4. Adaptive Morphology for Multi-Modal Locomotion

MultiMo-Bat [33] (1.69). This reduction is due to the additional mass of the deployable wings used only for ground locomotion and to the decreased mass of the battery.

Components		DALER v9 Mass [g]		DALER v9 Ad. Mass [g]	
Shared	Mechanics	162		162	
	Actuators	22		22	
	Electronics	27		27	
	Battery	130		90	
	$M_S$	341		301	
Ground	Mechanics	0		28	
	Actuators	0		14	
	Electronics	0		0	
	$M_G$	0		42	
	$M_G^{tot}$	$M_S + M_G$	341	$M_S + M_G$	343
Flight	Mechanics	10		10	
	Actuators	26		26	
	Electronics	14		14	
	$M_F$	50		50	
	$M_F^{tot}$	$M_S + M_F$	391	$M_S + M_F$	351
$M_{Robot}$		<b>391</b>		<b>393</b>	
Integration		$\frac{M_G^{tot} + M_F^{tot}}{M_{Robot}}$	<b>1.87</b>	$\frac{M_G^{tot} + M_F^{tot}}{M_{Robot}}$	<b>1.77</b>

Table 4.2: Mass distribution and integration analyses of the DALER v9 and v9 Adaptive.

### 4.7 Conclusion

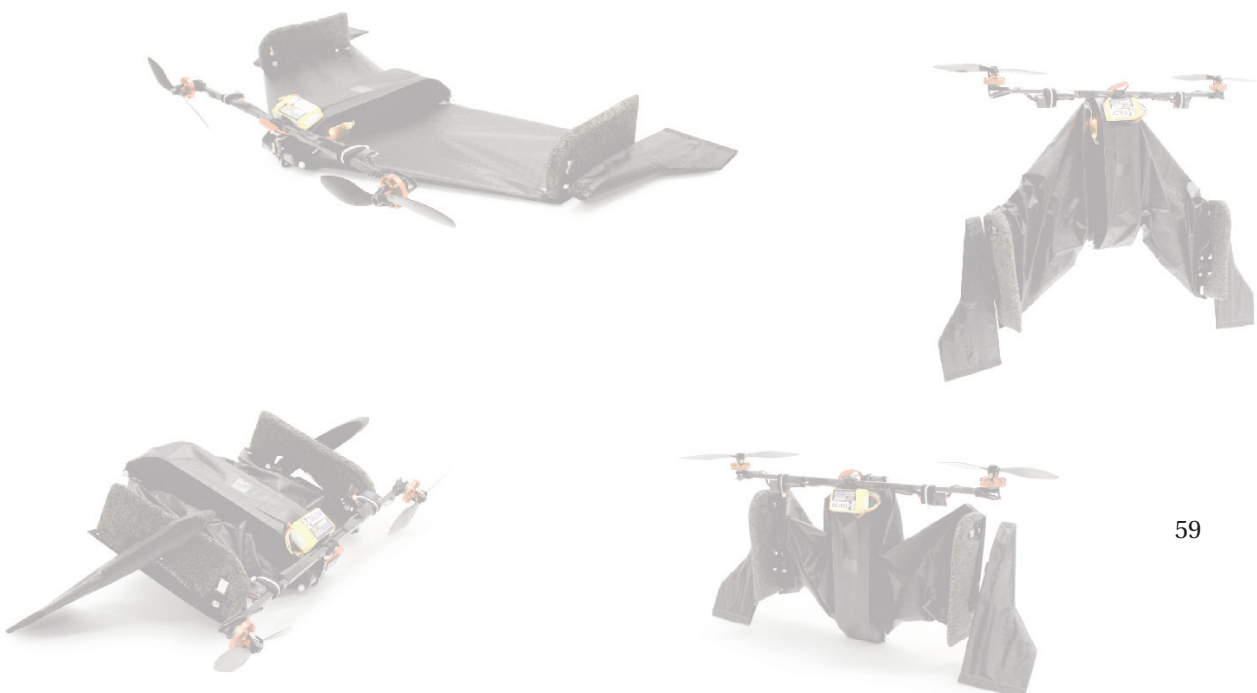
Many animals exploit adaptive morphologies in order to accommodate the requirements imposed by different modes of locomotion. This strategy is a good solution to shift trade-offs; a robot optimized for flight can improve its terrestrial capabilities with foldable wings. The following remarks can be made about the results presented in this chapter:

- Adaptive morphology can be used to increase the performance of a robot if two modes of locomotion impose opposing constraints on the placement of the center of mass. In our situation, the cost of transport of the robot on the ground is reduced by approximately 35% thanks to adaptive morphology and its speed is increased by 50%.
- Adaptive morphology has a cost in terms of weight added to the robot. In our situation, the weight added is balanced by a reduction of the weight of the battery. The forward flight performances are conserved but the autonomy is reduced by 33%.
- The mission requirements will decide if adaptive morphology is beneficial or not, depending on the distance that must be travelled in the air and on the ground.

## 5 Integrated & Adaptive Robot with Three Modes of Locomotion

A robot capable of forward flight and ground locomotion can be used in many applications such as exploration, search-and-rescue or monitoring of the environment. Forward flight can be used to quickly travel over long distances while ground locomotion can be used to explore a small region of interest. In order to be fully functional, such a robot must be capable to transition between these two modes of locomotion thus, it should be capable to take-off vertically and to hover in order to get back to the air autonomously. This additional mode of locomotion increases the versatility of the robot, yet it increases as well weight and complexity. This weight can be minimized by using the integrated design approach, as demonstrated in Chapter 3, and the efficiency in the hover mode of locomotion can be improve by adaptive morphology. This chapter presents, as a proof of concept, a robot capable of three modes of locomotion which is designed according to the integrated design approach and which has an adaptive morphology.

This chapter is based on the publication *DALER: Deployable Air Land Exploration Robot* [55].



### 5.1 Introduction

This chapter presents the design of the final version of the DALER prototype, the v11. This prototype can now additionally upright itself and hover. At first, the hovering configuration is discussed, and then the mechanical design of the prototype is explained. The locomotion results obtained with the prototype are analysed and finally, the mass integration metrics and a versatility metrics are used to evaluate the performance of the robot compared to other DALER prototypes presented in the previous chapters and to two other multi-modal robots.

### 5.2 Platform Configuration

In order to enable hover locomotion while keeping the same configuration of walkerons used both to control the flight and to walk on the ground (as for the DALER v9), a solution is to provide airflow on these walkerons during hover. The solution that requires the less additional actuators is to position one propeller above each walkeron (see Chapter 2). The ground and forward flight modes of locomotion require different placement of the center of mass of the robot (see Chapter 4). For ground locomotion, the axis of rotation of the walkerons must be close to the center of mass of the robot in order to avoid walkerons slipping on the ground, whereas for the forward flight the axis of rotation must be far from the center of mass in order to provide a sufficient torque to control the platform (see Fig. 5.1.A). Hover locomotion requires higher controllability than forward flight for stability reasons, which could be achieved by faster motion of the walkerons. Since the DC motors are already actuated at their maximum speed, another solution is to increase the distance between the axis of rotation of the walkerons and the center of mass during hover. The deployable wings must therefore take three different configurations in order to satisfy the constraints of the three modes of locomotion. Figures 5.1.B and C show the robot in these three different configurations for two different solutions of mounting propellers in order to provide airflow on the walkerons.

A solution presented in Fig. 5.1.B is to mount the propellers on the extremities of the deployable wings. The advantage of this solution is to have at any time the propellers above the walkerons, which ensures to have a constant airflow even during the transitions between hover and forward flight. However, this solution has many drawbacks; it adds weight on the extremities of the wings, which requires to increase the stiffness of all the deployable structure and consequently it increases the weight of the platform, moreover this weight increases the inertia in forward flight, and thus decreases the agility of the robot. In order to keep a good position of the centre of mass for forward flight and to keep the propellers away from the structure during hovering, brushless motors need to be mounted on carbon tubes, which increases the weight. During ground locomotion the propellers go higher towards the top and thus touch the ground. Finally, the cables which provide power to the brushless motors are relatively rigid and thus they increase the force needed to actuate the deployable mechanism of the foldable wings.

## 5.2. Platform Configuration

A second solution, presented in Fig. 5.1.C, is to mount the propellers on each extremities of a carbon tube mounted on the central frame of the robot. This solution has the advantage of solving all the drawbacks of the first solution, however it has two other inconveniences. First, during ground locomotion the propellers are slightly larger than the folded wings and second, the transitions between hover locomotion and forward flight are more difficult since, when the wings are fully deployed for forward flight, the walkerons are not any more in the airflow of the propellers. This second solution has more advantages than the first one and leads to a simpler design and is therefore selected.

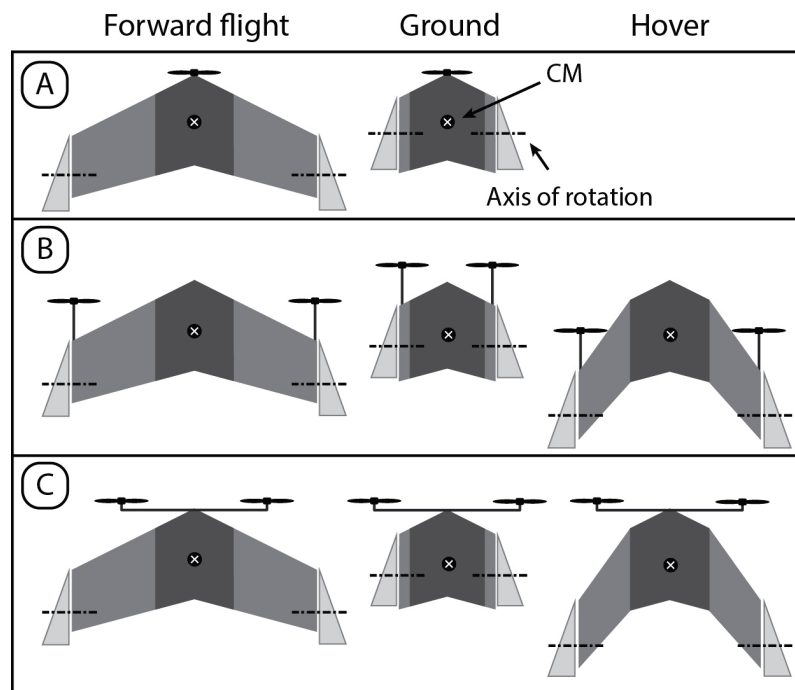


Figure 5.1: Solutions for adding hovering capabilities. A) Previous configuration of the robot capable of forward flight and walking on the ground, DALER v9 Adaptive. B) Solution 1, one propeller mounted on each extremities of the wings. C) Solution 2, propellers mounted on a carbon tube mounted on the central frame of the robot.

### 5.3 DALER v11 Mechanical Design

Figure 5.2 shows the mechanical design of the DALER v11 prototype. The robot is composed of five main sections: a central frame, two foldable sections and two walkerons. The skin of the wings is glued on the central ribs A and on the external ribs B. The skin is tensioned by the foldable mechanism while it is in the flight configuration. The two ribs A provide a casing which protects all the electronics and the wings' actuators. The central frame consist mainly in a carbon tube on which many parts are mounted. On this central tube, plastic parts are mounted to hold the shoulder joints, the cables for the parallelism of rib B, the tube on which the two brushless motors are mounted and the electronics. The foldable part of the wing is composed of two carbon fibre tubes and three joints connecting rib A to rib B. This structure transmits the forces between the central frame and the rib B. Cables are used to keep the parallelism between the central frame and the rib B, which are tensioned using turnbuckles. This solution is lighter than using two serial four-bar mechanisms and minimizes the backlash in the structure.

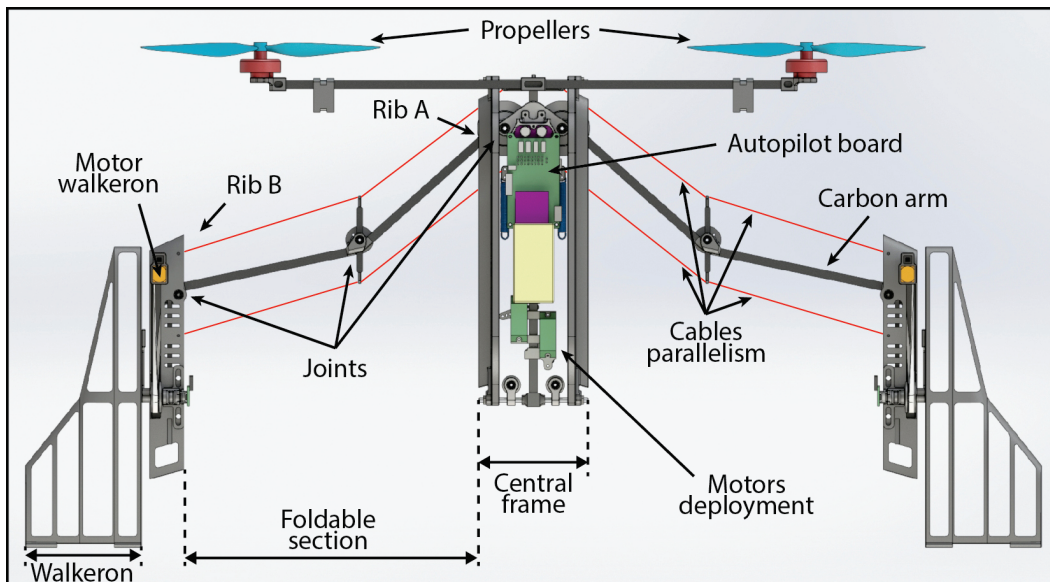


Figure 5.2: Mechanical design of the DALER v11. The prototype is composed of five main sections: one central frame, two foldable sections and two walkerons.

Figure 5.3 shows the three different configurations that the robot can take; flight, hover and ground configurations. In the flight configuration the two joints (i.e. elbows and shoulders) are fully deployed, leading to a half-wingspan of 371 mm and a distance between the center of mass and the axis of rotation of 119 mm. This configuration with widely spread wings offers good flight performances; the center of mass is positioned just in front of the aerodynamic pressure center and the large wingspan provides a high lift force. In the hover configuration, the shoulder joints are fully closed while the elbow joints are deployed. This configuration gives the largest possible distance between the center of mass of the platform and the center of rotation of the walkerons, thus increasing the manoeuvrability of the platform by increasing the torque produced by the walkerons. Furthermore, this configuration brings the walkerons below the propellers (i.e. in their airflow), which is essential for the hover control. The reduced wingspan during hover (17% wingspan reduction) reduces the impact of the wind on the platform and allows to go through smaller openings. In the last configuration, the ground configuration, all the joints are fully closed. The half-wingspan of the robot is reduced to its minimum, 245 mm (34% wingspan reduction), and the distance between the center of mass and the center of rotation of the walkerons as well, 36 mm only. This configuration maximizes the grip of the walkerons on the ground and allows to go through small gaps.

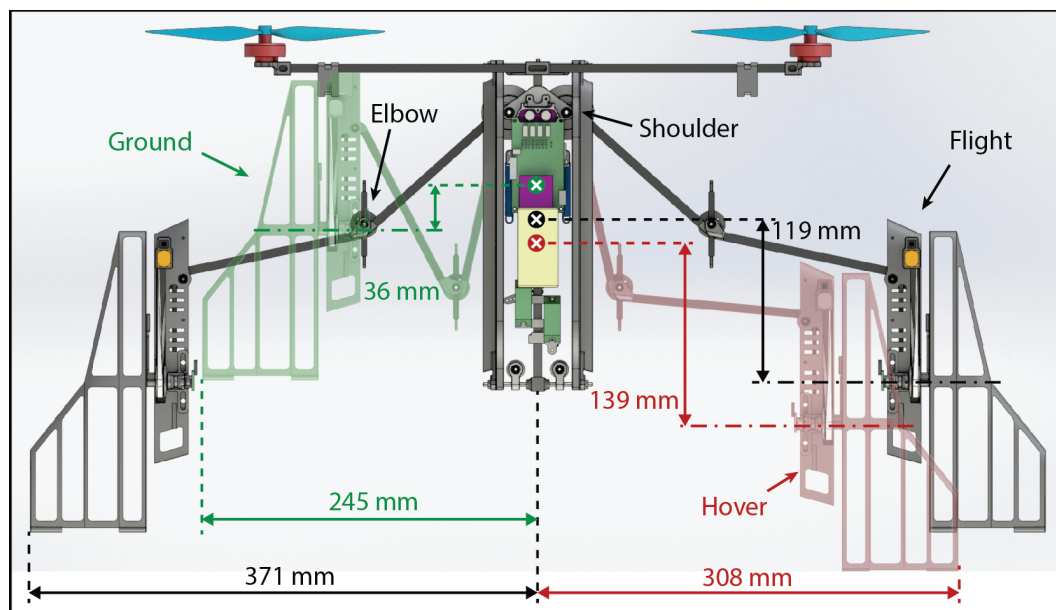


Figure 5.3: Morphology configurations of the DALER v11; the flight configuration (main image of the robot in colors), the hover configuration (red image on the right) and the ground configuration (green image on the left). The half-wingspan and the distance between the center of mass and the center of rotation of the walkerons are (371 mm; 119 mm), (308 mm; 139 mm) and (245 mm; 36 mm) for the flight, hover and ground configurations respectively.

## Chapter 5. Integrated & Adaptive Robot with Three Modes of Locomotion

In Fig. 5.4 the mechanism which actuates the wings deployment is shown, only the cables actuating one wing are shown for simplicity reasons. Each servo motor is dedicated to the actuation of two joints; one servo controls both elbows at the same time and the other one both shoulders. A shoulder joint is composed of two pulleys; one pulley is used to deviate the cables towards the elbow joint and the other holds the first carbon tube of the arm. Each joint is connected to a double arm mounted on a servo motor by two cables; one cable for opening and one for closing (i.e. when one cable is released the other one is pulled). The double arms of the servo motors can rotate 180 degrees, thus once in the open or closed positions (i.e. with the arm parallel with the cables) the cables do not produce any torque on the servo motors and the system is locked, reducing the power required by the servo motors to keep their positions. The diameter of each pulley is dimensioned in a way that the desired angles of the arms are reached when the servo motors move from 180 degrees. The two servo motors are mounted on plastic parts which can slide along the central tube. The servo motors are pulled backwards by cables which are pre-tensioned by springs. Thanks to this solution one of the two cables on each servo motor is always tensioned, reducing the backlash in the wings and providing tension in the skin. Furthermore, in case of a collision on the wings, the springs will absorb the energy of the impact and will prevent the deployable mechanism from breaking.

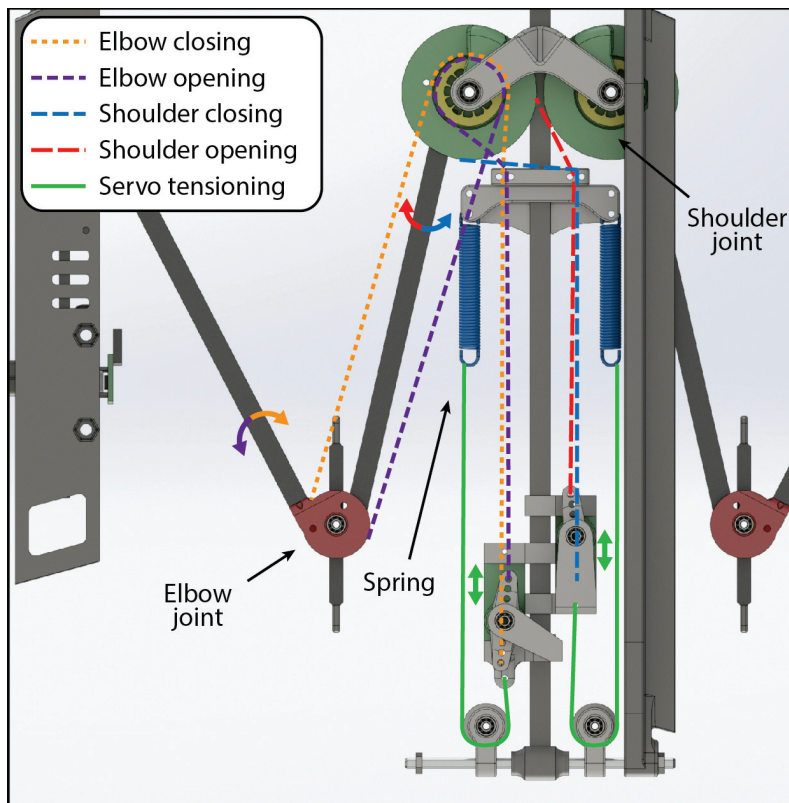


Figure 5.4: Wings' actuation mechanism.



### 5.3. DALER v11 Mechanical Design

The mechanical design of rib B and of the actuation of a walkeron is shown by Fig. 5.5. Rib B is reinforced by a carbon fibre tube which connects firmly the joint, the DC motor, the part that holds the axis of rotation of the walkeron and the two rods which hold the cables for the parallelism. The DC motor is held by a plastic part mounted on a carbon fibre tube and actuates the drive pulley. This drive pulley is connected to the driven pulley by a synchronous belt. This belt can be tensioned since the part which holds the walkeron's axis can slide on the rib B (held by two screws). The walkeron is connected to the driven pulley by magnets, therefore if the torque applied on the walkeron, in case of a collision, is greater than the holding torque of the magnets the walkeron will disengage instead of damaging the gears of the DC motor. A radially magnetised magnet is mounted on the axis of rotation of the walkeron and an Hall effect sensor is used to read the angle of the walkeron. The walkeron is made of a 3D printed plastic part reinforced with carbon fibre blades and covered by the same fabric used for the wings.

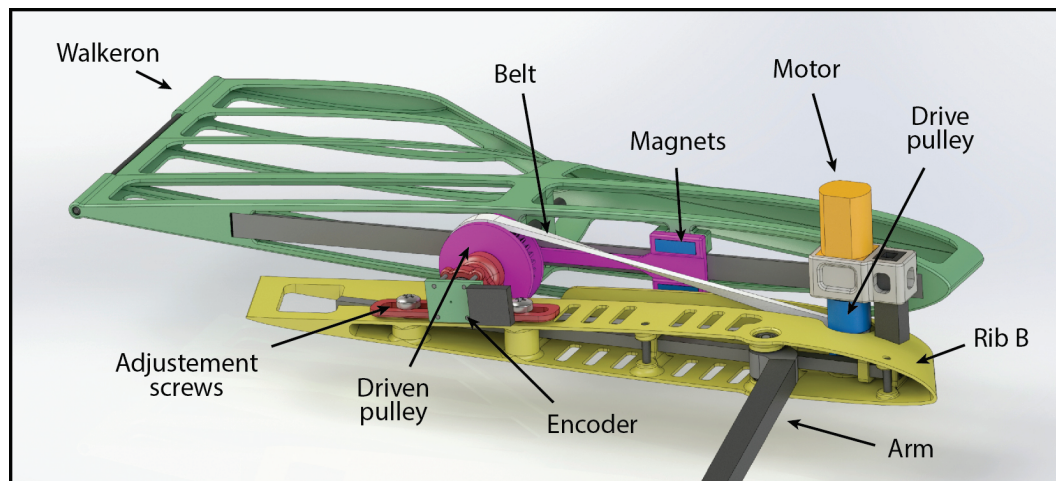


Figure 5.5: Mechanical design of the left rib B and its walkeron.

### 5.4 DALER v11 Prototype

This section presents the results of the manufactured DALER v11 prototype. Figure 5.6 shows A) the robot and B-D) enlarged pictures of the important parts of the design of the robot. The two brushless motors are mounted on a carbon fibre tube attached to the main frame of the robot, the ESCs which control the brushless motors are also mounted on this tube, next to the motors. The battery is attached with Velcro on top of the central frame, in order to be easily replaced. A winglet is added on each extremities of the wing, they increase the stability in the Y-axis during flight and enclose the DC motors and the transmission for the walkerons as shown in D. The coupling system that allows to disengage the walkerons in case of a collision, thus protecting the DC motor, is shown in B. A small wheel positioned at the tip of the central frame is shown in C, this wheel greatly reduces the friction with the ground while the robot is walking on flat terrains (e.g. asphalt, parquet, carpet) and C also shows the bolts that allow to adjust the position of the central frame's ribs. By pulling these ribs towards the center of the robot, the skin of the wings can be tensioned.

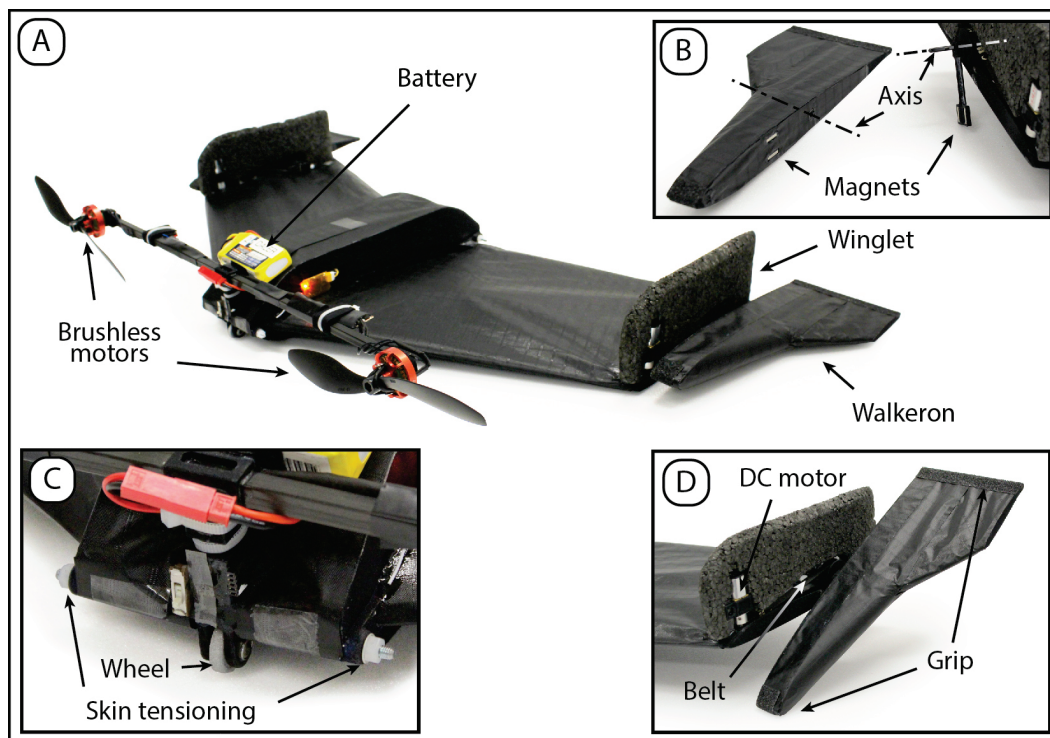


Figure 5.6: DALER v11 prototype. A) Placement of the brushless motors, battery, winglets and walkerons. B) System that allows to disengage the walkerons in case of a collision. C) Small wheel at the tip of the robot and bolts used to tighten the skin on the wings. D) DC motor, transmission and walkeron.

#### 5.4. DALER v11 Prototype

Figure 5.7 shows the different morphologies of the robot; from left to right, forward flight, ground and hover modes of locomotion. The measured wingspans, positions of axis of rotation and placements of center of mass are identical to the ones predicted by the CAD presented in Fig. 5.3. The robot can go from one morphology to another in less than one second.

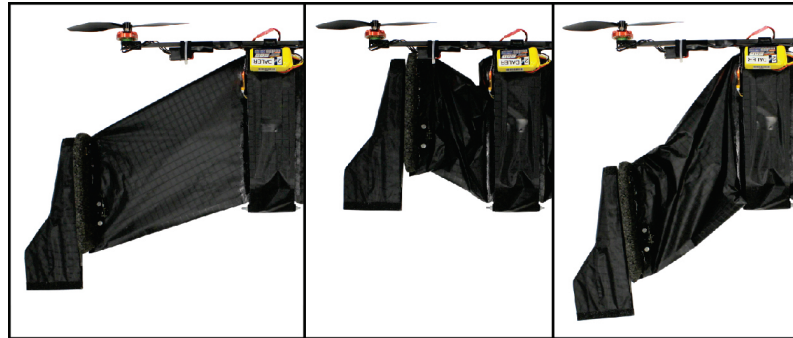


Figure 5.7: Morphology configurations of the DALER v11 prototype. From left to right, forward flight, ground and hover modes of locomotion morphologies.

Figure 5.8 shows the robot in the different modes; A) forward flight, B) hover, C) ground locomotion and D) shows the uprighted position. The robot should be capable to transition back and forth between forward flight and hover, land either in forward flight or in hover, upright itself from the ground locomotion configuration (C) to the take-off ready position (D), take-off from the ground in hover and finally be launched by hand by an operator either in hover or in forward flight (as indicated by the arrows).

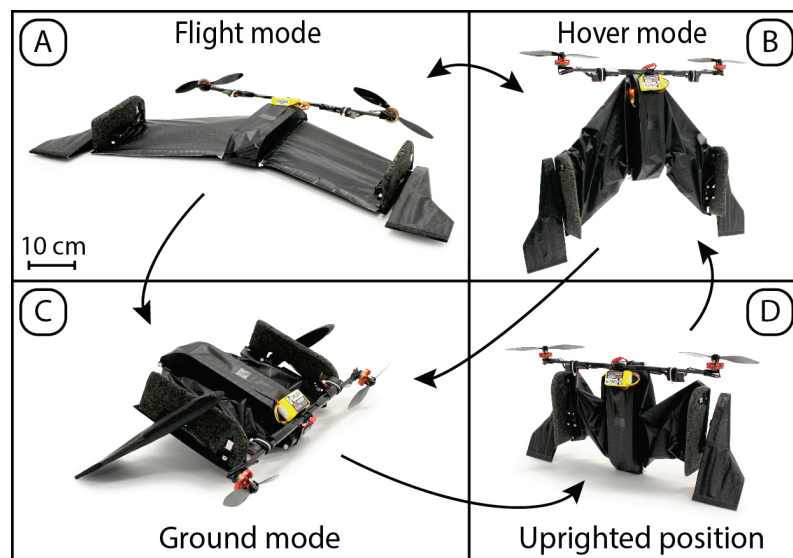


Figure 5.8: Modes of locomotion of the DALER v11 prototype. The arrows indicate the different possible transitions between the modes of locomotion.

## 5.5 Electronics Design

This section presents the electronics that is used to control the different subsystems of the robot (see Fig. 5.9). The high level control is implemented on an autopilot board developed at the *Laboratory of Intelligent Systems*, called *MAV'RIC*. This autopilot computes the attitude of the robot by means of an Inertial Measurement Unit (IMU), comprising a 3 axis gyroscope, a 3 axis accelerometer and a 3 axis magnetometer. A complementary filter fuses the information from these sensors and computes the output that must be sent to the actuators depending on the mode of locomotion, the inputs from the remote control and the ground station. The autopilot communicates by UART with a board which is dedicated to control the DC and servo motors. This DC board controller has been developed specifically for the DALER prototypes. It can control two DC motors (providing up to 30 A per motor) and 4 servo motors (providing up to 5 A in total). It can also measure the current drawn by the DC motors and send it back to the main autopilot for monitoring. Two servo motors are controlled by the DC board controller which actuate the deployable mechanism of the wings. The two DC motors controlled by this board actuate the walkerons. Radially magnetized magnets are mounted on the axis of rotation of the walkerons and magnetic encoders measure the orientation of these magnets. The DC board controller measures the values of these encoders through an SPI communication. The DC board can therefore control the walkerons in position, for hover and flight control, and in speed, for ground locomotion. Finally, the autopilot sends PWM signals to the two ESCs that control the brushless motors actuating the two propellers.

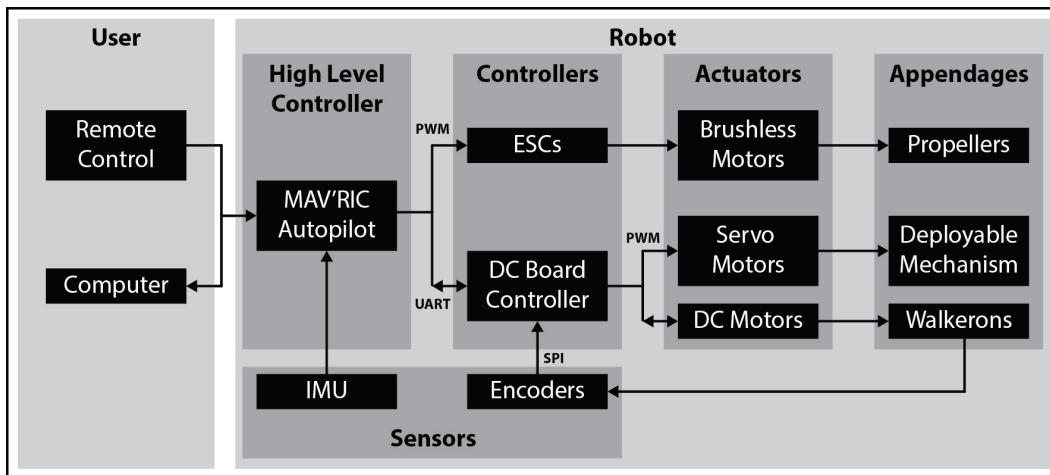


Figure 5.9: Schematic of the electronics of the DALER prototypes. An autopilot is responsible for the high level control of the robot which takes as input the commands from the user and from the IMU and then sends the commands to the low level controllers, two ESCs which control the brushless motors for the propellers and one DC board controller which controls two servo motors for the deployable wings and two DC motors for the walkerons.

## 5.6 DALER v11 Locomotion Capabilities

This section presents the locomotion capabilities of the robot, Table 5.1 summarizes the performance of the DALER v11 prototype compared to the DALER v9 Adaptive (see Chapter 4). The same ground experiments as presented in Chapters 3 and 4 for the v6, v9 and v9 Adaptive prototypes have been performed. The maximum gap that the robot can overcome is 9 cm. The maximum step that the robot can climb is 6 cm, which corresponds to 1 body-height (BH). The maximum upward slope, on a wooden floor, that the robot can walk on is  $15^\circ$ , which is more than for the v9 Adaptive ( $9^\circ$ ). The maximum forward speed measured on a flat wooden floor is 7 cm/s (0.23 BL/s) and the maximum rotational speed on spot of the robot is  $28^\circ/s$  (13 s for one complete revolution). On a flat wooden surface the maximum autonomy has been measured at close to 30 minutes and in rough terrains the robot can walk for about 15 minutes with a full battery (3 cells LiPo, 0.5 Ah). The prototype has been tested on different terrains, Fig. 5.10.a shows the robot A) on parquet, B) on slippery marble, C) on asphalt, D) on grass, E) going down a step and F) walking on a small stone. Figure 5.10.b shows the capability that the robot has to upright itself. The uprighting sequence takes less than 3 seconds to go from the horizontal position of the central frame (1) to the vertical take-off ready position (6).

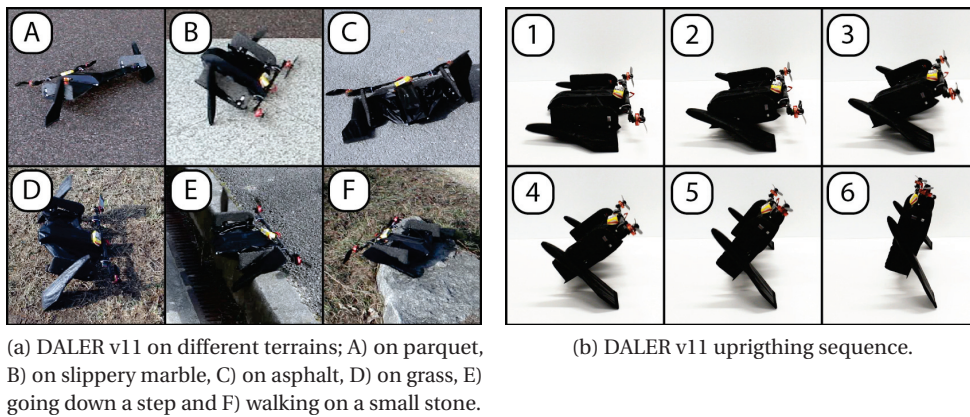


Figure 5.10: Ground locomotion capabilities of the DALER v11.

Forward flight has not been tested with this prototype. However, the flight performances should be similar as for the v9 and v9 Adaptive prototypes, the only difference is the weight added for the hovering components and for the adaptive morphology, which can be compensated by the use of a smaller battery. Table 5.1 gives the flight performances of the v9 Adaptive as a reference, yet the autonomy is estimated for the v11 prototype at 8 to 10 minutes. Hover flight has been tested with this prototype. A quaternion-based controller is used for the stabilization. The robot is given an attitude command as a unit quaternion. In the experiment shown in Fig. 5.12, the reference attitude is given by  $q_{ref} = [-0.123, -0.696, -0.123, 0.696]$ , which is equivalent to a heading of  $200^\circ$ , a pitch of  $90^\circ$ , and a roll of  $0^\circ$ . The robot manages to stay stable given this constant hovering command. The autonomy of the robot in hovering is about 4 to 5 minutes with a full battery (the robot in hover is shown in Fig. 5.11).

## Chapter 5. Integrated & Adaptive Robot with Three Modes of Locomotion

		DALER v9 Ad.	DALER v11	
Terrestrial	Speed	Gap max.	9 cm (0.25 BL)	9 cm (0.25 BL)
		Step max.	6 cm (1 BH)	6 cm (1 BH)
		Slope max.	9°	12°
	Obst.	Forward max.	6 cm/s (0.2 BL/s)	7 cm/s (0.23 BL/s)
		Rotational max.	24°/s	28°/s
		Autonomy	30-60 min.	15-30 min.
Aerial	Speed	Speed min.	6 m/s	-
		Speed max.	20 m/s	-
		Cont. pitch rate	120°/s	-
		Cont. roll rate	180°/s	-
		Flight autonomy	15-20 min.	(8-10 min.)
		Hover autonomy	NA	4-5 min.
Adaptive Morphology	Ground	Wingspan tot.	50 cm	49 cm
		Foldable section	6 cm	9 cm
		$d_{axis} - d_{CM}$	9 cm	4 cm
	Hover	Wingspan tot.	NA	62 cm
		Foldable section	NA	15 cm
		$d_{axis} - d_{CM}$	NA	14 cm
	Flight	Wingspan tot.	72 cm	74 cm
		Foldable section	17 cm	21 cm
		$d_{axis} - d_{CM}$	13 cm	12 cm
Battery capacity		1 Ah	0.5 Ah	

Table 5.1: Summary of performance of the DALER v11.



Figure 5.11: Hover capabilities of the DALER v11. Screen-shot from a hover flight video.

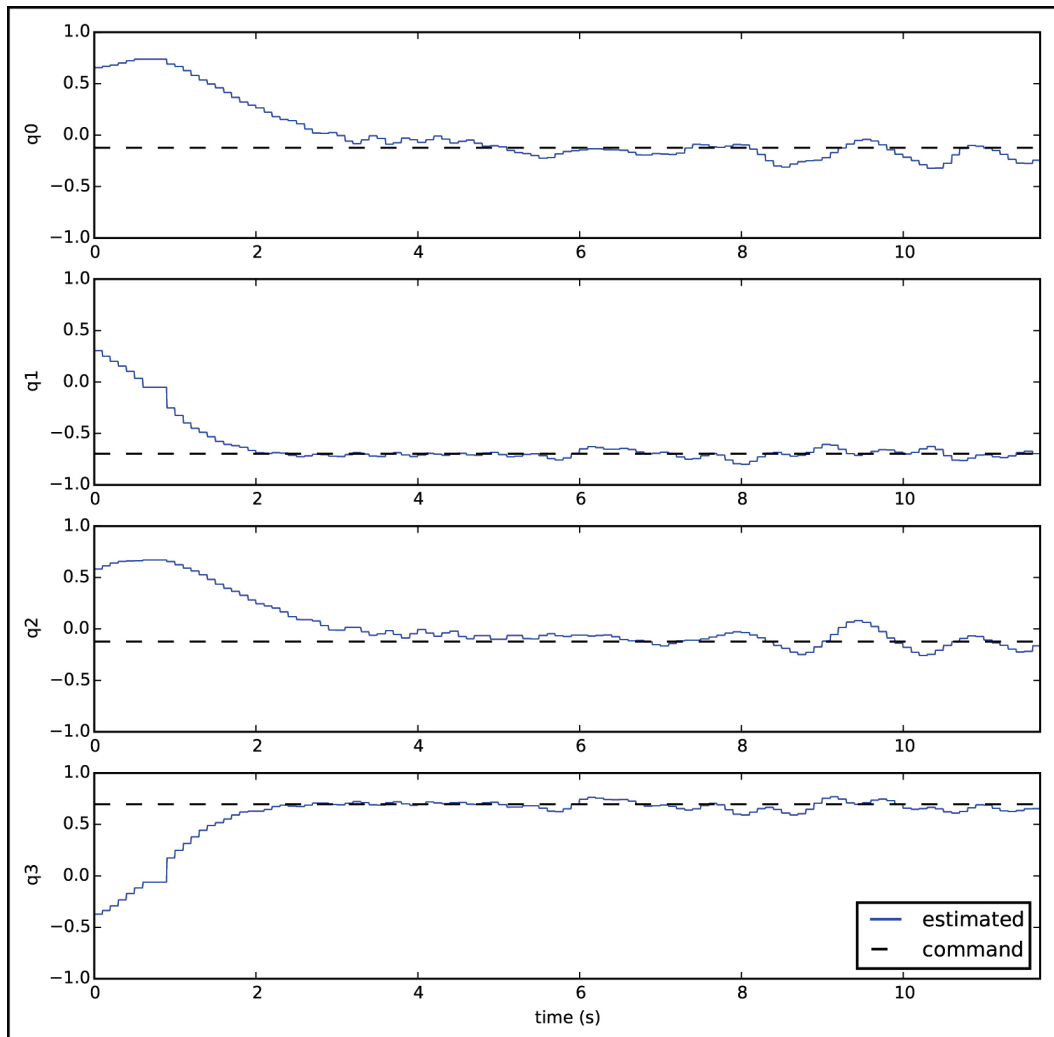


Figure 5.12: Attitude log during a hover flight. The given reference attitude is equivalent to a heading of  $200^\circ$ , a pitch of  $90^\circ$ , and a roll of  $0^\circ$  ( $q_{ref} = [-0.123, -0.696, -0.123, 0.696]$ ).

### 5.7 Multi-Modal Locomotion Analysis

This section first presents the mass distribution and integration analyses of the DALER v11 compared to other DALER prototypes and to other flying robots. Then, the DALER v11 is evaluated against other multi-modal robots, based on versatility and complexity metrics.

#### 5.7.1 Mass Distribution & Integration Analyses

The level of integration of the prototype has been evaluated based on the method defined by [33] (as explained in section 3.4). Table 5.2 provides the mass distribution of the prototype, compared to the DALER v9 Adaptive. The components are sorted into four categories; the components shared for the three modes of locomotion, those added for the adaptive morphology (i.e. the deployable wings), the components used only for forward flight and those used only for hover. Figure 5.13 gives a visual representation of the mass distribution; each color represents one of the four categories.

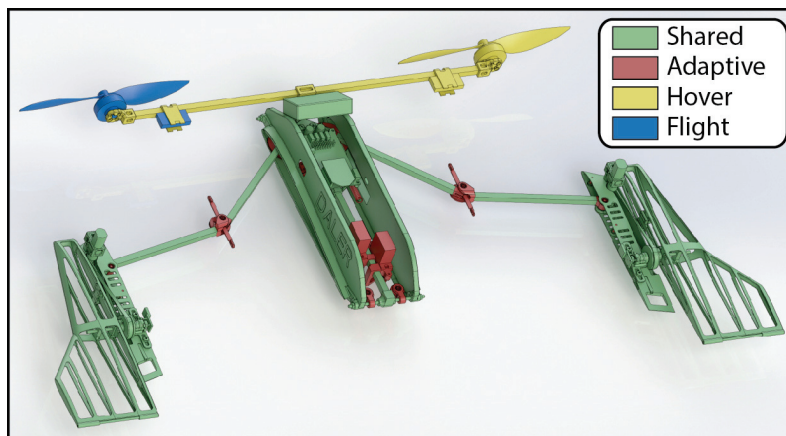


Figure 5.13: Mass distribution by modes of locomotion of the components.

The shared components are divided into four sub-categories: the *Mechanics* which is composed of all the parts which are needed to build a fixed wing without deployable wings (i.e. central frame, ribs, carbon rods, walkerons, transmission and fabric), the *Actuators* which are the DC motors that actuate the walkerons, the *Electronics* which includes the autopilot board, the DC board, the satellite receiver, the walkerons' encoders and the XBee module and finally the *Battery*. These shared components weigh a total of 260 g. The components which are added only for the adaptive morphology includes all the joints, bearings, springs, cables and servo motors which are added to include the folding of the wings. The mass added for having adaptive morphology is 88 g. That mass is shared between the hover and ground modes of locomotion since both benefit from adapting the morphology of the robot from the original forward flight configuration, which does not need adaptive morphology. There are no components added only for ground locomotion, thus the weight of the ground mode of locomotion is the sum of the shared components and of half of the adaptive morphology, which represents



## 5.7. Multi-Modal Locomotion Analysis

304 g. The parts used only for the flight are one propulsion system (i.e. one brushless motor, one propeller and a speed controller) and the two winglets, these components weigh 44 g in total, which brings the mass for the flight mode of locomotion to 304 g. The parts added for hovering are a second propulsion system and the parts that hold the brushless motors. These components weigh 64 g, which brings the total mass for the hover mode of locomotion to 368 g. The total mass of the robot is 456 g. The mass integration value of the DALER v11 prototype is 2.14 according to the metric defined by [33] ( $Int. = (M_G^{tot} + M_F^{tot} + M_H^{tot})/M_{Robot}$ ). A complete integration of the modes of locomotion would represent a mass integration value of 3 and no integration would be 1. There is no other multi-modal robot with three modes of locomotion which has been evaluated with this metrics, therefore no comparison can be made. Nevertheless, this prototype can be used as a benchmark for new designs.

Components		DALER v9 Ad. Mass [g]	DALER v11 Mass [g]
Shared	Mechanics	162	141
	Actuators	22	23
	Electronics	27	47
	Battery	90	49
	$M_S$	301	260
Adap.	Mechanics	28	60
	Actuators	14	28
	$M_A$	42	88
	$M_G$	0	0
Gr.	$M_G^{tot}$	$M_S + M_A + M_G$ 343	$M_S + \frac{M_A}{2} + M_G$ 304
Flight	Mechanics	10	9
	Actuators	26	25
	Electronics	14	10
	$M_F$	50	44
	$M_F^{tot}$	$M_S + M_F$ 351	$M_S + M_F$ 304
Hover	Mechanics		25
	Actuators		25
	Electronics		14
	$M_H$		64
	$M_H^{tot}$		$M_S + \frac{M_A}{2} + M_H$ 368
	$M_{Robot}$	<b>393</b>	<b>456</b>
	Integration	$\frac{M_G^{tot} + M_F^{tot}}{M_{Robot}}$ <b>1.77</b>	$\frac{M_G^{tot} + M_F^{tot} + M_H^{tot}}{M_{Robot}}$ <b>2.14</b>

Table 5.2: Mass distribution and integration analyses of the DALER v9 Adaptive and v11.

## Chapter 5. Integrated & Adaptive Robot with Three Modes of Locomotion

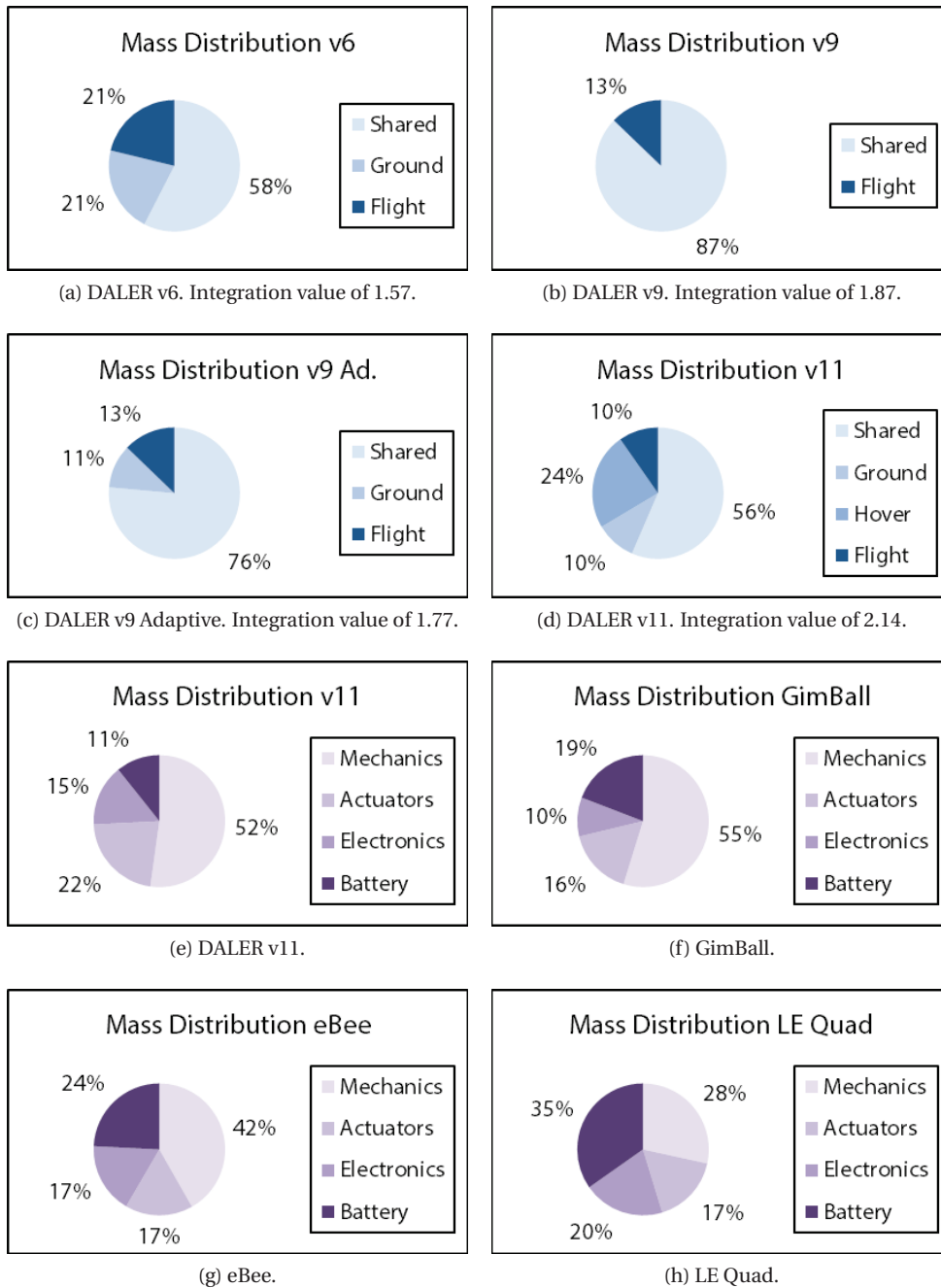


Figure 5.14: Mass distribution by modes of locomotion of a) the v6, b) the v9, c) the v9 Adaptive and d) the v11. And mass distribution by components' purpose of e) the v11, f) the GimBall robot, g) a fixed wing (eBee, from senseFly) and h) a quadrotor (LE Quad, developed at LIS).

Figures 5.14.(a-d) show the mass distribution between the shared mass and the mass added for each mode of locomotion for a) the v6, b) the v9, c) the v9 Adaptive and d) the v11. For the v11, 56% of the mass is shared between the three modes of locomotion, 10% is added for the flight, 10% for the ground mode of locomotion and 24% for hovering. The hovering mode of locomotion has a large mass since it is composed of half of the mass of the adaptive morphology, a second propulsion system and an additional structure for the brushless motors. Furthermore, the v11 has a smaller battery (0.5 Ah) than the v9 Adaptive (1 Ah), which reduces the percentage of shared mass. The level of mass integration of the v11 is similar to the v6, yet it has three modes of locomotion.

For this analysis, the mass of all the components of the robot were measured and assigned to a category (i.e. shared components, adaptive morphology or one of the modes of locomotion), another way to regroup these components is by purpose; mechanical parts, actuators, electronics and battery. Figures 5.14.(e-h) show the mass repartition of the components in these four categories for e) the v11, f) the GimBall robot [23], g) a fixed wing (eBee, from senseFly) and h) a quadrotor (LE Quad, developed at LIS). For the DALER v11, more than half of the mass (52%) is in the structure of the robot, which is similar to the GimBall robot (55%). The GimBall (see Fig. 1.2.B) has a protective frame and a gimbal system which add weight. However, it does not have additional actuators for the ground locomotion thus it has a larger battery percentage (19%) than the DALER v11 (11%). For the eBee and for similar fixed wing UAVs the percentage of mass for the mechanics is 40-50%, for the actuators 15-20%, for the electronics 10-20% depending on the level of autonomy of the UAV (i.e. ranging from remote controlled to fully autonomous) and for the battery 20-30% depending on the mission requirements, there is a trade-off between payload mass and flight time (with a 100 g payload the eBee can fly for 50 minutes). For LE Quad or similar quadrotors, the percentage of mechanical mass is lower since the structure is much simpler (it does not have wings) and is typically 25-30%. Therefore, for similar percentages of electronics and actuators masses the battery percentage is higher (35%) than for fixed wing UAVs. However, the energy consumption is also higher, leading to a shorter flight time (LE Quad can fly 20 minutes without payload and about 15 minutes with a 100 g payload). For the DALER v11, the mass of the mechanics and of the actuators are already minimized, however the mass of the electronics can still be reduced by designing a new custom board which could replace the two boards used on the current prototype. The goal would be to reach 20% of battery mass in order to guaranty a sufficient autonomy to perform a mission.

### 5.7.2 Versatility and Complexity Analyses

The versatility and complexity metrics defined in [13] have been used to evaluate four versions of the DALER prototypes (v6, v9, v9 Adaptive and v11). The versatility metrics is defined by [13] as “an extension of mobility that includes operation in and transition among multiple domains”, and the complexity metrics is defined as the number of actuators multiplied by the number of degrees of freedom (DOF) of the robot. The objectiveness of the versatility metrics

## Chapter 5. Integrated & Adaptive Robot with Three Modes of Locomotion

is questionable since arbitrary grades are given by the person doing the evaluation of a given robot. However, to the best of the author's knowledge, there is no objective metrics to evaluate the versatility of a mobile robot.

				DALER v6	DALER v9	DALER v9Ad.	DALER v11	BOLT [17]	MMALV [19]
Terrestrial	Manoeuvrability	Smooth	X	2	1	2	2	1	2
			$\gamma$	1	1	1	1	0	1
		Rough	X	2	1	2	2	1	1
			$\gamma$	1	1	1	1	0	1
		Def.	X	2	1	2	2	1	1
			$\gamma$	1	1	1	1	0	1
	Obstacle	NA	Gap < 0.5 BL	1	1	1	1	0	0
			Obs. < BH	2	1	2	2	1	1
			Obs. $\geq$ BH	1	1	1	1	0	0
		Smooth	Slope 0-30°	1	1	1	1	2	1
			Slope 30-60°	0	0	0	0	2	0
		Rough	Slope 0-30°	1	1	1	1	0	1
			Slope 30-60°	1	1	1	1	2	1
		Def.	Slope 0-30°	0	0	0	0	1	0
Slope 30-60°	0		0	0	0	1	0		
Aerial	NA	NA	X	1	2	2	(1)	1	2
			$\alpha$	1	2	2	2	0	0
			$\beta$	1	2	2	2	1	1
			$\gamma$	0	0	0	2	1	1
			H	0	0	0	1	1	0
Tran.	NA	NA	A to T	1	1	1	2	1	1
			T to A	0	0	0	(2)	1	0
Total				0.141	0.157	0.183	0.253	0.118	0.128

Table 5.3: Versatility analysis. Grades in brackets have not been demonstrated yet.

The DALER prototypes are compared to BOLT [17] and MMALV [19]; they are the only robots with wings that can also move on the ground. Table 5.3 shows the results of these evaluations (refer to [13] for the details). The robots are graded for their capabilities in the aerial and terrestrial domains and for their capability of transition between these domains; they obtain a grade between 0 (cannot do it) and 2 (does it well) for each "mobility". Some of these grades are based on measured values given in Tables 4.1 and 5.1 and some are evaluated by the authors. The mobilities in the terrestrial domain are further categorized between the manoeuvrability and the capacity to overcome different types of obstacles. The versatility of the DALER v11 is 0.253 (assuming that the grades given between brackets can be demonstrated) which is

## 5.7. Multi-Modal Locomotion Analysis

much higher than for the other prototypes; 0.183 for the v9 Adaptive, 0.157 for the v9, 0.141 for the v6, 0.128 for MMALV and 0.118 for BOLT. The v6 has lower flight performances than the v9 but has higher ground locomotion capabilities however, the total versatility is higher for the v9. The v9 Adaptive has a higher versatility than the v9 since it has better ground locomotion capabilities and the v11 has a higher versatility than the v9 Adaptive because it can also hover. According to Fig. 4 of [13], which shows the versatility of many mobile robots, none of them has a versatility higher than 0.16, demonstrating the very high versatility of the DALER prototypes compared to the state of the art of mobile robots.

	Actuators	DOF	Complexity
DALER v6	7	7	49
DALER v9	3	3	9
DALER v9 Ad.	4	4	16
DALER v11	6	6	36
BOLT	3	4	12
MMALV	6	6	36

Table 5.4: Complexity analysis.

The complexity of these six robots has also been evaluated with the metric defined by [13] (see Table 5.4). The v6 has a complexity of 49, it has 7 actuators and 7 DOFs, the v9 has a complexity of 9, 3 actuators and 3 DOFs, the v9 Adaptive has a complexity of 16, 4 actuators and 4 DOFs, the v11 has a complexity of 36, 6 actuators and 6 DOFs, BOLT has a complexity of 12, 3 actuators and 4 DOFs (its wings and legs are powered with a single actuator) and MMALV has a complexity of 36, 6 actuators and 6 DOFs. Figure 5.15 gives the versatility versus complexity of these robots. The v9 has a higher versatility and a lower complexity than the v6, MMALV and BOLT. The v9 Adaptive is more versatile and also more complex than the v9. Finally, the v11 has the highest versatility with a relatively low complexity. It can be observed that the complexity increases exponentially with the versatility. Furthermore, the autonomy of the robot decreases linearly with the versatility, as shown in Fig. 5.16.

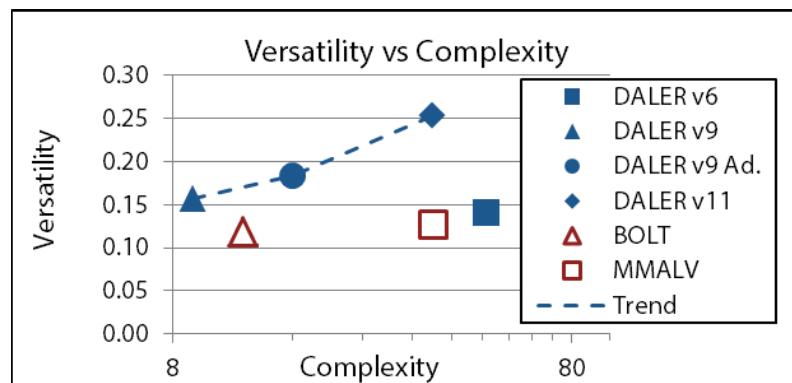


Figure 5.15: Versatility versus complexity of multi-modal robots.

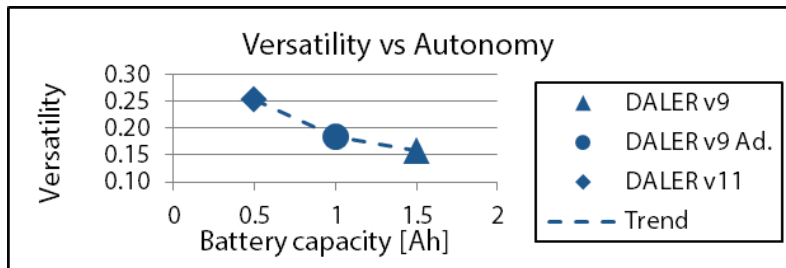


Figure 5.16: Versatility versus autonomy of DALER prototypes.

## 5.8 Conclusion

The final prototype presented in this chapter, the DALER v11, demonstrated having a very high versatility thanks to its three complementary modes of locomotion. The following remarks can be made about the integration, versatility and complexity analyses:

- The integrated design approach allows to minimize the weight and complexity of a multi-modal robot. An additive approach for a design with three modes of locomotion would probably not lead to a feasible solution.
- Adaptive morphology increases the performance of the robot in the additional modes of locomotion. The morphology of the wings of the DALER v11 can be adapted either to the ground or hover mode of locomotion, in order to increase efficiency. However, adaptive morphology increases the weight and the complexity of the robot. The additional weight can be balanced by a smaller battery; conserving good locomotion capabilities but decreasing the autonomy of the robot.
- There is a trade-off between versatility and complexity as shown in Fig. 5.15; complexity increases almost exponentially with versatility as shown by the line formed by the data points of the DALER v9, v9 Adaptive and v11. A new possible design would be a prototype similar to the v11 which would adapt its shape only to ground locomotion. Wings with one degree of freedom instead of two would reduce the weight and complexity of adaptive morphology but would also reduce the performance in hover; this design should be on the trend line between the v9 Adaptive and the v11.
- The robot's autonomy is not considered in the versatility metrics proposed by [13]. The autonomy of the robot is an important aspect which should be included in the performance analysis of a multi-modal robot. An option could be to multiply the versatility value obtained for each mode of locomotion by the autonomy of the robot in that mode. Finally, another option could be to represent the autonomy of the robot in a third dimension of the versatility versus complexity plot, by plotting the battery/robot mass ratio, for example.

## 6 Concluding Remarks

This chapter summarizes the main contributions of this thesis in the topic of adaptive morphology for multi-modal locomotion. A generalized design method is proposed in order to give guidelines for the design of multi-modal mobile robots. The concepts of integrated design and adaptive morphology showed interesting results for improving the versatility of mobile robots, thus future research directions are proposed in order to continue this work.



### 6.1 Main Accomplishments

This section summarizes the main contributions of this thesis, three main contributions can be extracted from this work. The first contribution is the research done on the integrated design approach. The second contribution is the study of using adaptive morphology to improve the efficiency of a multi-modal robot. Finally, the last contribution is a new highly versatile robot capable of three modes locomotion, designed according to the integrated design approach and which can adapt its morphology. Furthermore, the design of this multi-modal flying, hovering and walking robot brought together many different topics such as mechanical design, electronics, control theory and aerodynamics, which are presented throughout this thesis.

#### Integrated Design Approach

The integration of the structure only (i.e. not the actuation) for multiple modes of locomotion allows to reduce the total mass of a multi-modal robot, which increases its locomotion performances. If different actuators are used for two modes of locomotion, each mode can be individually optimized. The dynamics and the placement of the actuators are tuned specifically for one mode of locomotion. For the DALER v6, it led to high ground locomotion capabilities. However, the total weight of this robot was high, which reduced its flight capabilities and its autonomy. A fully integrated design approach, where the structure and the actuators are shared, allows to further minimize the total weight of the robot. If the same locomotor system is to be used for multiple modes of locomotion, then these modes should be dynamically compatible (i.e. they should require compatible speeds and torques). Morphology optimization can be used in order to make two modes of locomotion dynamically compatible. The DALER v9 had good flight capabilities and a high autonomy, however the ground locomotion capabilities were sub-optimal since the placement of the axis of rotation of the walkerons was constrained by flight requirements.

#### Adaptive Morphology

Adaptive morphology can be used to increase the performance of a robot if two modes of locomotion impose opposing constraints on the placement of the center of mass or of the locomotor system. For the DALER v9 Adaptive, the cost of transport of the robot on the ground was reduced by 35% thanks to adaptive morphology and its speed could be increased by 50%. Adaptive morphology has a cost in terms of weight added to the robot. For the DALER v9 Adaptive, the weight added was balanced by a reduction of the weight of its battery. The forward flight performances were conserved but the flight time was reduced by 33%. Therefore, the mission requirements decide if adaptive morphology is beneficial or not, depending on the distance that must be travelled in the air and on the ground.



### **Highly Versatile Robot**

Three complementary modes of locomotion give a very high versatility to a mobile robot; the versatility of the DALER v11 is far above the state of the art of mobile robots. Adaptive morphology can be used to increase the performance of the robot in the additional modes of locomotion; the wings can be adapted either to the ground or hover mode of locomotion, in order to increase efficiency. However, adaptive morphology increases the weight and the complexity of the robot. The additional weight can be balanced by a smaller battery; conserving good locomotion capabilities but decreasing the autonomy of the robot. Furthermore, there is a trade-off between versatility and complexity; complexity increases almost exponentially with versatility. Finally, even if the DALER v11 demonstrated a very high versatility, its autonomy is limited; solutions to reduce the weight should be found for future designs (e.g. new optimized electronics or new technology for adaptive morphology).

## 6.2 Future Work

This section summarizes the work that has been started during this thesis but which is not sufficiently mature to be included in the main chapters. Directions are proposed in order to continue this work in the future.

### Advanced Walking with Deployable Wings

Adaptive morphology is presented in this thesis as a way to improve the performance of a multi-modal robot (see Chapter 4). The DALER v11 has deployable wings which have two degrees of freedom actuated by two servo motors. This mechanism was used only to adapt the morphology of the robot to either forward flight, hover or ground locomotion. It is used solely during the transitions between the modes and not during locomotion, an idea is to use the deployable wings during ground locomotion, in order to increase the length of each step of the robot. The wings move in front of the robot when the walkerons are in parallel with the ground and then come backward while the walkerons are turning of 180 degrees, thus propelling the central frame of the robot on a greater distance. The optimization of this new gait should start with an analysis of the ground locomotion mode; there are several constraints for the range of the deployable mechanism, the first is the mechanical limit of the deployable mechanism itself and the second is the skin of the wings that is inextensible (see Fig. 6.1). Experimental results demonstrated that the mean speed of the robot on a flat wooden ground can be increased from 7 cm/s to 10 cm/s. However, the cost of transport of the robot with this new gait has not been measured yet, thus no conclusion can be drawn on the efficiency.

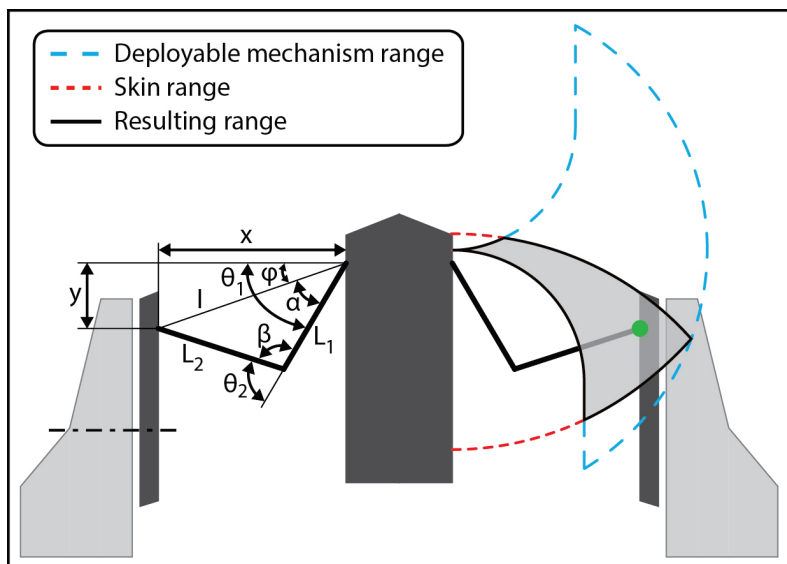


Figure 6.1: Model of the deployable wings. Left) Joints angles to achieve a given position. Right) Range of the green point given by the deployable wings' mechanism and the skin.

### Performance of Walkerons' Controlled Flight

The use of walkerons as control surfaces already demonstrated great flight capabilities with the DALER prototypes thus, an aerodynamical study of the wing and of the walkerons has been started. The DALER prototypes presented in this thesis have self-stabilizing airfoil profiles however, walkerons bring the possibility to stabilize the wing like a tail does for a traditional aircraft. The use of walkerons as stabilizers should then allow the use of an airfoil profile which is not self-stabilizing and which has thus better aerodynamic characteristics, leading to higher flight performance of the robot. Two prototypes were built to test this hypothesis and to compare their flight performances; one with elevons as control surfaces and a self-stabilizing airfoil profile and one with walkerons and an optimized airfoil profile (see Fig. 6.2). Theoretical studies showed promising aerodynamical performances with the use of walkerons for control. The new design shows good flight performances yet, more flight tests should be performed.

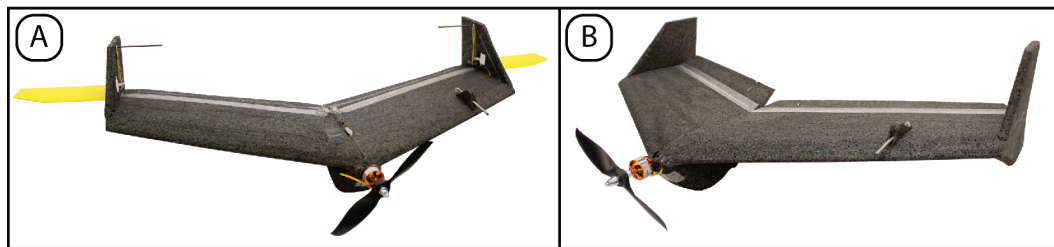


Figure 6.2: Prototypes used to compare flight performance.

### Transitions

The transition between hover and forward flight has been implemented on a test prototype that is similar to the DALER v10 but without adaptive morphology (see Fig. 6.3.a). Successful manoeuvres demonstrated that the transitions are feasible with this configuration (see Fig. 6.3.b). However, there are still improvements that need to be done on the DALER prototype before it can do similar manoeuvres. Chapter 5 showed that the prototype is capable of hovering for a short time yet, if the robot loses its balance due to an external force (e.g. wind), it cannot stabilize itself again due to its too low agility; the speed of the walkerons during hover should be increased in order to improve the stability of the robot. Thus, it would require to build a new prototype with improvements in the hardware in order to perform transitions with the DALER prototype. Table 6.1 shows the transition capabilities of a DALER prototype.

From\to	Ground	Hover	Flight
Ground	-	Yes*	No
Hover	Yes*	-	Yes*
Flight	Yes*	Yes*	-

Table 6.1: Transition capabilities; \* tested with test prototype and \* tested with DALER v11.

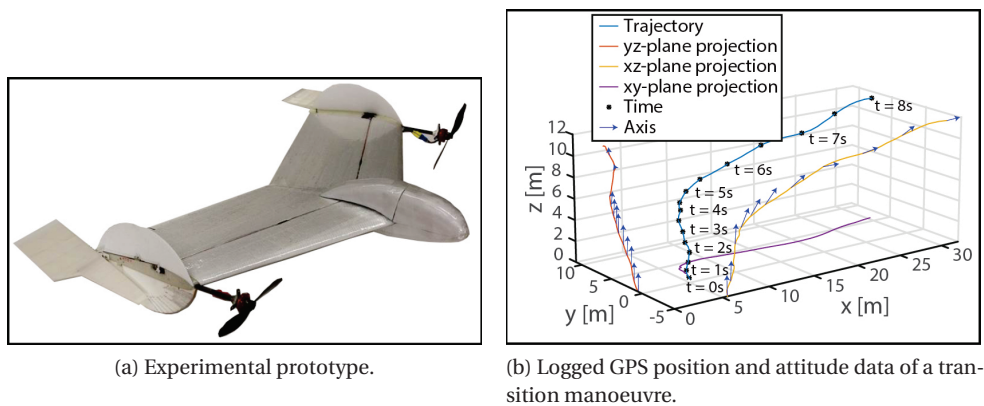


Figure 6.3: Experimental prototype used to test the hover controller and transitions between hover and forward flight.

### Mass & Power Model

A mass-and-power model can be used to define the optimal wingspan and chord of the robot for a given mission scenario. A model has been implemented in a Matlab script based on an existing mass-and-power model developed for a flying wing [56]. This model takes as inputs the mass and the power consumption of the payload, the mission duration and the cruise flight speed and gives as outputs the wingspan, the chord, the total mass of the platform, the stall speed, the power consumption of the motors and the battery requirements (i.e. capacity and voltage). The model has been modified in order to take into account the mass and power models of the hovering and ground locomotion modes as well as the mass model of the deployable wings (see Fig 6.4). To start the process, an arbitrary total mass is defined, then the power models provide the initial power values which meet the requirements of the mission. These powers are re-injected into the mass models of each component, which are directly related to the power they deliver. A new total mass is then calculated and the power models are re-evaluated, and so on until it converges to a solution. This model converges towards different wings geometries depending on the mission parameters; for missions that require long time of flight, the model converges to large wingspans with high aspect ratios while if the mission requires more hover or ground locomotion, it converges towards shorter wingspans and longer chords. However, these configurations have been defined and optimized after many approximations and assumptions, which raises questions about the validity of the model. This model should be experimentally validated.

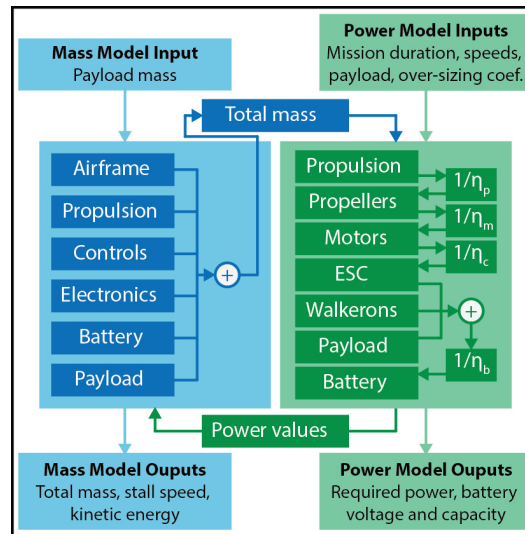


Figure 6.4: Mass-and-power model diagram.

### Control and Sensing

Once the robot will be optimized for a specific mission scenario, will be capable to perform transitions between the three modes of locomotion, will have optimized flight performances and will possibly use its deployable wings for performing more advanced gaits on the ground, it will still require a high level controller and sensing capabilities in order to perform autonomously a mission. To do so, a 3D vector field navigation algorithm has been implemented on quadrotors for testing and gave promising results. This solution could be used to drive the robot in the three modes of locomotion and also during the transitions, the algorithm would provide a speed vector in 3D and different controllers, depending on the mode of locomotion, would calculate the motors output commands in order to follow this vector.

## 6.3 Outlook

Both the integrated and the additive strategies to multi-modal locomotion can be observed in Nature. Some animals use multiple locomotor apparatus for the different modes of locomotion; for example, birds use legs for walking on the ground and for perching, but use wings for flying. Some species of bats, such as the *Desmodus rotundus* evolved rather an integrated approach, they use their pectoral muscles and their wings for both flying and running on the ground. *D. rotundus* evolved impressive ground locomotion capabilities, which do not appear to negatively affect their flight ability [32]. In Nature, it is difficult to compare which strategy is better between the integrated and the additive since, natural evolution leads to viable solutions and not to optimal solutions. However, it can be observed that the *D. rotundus* can locomote faster on the ground than birds, suggesting that the integrated approach is more appropriate when high performances are required in both modes of locomotion.

## Chapter 6. Concluding Remarks

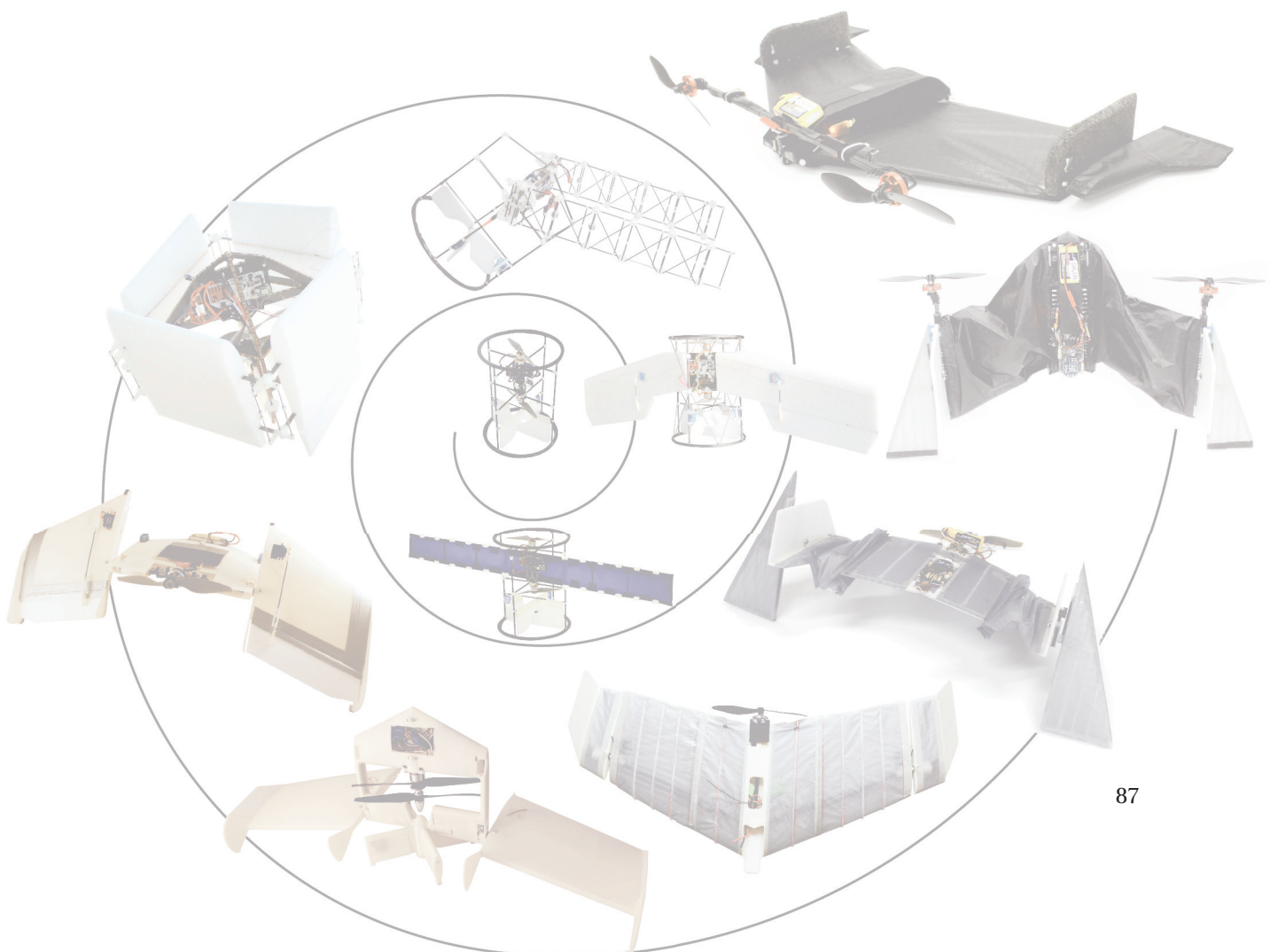
---

These two strategies can be successfully applied to the development of robots with multi-modal locomotion capabilities. A comparison between a semi-integrated design (i.e. integrated structure), DALER v6, and a fully integrated design (i.e. integrated structure and actuation), DALER v9, showed that both of these solutions are feasible. It has been demonstrated in this thesis that a fully integrated strategy is beneficial only if the two modes of locomotion require compatible dynamics, meaning that the dynamics imposed by the secondary mode of locomotion are compatible with the operating range of the actuator used for the first mode of locomotion. In this condition, the secondary mode of locomotion can be added with minimal impact on the primary locomotion mode. If this condition cannot be satisfied through an optimization of the morphology of the robot, due to too different dynamical requirements, then a semi-integrated approach would be more suitable, since different actuators could be individually optimized for a particular mode of locomotion. In both designs, the integration of the structure allows to minimize the weight of the robot. While the fully integrated design led to a higher weight integration and good performance in both modes of locomotion, the semi-integrated design had higher ground locomotion capabilities thanks to an optimal placement of the actuators for walking.

Furthermore, the study of multi-modal locomotion in robotics could potentially help to understand the concept of dynamically compatible modes of locomotion for animals. It could explain why the *D. rotundus* does not show loss of flight performances due to terrestrial competences, it could be possible to show that this bat evolved a running gait which is dynamically compatible with a locomotor apparatus already optimized for flight [32]. Finally, a solution to improve the efficiency of a fully integrated design is adaptive morphology, also used by the *D. rotundus*, which partially folds its wings during walking in order to accommodate the requirements imposed by ground locomotion. It has been shown, with the DALER v11, that a robot optimized for flight can adapt the shape of its wings either to ground locomotion or to hover. Adaptive morphology increases the efficiency of the secondary mode of locomotion by adapting the shape of the robot to its requirements. This solution not only permits to switch between different modes of locomotion but should be used to continuously adapt the morphology of the robot in order to maximize its performance. For example, adaptive wings can also be used during flight to adapt to specific flight conditions; widely spread wings for slow flight or partially folded wings for aggressive manoeuvres (e.g. dive, sharp turns). To conclude, there is still a lot of work to be done before reaching the incredibly high multi-modal performance of bats, but perhaps this thesis brought that dream a little bit closer.

# A History of the DALER Project

More than 20 prototypes have been manufactured during this project, this appendix presents a selection of the main platforms manufactured and tested during this thesis which led to the final design of the DALER. For each prototype the locomotion capabilities and the number of actuators are given and the main innovation is described.



## Appendix A. History of the DALER Project

---

### Introduction

At the beginning of this project, the design of the first prototype has been inspired by the AirBurr project from LIS [57]. The AirBurr is an indoor hovering robot that is designed to survive to collisions with its environment. One version of the AirBurr [58] is equipped with deployable legs, these legs allow the robot to upright itself after it has fallen to the ground and therefore get back in the air. The main limitation of this robot is that it cannot move on the ground; if it gets stuck below an obstacle (e.g. a table) it cannot move to a location where there is enough space to upright and take-off. The second main limitation of this robot is its autonomy of 4-5 minutes only, due to the high energy consumption of hover locomotion. Therefore, the idea of designing a robot which can fly forward, hover and move on the ground came from the analysis of the limitations of the AirBurr robot.

### DALER v1

The first DALER prototype (see Fig. A.1), as mentioned above, has been inspired by the design of a prototype of the AirBurr project [58]. The main idea behind this prototype was to use the same actuators for hovering and for ground locomotion. DALER v1 has the shape of a cylinder, two carbon fibre rings are connected by four carbon fibre tubes. A central frame hosts two brushless motors for the propellers and an autopilot. Below the propellers, two flaps are actuated by servo motors, which are used to control the attitude of the platform during hover. When the robot is at the vertical, it can hover by the use of the two contra-rotating propellers and the two control flaps, and when it is at the horizontal, it can roll sideways by spinning the two propellers in the same direction. The torque produced by the propellers moving in the air creates a counter-rotating torque on the platform, which induces the rolling motion. This prototype can hover and roll on flat grounds by using only four actuators, however it cannot transition from ground to hover and the ground locomotion are limited since it cannot overcome obstacles and it cannot steer.

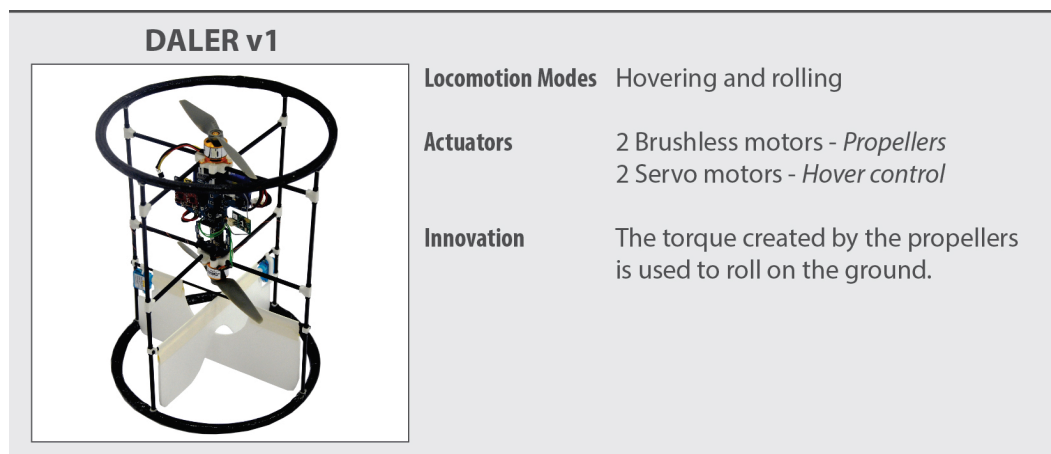


Figure A.1: DALER v1.



---

## DALER v2

DALER v2 (see Fig. A.2) has additional deployable "wings" that can be deployed using two DC motors. These wings made out of a carbon fibre skeleton covered by a layer of latex can be wrapped around the central frame of the robot, inside of the outer cylinder. Thus, when the wings are folded, the robot has the same capabilities as the DALER v1. When the robot encounters an obstacle on the ground that cannot be overcome by the torque created by the propellers, it can open one wing in order to push against the ground, increasing the rolling torque. However, these wings were used only to investigate ground locomotion and not forward flight, since they do not have elevons to control roll.

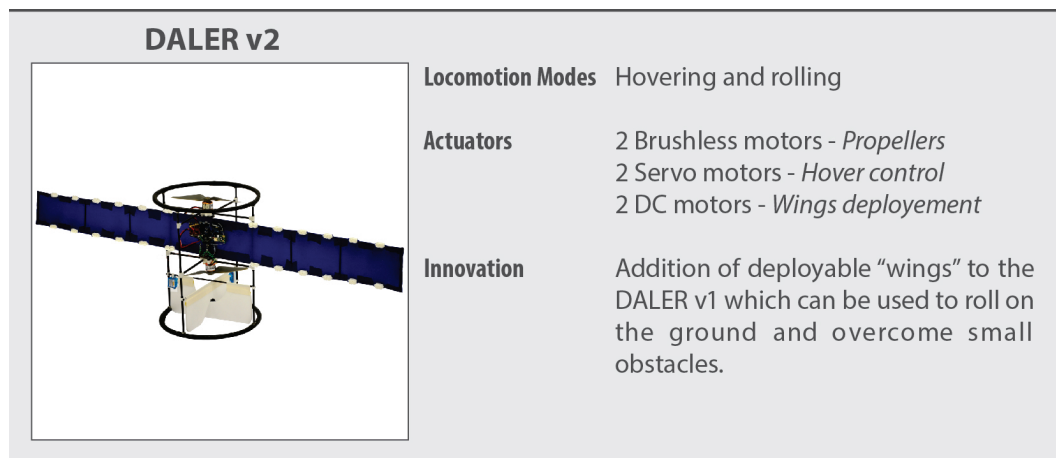


Figure A.2: DALER v2.

## Appendix A. History of the DALER Project

---

### DALER v3

The goal of DALER v3 was to investigate forward flight with the design of the DALER v1. For this purpose, rigid wings were added on the platform. These wings are equipped with elevons in order to control forward flight; experiments showed that the torque created by the differential thrust of the contra-rotating propellers is not sufficient to control the roll axis of the robot. This prototype could fly on a short distance, however due to a wrong placement of the center of mass, forward flight was not stable.

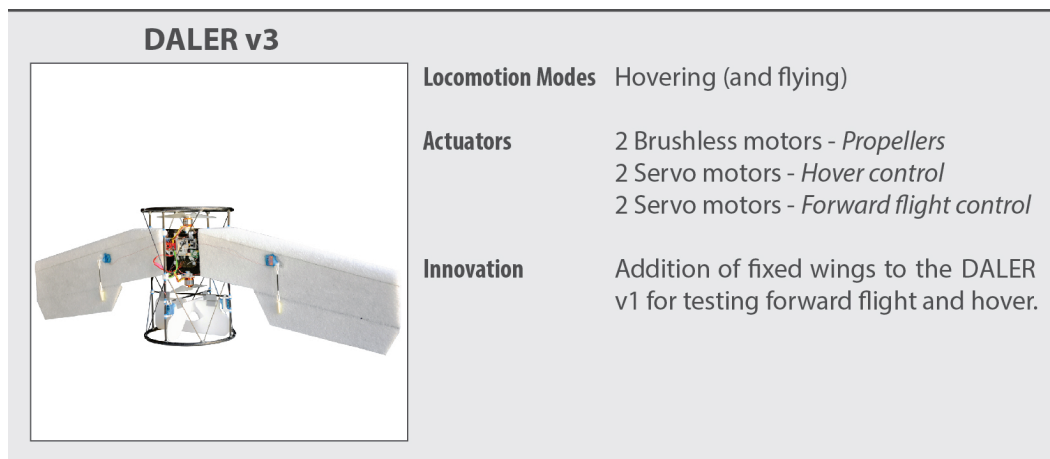


Figure A.3: DALER v3.

---

#### DALER v4

DALER v4 (see Fig. A.4) is based on the design of the DALER v2 with deployable wings. The wings are now mounted on servo motors which allow the robot to upright itself. As before, the two wings can be wrapped around the central frame of the robot, they can be extended until being at 90 degrees with respect to the plane of the central frame and thus they can be used for uprighting. The wings are used both for ground rolling and for uprighting, but they require two motors each and a complex mechanism to be locked at 90 degree during uprighting. The wings are closed by pre-constrained springs and opened by cables driven by DC motors. Each wing is made out of 6 segments which means that 12 springs are needed for the robot, leading to a very complex and heavy prototype.

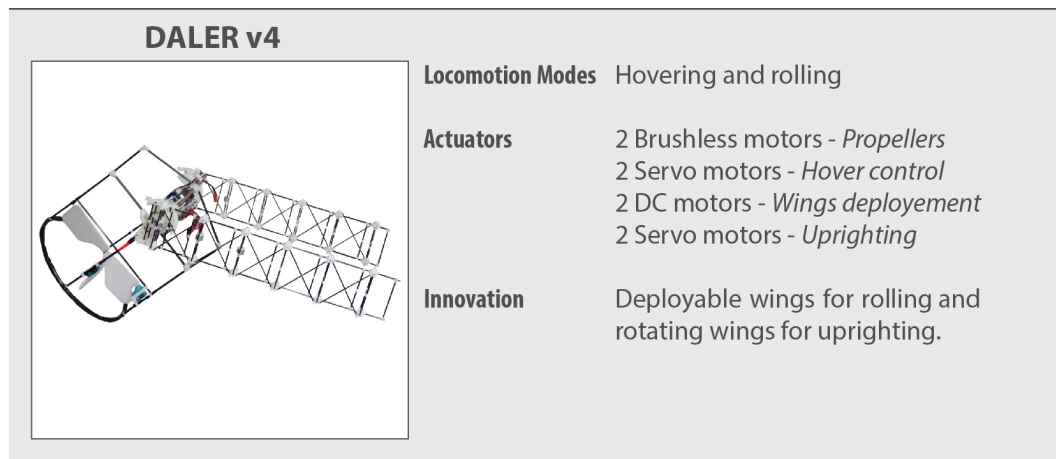


Figure A.4: DALER v4.

## Appendix A. History of the DALER Project

### DALER v5

The concepts investigated in the four first versions of the DALER (v1 to v4) were used to design the DALER v5 (see Fig. A.5). The DALER v5 could in theory, hover, fly forward, roll on the ground and transition between these three modes of locomotion. Its design is similar to the DALER v4; it has two deployable wings actuated by DC motors which are mounted on servo motors, which allow the robot to upright itself. The prototype showed good hovering capabilities and was capable to move slowly on the ground in one direction. It was also capable to upright itself thanks to the two servo motors that rotates the wings. However, the prototype was not capable to fly forward due to a bad design of the wings (i.e. inappropriate airfoil profile, geometry and centre of mass). At the beginning of the project, we have started from a hovering platform (e.g. similar to the AirBurr design) and then added ground locomotion and forward flight capabilities. This approach appeared to be very difficult because forward flight imposes specific constraints on the design of the platform. A fixed wing platform, requires a specific airfoil profile, geometry of the wing and placement of the centre of mass relative to the aerodynamic pressure center. Thus, the design of the DALER platform had to be completely rethought; instead of starting from a hovering platform, it has been decided to start from a fixed wing platform and then add hovering and ground locomotion capabilities.

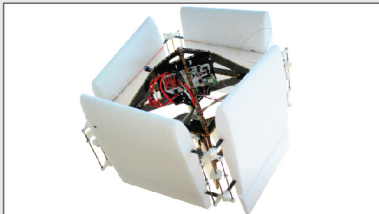
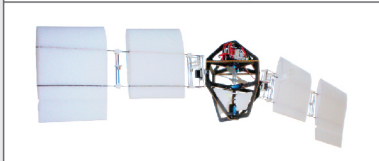
DALER v5	
	<b>Locomotion Modes</b> Hovering, rolling (and flying)
	<b>Actuators</b> 2 Brushless motors - <i>Propellers</i> 2 Servo motors - <i>Hover control</i> 2 DC motors - <i>Wings deployment</i> 2 Servo motors - <i>Uprighting</i>
	<b>Innovation</b> Simplification of DALER v4 and addition of wings for forward flight.

Figure A.5: DALER v5.

---

### DALER v6

The DALER v6 (see Fig. A.6) is very different from the DALER v5, since its design is based on a flying wing. The DALER v6 can use its wings both to produce lift during flight and to move on the ground. This robot uses different actuators for flight control (servo motors are used to actuate elevons on the wings) and for ground locomotion (DC motors actuate the rotation of the wings). In order to avoid backlash in the wings during forward flight, which would cause instabilities, two servo motors are added to actuate a mechanism to lock the wings in the flight configuration. The advantage of this design is that no additional structure is needed for the ground locomotion however, it has 7 actuators, which add weight.

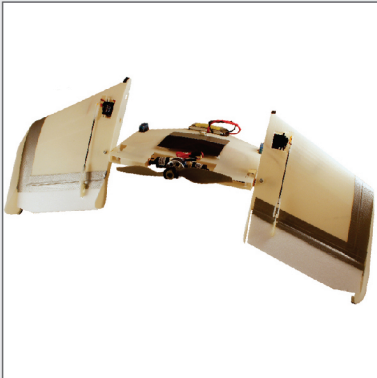
DALER v6	
	<p><b>Locomotion Modes</b> Flying and walking</p> <p><b>Actuators</b> 1 Brushless motor - <i>Propeller</i> 2 Servo motors - <i>Flight control</i> 2 DC motors - <i>Walking</i> 2 Servo motors - <i>Locking wings</i></p> <p><b>Innovation</b> The same structure is used for forward flight and for walking on the ground.</p>

Figure A.6: DALER v6.

## Appendix A. History of the DALER Project

---

### DALER v7

DALER v7 (see Fig. A.7) builds on top of the DALER v6. The goal was to add hovering capabilities to the design of the DALER v6 with the same principle as on the DALER v5; two coaxial contra-rotating propellers and two flaps in their airflow. The robot could also upright itself thanks to its wings and takeoff vertically as shown on Fig. A.7, however this design is very complex and heavy. This robot has 10 actuators and 4 control surfaces (i.e. 2 elevons for flight control and 2 flaps for hover control). This design was less efficient during ground locomotion than the DALER v6 and was too heavy for forward flight and hovering. As a result, it has been decided to go back to the design of the DALER v6 and try simplifying it before adding hovering capabilities (at this time the analysis presented in Chapter 2 has been done).

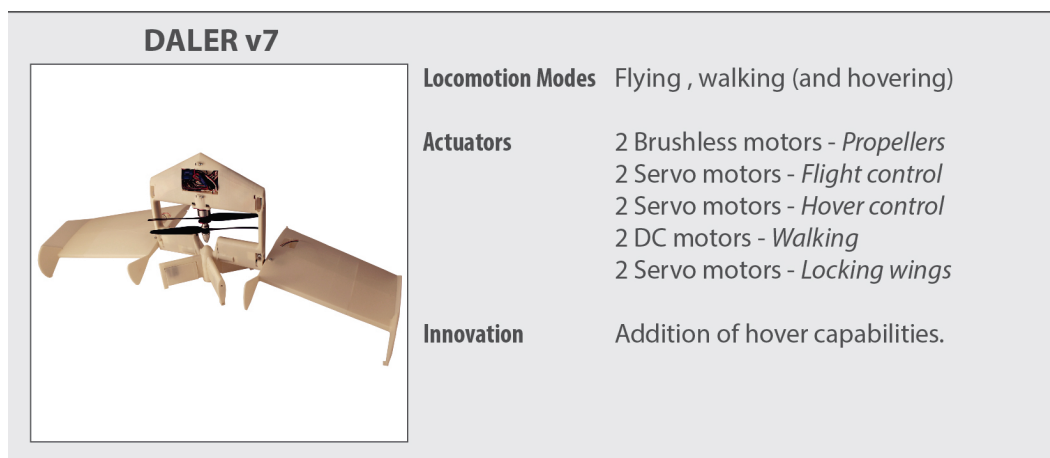


Figure A.7: DALER v7.

---

### DALER v8

With the aim of simplifying the design of the DALER v6, DALER v8 (see Fig. A.8) was a test prototype that can control forward flight by rotating the extremities of its wings. This prototype is made out of a carbon fibre skeleton covered by a layer of fabric. The extremities of the wings are actuated by servo motors. DALER v8 showed very good flight performances and high manoeuvrability. Therefore, this solution of using a portion of the wings for flight control was kept for the next designs since, these appendages can also be used to move on the ground.


DALER v8	
	<p><b>Locomotion Modes</b> Flying</p> <p><b>Actuators</b> 1 Brushless motor - <i>Propeller</i> 2 Servo motors - <i>Flight control</i></p> <p><b>Innovation</b> Control of forward flight by using two portions of the wing as control surfaces. New manufacturing technique with carbon fiber skeleton covered by a layer of fabric.</p>

Figure A.8: DALER v8.

## Appendix A. History of the DALER Project

---

### DALER v9

DALER v9 (see Fig. A.9) can walk on the ground and control forward flight with the same locomotor system, called walkerons. The prototype has similar capabilities as the DALER v6 but with a higher level of integration since the same actuators are used for ground locomotion and flight control. Furthermore, the prototype is equipped with foldable wings that allow to change the morphology of the robot. During ground locomotion the robot can close its wings in order to be more efficient. In this configuration the axis of rotation of the walkerons is closer to the center of mass of the robot, thus the walkerons slip less on the ground, making the robot faster. Moreover, the reduced wingspan allows the robot to go easily between obstacles on the ground.

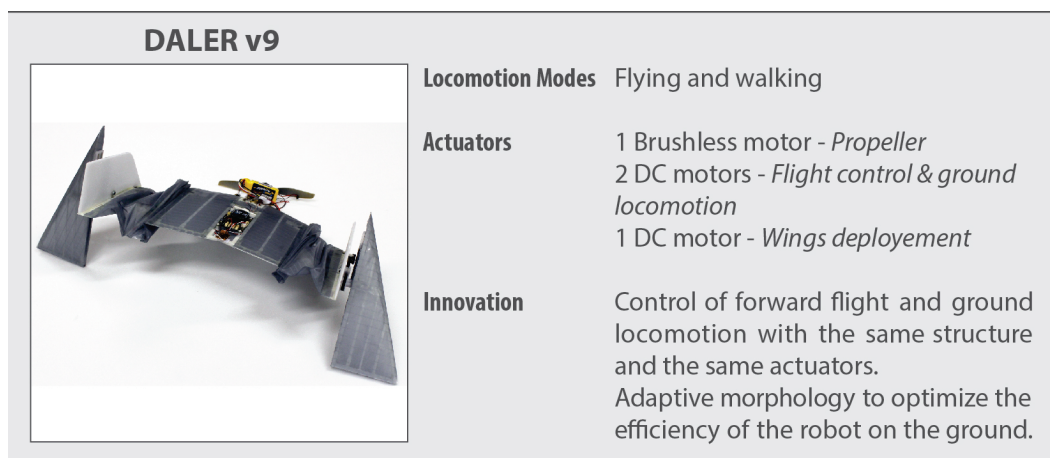


Figure A.9: DALER v9.



---

### DALER v10

The DALER v10 (see Fig. A.10) builds directly on the design of the DALER v9. The goal here was to add hovering capabilities to the prototype. Instead of having one propeller in the center of the robot as on the DALER v9, this version has one propeller at each extremities of the wings, providing airflow on the walkerons. Thus, allowing control during hover and transitions between forward flight and hover. This prototype can walk on the ground and upright itself in a take-off ready position, however the design is too heavy and the weight of the motors added at the extremities of the wings put a lot of constraints on the foldable mechanism of the wings. In order to keep the walkerons parallel to the centre of the robot, the foldable mechanism is made out of two serial parallelograms composed of carbon fibre tubes and rods. An issue with this design is that the propellers are going too high in front of the robot during ground locomotion and are thus too close from the ground. Moreover, during hover they come too close to the wings and might damage the fabric (see Fig. A.10).

DALER v10	
	<b>Locomotion Modes</b> Walking (flying and hovering)
<b>Actuators</b>	2 Brushless motors - <i>Propellers</i> 2 DC motors - <i>Flight control &amp; ground locomotion</i> 2 DC motor - <i>Wings deployment</i>
<b>Innovation</b>	Addition of hover locomotion. Addition of a second degree of freedom in the deployable wings.

Figure A.10: DALER v10.

## Appendix A. History of the DALER Project

---

### DALER v11

The DALER v11 (see Fig. A.11) is the final prototype built during this thesis. The main difference with respect to the design of the DALER v10 is that the propellers are now directly connected to the central frame of the robot. This allows to reduce the weight at the extremities of the wings and to avoid having the propellers going too high during ground locomotion or going too close to the fabric during hover. Each parallelogram of the deployable mechanism is replaced by a single carbon tubes and two cables tensioned on each side of this tube that keep the parallelism. This solution reduces the weight and the backlash of the foldable wings. This final prototype can walk on the ground, upright itself and hover. Moreover, the wings can adapt their shape in order to increase the efficiency during ground locomotion and hover. These impressive capabilities can be achieved due to the high level of integration of the design; the robot has only 6 actuators, which minimizes its total weight and complexity.



Figure A.11: DALER v11.

## B Weight of Criteria for Platform Configuration Selection

This appendix presents how the weights for the evaluation of the solutions presented in Chapter 2 are defined. The method of pairwise comparison is used, the importance of each criterion is compared to the others. If a criterion is more important than another one then it gets 2 and the other one 0, if they are of equal importance they both get 1.

For providing lift, Table B.1 gives the weight of each criterion; the most important criteria are reuseability (2.00), robustness (1.20), weight (1.20), and complexity (1.20), wind resistance (0.20) and safety (0.20) are less important.

<b>Provide lift</b>	Robustness	Weight	Wind resistance	Complexity	Safety	Reuseability
Robustness	-	1	0	1	0	2
Weight	1	-	0	1	0	2
Wind resistance	2	2	-	2	1	2
Complexity	1	1	0	-	0	2
Safety	2	2	1	2	-	2
Reuseability	0	0	0	0	0	-
Total	6	6	1	6	1	10
Weight	1.20	1.20	0.20	1.20	0.20	2.00

Table B.1: Weights calculation based on pairwise comparison for providing lift.

## Appendix B. Weight of Criteria for Platform Configuration Selection

For providing thrust, Table B.2 gives the weight of each criterion; the dominant criteria are reuseability (2.00) and force/weight ratio (1.20) since we want to minimize the total weight of the platform. Then two important criteria are efficiency (1.00) and complexity (1.00). Finally, robustness (0.40) and safety (0.40) are less important criteria for this function.

<b>Provide thrust</b>	Force/weight	Robustness	Efficiency	Complexity	Safety	Reuseability
Force/weight	-	0	1	1	0	2
Robustness	2	-	2	1	1	2
Efficiency	1	0	-	1	1	2
Complexity	1	1	1	-	0	2
Safety	2	1	1	2	-	2
Reuseability	0	0	0	0	0	-
<b>Total</b>	<b>6</b>	<b>2</b>	<b>5</b>	<b>5</b>	<b>2</b>	<b>10</b>
<b>Weight</b>	<b>1.20</b>	<b>0.40</b>	<b>1.00</b>	<b>1.00</b>	<b>0.40</b>	<b>2.00</b>

Table B.2: Weights calculation based on pairwise comparison for providing thrust.

For controlling the orientation, Table B.3 gives the weight of each criterion; reuseability (2.00) is always the most important criterion since the same actuators and structure should be used for different purposes. Power/weight (1.33) is an important criterion, for the same reasons as above. Finally, robustness (0.33) and complexity (0.33) are less important criteria for this function.

<b>Control orientation</b>	Power/weight	Robustness	Complexity	Reuseability
Power/weight	-	0	0	2
Robustness	2	-	1	2
Complexity	2	1	-	2
Reuseability	0	0	0	-
<b>Total</b>	<b>4</b>	<b>1</b>	<b>1</b>	<b>6</b>
<b>Weight</b>	<b>1.33</b>	<b>0.33</b>	<b>0.33</b>	<b>2.00</b>

Table B.3: Weights calculation based on pairwise comparison for controlling orientation.

Finally, for moving on the ground, Table B.4 gives the weight for each criterion; the most important criteria are reuseability (2.00) and weight (1.50); again because the total weight should be minimized. The modifications added to the platform for the ground locomotion should not, if possible, increase the weight. The third most important criterion is complexity (1.33). Manoeuvrability (1.00) is also an important criterion; the locomotion capabilities of the platform should be as good as possible in order to maximize versatility. Finally, speed (0.50) is a little bit less important and so are robustness (0.33) and efficiency (0.33).

<b>Ground</b>	Weight	Robustness	Complexity	Speed	Efficiency	Manoeuvrability	Reuseability
Weight	-	0	1	0	0	0	2
Robustness	2	-	2	1	1	2	2
Complexity	1	0	-	0	0	1	2
Speed	2	1	2	-	1	1	2
Efficiency	2	1	2	1	-	2	2
Manoeuvrability	2	0	1	1	0	-	2
Reuseability	0	0	0	0	0	0	-
<b>Total</b>	<b>9</b>	<b>2</b>	<b>8</b>	<b>3</b>	<b>2</b>	<b>7</b>	<b>12</b>
<b>Weight</b>	<b>1.50</b>	<b>0.33</b>	<b>1.33</b>	<b>0.50</b>	<b>0.33</b>	<b>1.17</b>	<b>2.00</b>

Table B.4: Weights calculation based on pairwise comparison for moving on the ground.



## Bibliography

- [1] T. Chung, G. Hollinger, and V. Isler, "Search and pursuit-evasion in mobile robotics: A survey," *Autonomous robots*, vol. 31, no. 4, pp. 299–316, 2011.
- [2] S. Tadokoro, *Rescue Robotics: DDT Project on Robots and Systems for Urban Search and Rescue*. Springer Verlag, 2009.
- [3] R. Murphy, J. Kravitz, S. Stover, and R. Shoureshi, "Mobile robots in mine rescue and recovery," *Robotics & Automation Magazine, IEEE*, vol. 16, no. 2, pp. 91–103, 2009.
- [4] K. Nagatani, S. Kiribayashi, Y. Okada, K. Otake, K. Yoshida, S. Tadokoro, T. Nishimura, T. Yoshida, E. Koyanagi, M. Fukushima, *et al.*, "Emergency response to the nuclear accident at the fukushima daiichi nuclear power plants using mobile rescue robots," *Journal of Field Robotics*, vol. 30, no. 1, pp. 44–63, 2013.
- [5] R. Siddall and M. Kovač, "Launching the aquamav: bioinspired design for aerial–aquatic robotic platforms," *Bioinspiration & biomimetics*, vol. 9, no. 3, p. 031001, 2014.
- [6] J.-D. Nicoud and J.-C. Zufferey, "Toward indoor flying robots," *IEEE/RSJ International Conference on Robots and Systems (IROS'02), Lausanne*, pp. 787–792, 2002.
- [7] S. Bouabdallah, P. Murrieri, and R. Siegwart, "Towards autonomous indoor micro vtol," *Autonomous Robots*, vol. 18, no. 2, pp. 171–183, 2005.
- [8] G. De Croon, K. De Clercq, R. Ruijsink, B. Remes, and C. De Wagter, "Design, aerodynamics, and vision-based control of the delfly," *International Journal of Micro Air Vehicles*, vol. 1, no. 2, pp. 71–97, 2009.
- [9] W. Green and P. Oh, "Autonomous hovering of a fixed-wing micro air vehicle," in *Robotics and Automation, 2006. ICRA 2006. Proceedings 2006 IEEE International Conference on*, pp. 2164–2169, IEEE, 2006.
- [10] J. Zufferey, A. Guanella, A. Beyeler, and D. Floreano, "Flying over the reality gap: From simulated to real indoor airships," *Autonomous Robots*, vol. 21, no. 3, pp. 243–254, 2006.
- [11] H. Tennekes and H. Tennekes, *The simple science of flight: from insects to jumbo jets*. The MIT Press, 2009.

## Bibliography

---

- [12] D. Lentink and M. Dickinson, "Biofluiddynamic scaling of flapping, spinning and translating fins and wings," *Journal of Experimental Biology*, vol. 212, no. 16, p. 2691, 2009.
- [13] C. Nie, X. Pacheco-Corcho, and M. Spenko, "Robots on the move: Versatility and complexity in mobile robot locomotion," *Robotics Automation Magazine, IEEE*, vol. 20, pp. 72–82, Dec 2013.
- [14] R. J. Lock, S. C. Burgess, and R. Vaidyanathan, "Multi-modal locomotion: from animal to application," *Bioinspiration & Biomimetics*, vol. 9, no. 1, p. 011001, 2014.
- [15] A. Kossett, R. D'Sa, J. Purvey, and N. Papanikolopoulos, "Design of an improved land/air miniature robot," in *Robotics and Automation (ICRA), 2010 IEEE International Conference on*, pp. 632–637, IEEE, 2010.
- [16] M. Kovac, W. Hraiz, O. Fauria, J.-C. Zufferey, and D. Floreano, "The epfl jumpglider: A hybrid jumping and gliding robot with rigid or folding wings," in *Robotics and Biomimetics (ROBIO), 2011 IEEE International Conference on*, pp. 1503–1508, IEEE, 2011.
- [17] K. Peterson and R. S. Fearing, "Experimental dynamics of wing assisted running for a bipedal ornithopter," in *Intelligent Robots and Systems (IROS), 2011 IEEE/RSJ International Conference on*, pp. 5080–5086, IEEE, 2011.
- [18] F. Li, W. Liu, X. Fu, G. Bonsignori, U. Scarfogliero, C. Stefanini, and P. Dario, "Jumping like an insect: Design and dynamic optimization of a jumping mini robot based on bio-mimetic inspiration," *Mechatronics*, vol. 22, no. 2, pp. 167–176, 2012.
- [19] R. J. Bachmann, F. J. Boria, R. Vaidyanathan, P. G. Ifju, and R. D. Quinn, "A biologically inspired micro-vehicle capable of aerial and terrestrial locomotion," *Mechanism and Machine Theory*, vol. 44, no. 3, pp. 513–526, 2009.
- [20] J. R. Lovvorn, D. A. Croll, and G. A. Liggins, "Mechanical versus physiological determinants of swimming speeds in diving brunnich's guillemots," *Journal of Experimental Biology*, vol. 202, no. 13, pp. 1741–1752, 1999.
- [21] D. K. Riskin, S. Parsons, W. A. Schutt, G. G. Carter, and J. W. Hermanson, "Terrestrial locomotion of the new zealand short-tailed bat *mystacina tuberculata* and the common vampire bat *desmodus rotundus*," *Journal of Experimental Biology*, vol. 209, no. 9, pp. 1725–1736, 2006.
- [22] K. H. Elliott, R. E. Ricklefs, A. J. Gaston, S. A. Hatch, J. R. Speakman, and G. K. Davoren, "High flight costs, but low dive costs, in auks support the biomechanical hypothesis for flightlessness in penguins," *Proceedings of the National Academy of Sciences*, vol. 110, no. 23, pp. 9380–9384, 2013.
- [23] A. Briod, P. M. Kornatowski, J.-C. Zufferey, and D. Floreano, "A collision resilient flying robot," *Journal of Field Robotics*, vol. 31, no. 4, pp. 469–509, 2014.



- [24] M. Itasse, J.-M. Moschetta, Y. Ameho, and R. Carr, "Equilibrium transition study for a hybrid mav," *International Journal of Micro Air Vehicles*, vol. 3, no. 4, pp. 229–246, 2011.
- [25] A. Kalantari and M. Spenko, "Design and experimental validation of hytaq, a hybrid terrestrial and aerial quadrotor," in *Robotics and Automation (ICRA), 2013 IEEE International Conference on*, pp. 4445–4450, IEEE, 2013.
- [26] K. Kawasaki, M. Zhao, K. Okada, and M. Inaba, "Muwa: Multi-field universal wheel for air-land vehicle with quad variable-pitch propellers," in *Intelligent Robots and Systems (IROS), 2013 IEEE/RSJ International Conference on*, pp. 1880–1885, IEEE, 2013.
- [27] C. Thipyopas, "Aerodynamic comparison of tilt-rotor,-wing and-body concept for multi task mavs," 2008.
- [28] A. J. Gaston and I. L. Jones, *The Auks: Alcidae*. Oxford University Press, 1998.
- [29] U. M. Norberg and J. M. Rayner, "Ecological morphology and flight in bats (mammalia; chiroptera): wing adaptations, flight performance, foraging strategy and echolocation," *Philosophical Transactions of the Royal Society of London. Series B, Biological Sciences*, pp. 335–427, 1987.
- [30] D. K. Riskin and J. W. Hermanson, "Biomechanics: Independent evolution of running in vampire bats," *Nature*, vol. 434, no. 7031, pp. 292–292, 2005.
- [31] W. Schutt, J. S. Altenbach, Y. Chang, D. M. Cullinane, J. W. Hermanson, F. Muradali, and J. Bertram, "The dynamics of flight-initiating jumps in the common vampire bat *desmodus rotundus*," *The Journal of experimental biology*, vol. 200, no. 23, pp. 3003–3012, 1997.
- [32] D. K. Riskin, J. E. Bertram, and J. W. Hermanson, "Testing the hindlimb-strength hypothesis: non-aerial locomotion by chiroptera is not constrained by the dimensions of the femur or tibia," *The Journal of experimental biology*, vol. 208, no. 7, pp. 1309–1319, 2005.
- [33] M. A. Woodward and M. Sitti, "Multimo-bat: A biologically inspired integrated jumping-gliding robot," *The International Journal of Robotics Research*, vol. 33, no. 12, pp. 1511–1529, 2014.
- [34] J. J. Socha, "Kinematics: Gliding flight in the paradise tree snake," *Nature*, vol. 418, no. 6898, pp. 603–604, 2002.
- [35] J. J. Socha, T. O'Dempsey, and M. LaBarbera, "A 3-d kinematic analysis of gliding in a flying snake, *chrysopelea paradisi*," *Journal of Experimental Biology*, vol. 208, no. 10, pp. 1817–1833, 2005.
- [36] L. C. Johansson and B. S. W. Aldrin, "Kinematics of diving atlantic puffins (*fratercula arctica* L.): evidence for an active upstroke," *Journal of experimental biology*, vol. 205, no. 3, pp. 371–378, 2002.

## Bibliography

---

- [37] A. J. Ijspeert, A. Crespi, D. Ryczko, and J.-M. Cabelguen, "From swimming to walking with a salamander robot driven by a spinal cord model," *Science*, vol. 315, no. 5817, pp. 1416–1420, 2007.
- [38] M. García-París and S. M. Deban, "A novel antipredator mechanism in salamanders: rolling escape in hydromantes platycephalus," *Journal of herpetology*, vol. 29, no. 1, pp. 149–151, 1995.
- [39] M. Kovac, J. Zufferey, and D. Floreano, "Towards a self-deploying and gliding robot," *Flying insects and robots*, 2009.
- [40] S. Barbarino, O. Bilgen, R. M. Ajaj, M. I. Friswell, and D. J. Inman, "A review of morphing aircraft," *Journal of Intelligent Material Systems and Structures*, vol. 22, no. 9, pp. 823–877, 2011.
- [41] J. C. Gomez and E. Garcia, "Morphing unmanned aerial vehicles," *Smart Materials and Structures*, vol. 20, no. 10, p. 103001, 2011.
- [42] D. Lentink, U. Müller, E. Stamhuis, R. De Kat, W. Van Gestel, L. Veldhuis, P. Henningsson, A. Hedenström, J. J. Videler, and J. L. Van Leeuwen, "How swifts control their glide performance with morphing wings," *Nature*, vol. 446, no. 7139, pp. 1082–1085, 2007.
- [43] D. T. Grant, M. Abdulrahim, and R. Lind, "Design and analysis of biomimetic joints for morphing of micro air vehicles," *Bioinspiration & biomimetics*, vol. 5, no. 4, p. 045007, 2010.
- [44] P. G. Ifju, D. A. Jenkins, S. Ettinger, Y. Lian, W. Shyy, and M. R. Waszak, "Flexible-wing-based micro air vehicles," *AIAA paper*, vol. 705, no. 2001-3290, pp. 1–11, 2002.
- [45] L. Daler, J. Lecoeur, P. B. Hählen, and D. Floreano, "A flying robot with adaptive morphology for multi-modal locomotion," in *IROS 13*, 2013.
- [46] L. Daler, S. Mintchev, C. Stefanini, and D. Floreano, "A bioinspired multi-modal flying and walking robot," *Bioinspiration & Biomimetics*, vol. 10, no. 1, p. 016005, 2015.
- [47] L. J. Clancy, *Aerodynamics*. Pitman, 1975.
- [48] B. Etkin and L. D. Reid, *Dynamics of flight: stability and control*. Wiley New York, 1996.
- [49] L. Rome, R. Funke, R. Alexander, G. Lutz, H. Aldridge, F. Scott, and M. Freadman, "Why animals have different muscle fibre types," *Nature*, vol. 335, no. 6193, pp. 824–827, 1988.
- [50] C. Pennycuick, "Adapting skeletal muscle to be efficient," *Efficiency and economy in animal physiology*, pp. 33–42, 1991.
- [51] R. J. Lock, R. Vaidyanathan, and S. C. Burgess, "Impact of marine locomotion constraints on a bio-inspired aerial-aquatic wing: experimental performance verification," *Journal of Mechanisms and Robotics*, vol. 6, no. 1, p. 011001, 2014.

- [52] I. W. Hunter and S. Lafontaine, "A comparison of muscle with artificial actuators," in *Solid-State Sensor and Actuator Workshop, 1992. 5th Technical Digest., IEEE*, pp. 178–185, IEEE, 1992.
- [53] J. Huber, N. Fleck, and M. Ashby, "The selection of mechanical actuators based on performance indices," *Proceedings of the Royal Society of London. Series A: Mathematical, Physical and Engineering Sciences*, vol. 453, no. 1965, pp. 2185–2205, 1997.
- [54] V. A. Tucker, "The energetic cost of moving about," *Am. Sci.*, vol. 63, no. 4, pp. 413–419, 1975.
- [55] L. Daler, S. Mintchev, J. Lecoecur, and D. Floreano, "Daler: Deployable air land exploration robot," in *IROS 15*, In review.
- [56] S. Leven, *Enabling Large-Scale Collective Systems in Outdoor Aerial Robotics Bioinspired*. PhD thesis, Lausanne, 2011.
- [57] A. Klaptocz, *Design of Flying Robot for Collision Absorption and Self-Recovery*. PhD thesis, Lausanne, 2012.
- [58] A. Klaptocz, L. Daler, A. Briod, J.-C. Zufferey, and D. Floreano, "An active uprighting mechanism for flying robots," *Robotics, IEEE Transactions on*, vol. 28, no. 5, pp. 1152–1157, 2012.



# Ludovic Daler

Rue Etraz 16  
1003 Lausanne  
Switzerland  
☎ +41 78 790 13 76  
✉ ludovic.daler@gmail.com



## Education

2011

**PhD in Manufacturing Systems and Robotics**, *École Polytechnique Fédérale de Lausanne*, Lausanne, Switzerland.

2011

**Master of science in Robotics and Autonomous Systems**, *École Polytechnique Fédérale de Lausanne*, Lausanne, Switzerland.

2009

**Bachelor of science in Micro-Engineering**, *École Polytechnique Fédérale de Lausanne*, Lausanne, Switzerland.

2006

**Maturité Fédérale**, *Gymnase de Chamblandes*, Pully, Switzerland.  
Option: Mathematics and physics.

## PhD thesis

title *Adaptive Morphology for Multi-Modal Locomotion.*  
supervisors Prof. Dario Floreano and Prof. Auke Ijspeert.

## Master thesis

title *Design, Manufacturing and Implementation of Fiber Adhesives based Perching Mechanism for Flying Robots.*  
supervisors Prof. Dario Floreano and Prof. Metin Sitti.

## Achievements

- Received best student paper award finalist at IROS 2013 conference.

## Languages

French **Native**  
English **Fluent**

*Mother Tongue*  
*Daily practice, all work performed in English*

## Skills

**Languages** C, C++, Assembler.

**Software** MS Office, LaTeX, Matlab, Pro-Engineer, Solidworks, Eagle, Photoshop, Illustrator, Premiere.



# Publications

## Peer-Reviewed Journal Papers

L. Daler, S. Mintchev, C. Stefanini, and D. Floreano, "A Bioinspired Multi-Modal Flying and Walking Robot," in *Bioinspiration & Biomimetics*, vol. 10, num. 1, 2015.

A. Klaptocz, L. Daler, A. Briod, J.-C. Zufferey and D. Floreano, "An Active Uprighting Mechanism for Flying Robots," in *IEEE Transactions on Robotics*, vol. 28, num. 5, p. 1152-1157, 2012.

## Peer-Reviewed Conference Proceedings

L. Daler, S. Mintchev, J. Lecoœur, and D. Floreano, "DALER: Deployable Air Land Exploration Robot," in *IEEE/RSJ International Conference on Intelligent Robots and Systems*. Hamburg, Germany, September 28-October 02, 2015. In review.

L. Daler, J. Lecoœur, P. B. Haehlen and D. Floreano, "A Flying Robot with Adaptive Morphology for Multi-Modal Locomotion," in *IEEE/RSJ International Conference on Intelligent Robots and Systems*. Tokyo, Japan, November 3-7, 2013.

L. Daler, A. Klaptocz, A. Briod, M. Sitti and D. Floreano, "A Perching Mechanism for Flying Robots Using a Fibre-Based Adhesive," in *IEEE International Conference on Robotics and Automation*. Karlsruhe, Germany, May 6-7, 2013.

S. Mintchev, L. Daler, G. L'Eplattenier, L. Saint-Raymond, and D. Floreano, "Foldable and Self-Deployable Pocket Sized Quadrotor," in *IEEE International Conference on Robotics and Automation*. Seattle, USA, May 26-30, 2015. Accepted.

A. Klaptocz, A. Briod, L. Daler, J.-C. Zufferey and D. Floreano, "Euler Spring Collision Protection for Flying Robots," in *IEEE/RSJ International Conference on Intelligent Robots and Systems*. Tokyo, Japan, November 3-7, 2013.

J. Auerbach, D. Aydin, A. Maesani, P. Kornatowski, T. Cieslewski, G. Heitz, P. Fernando, I. Loshchilov, L. Daler and D. Floreano, "RoboGen: Robot Generation through Artificial Evolution," in *Artificial Life 14: International Conference on the Synthesis and Simulation of Living Systems*. New York, NY, USA, July 30-August 2, 2014.